

TD-03-034

7/25/03

Quench Data Analysis with Correction of Inductive Voltage and HFDM-02 Magnet Quench Events with BICC

Ryuji Yamada and Eric Marscin

July 25, 2003

1. Introduction

When we are testing a short length superconducting model magnet, the time constant of the system is very short due to the very small inductance of the magnet and the small resistance value of the dump resistor. This situation causes the rapid decay of the current, inducing large inductive voltages in the observed voltage signals. At times, this caused some problems for the interpretation of the experimental data.

The voltage tap signals over some distance of the coil are affected by the local effective inductance value. After the magnet quenches, the observed voltage signals are composed with the signal of the true normal resistance signal and the locally induced voltage signal. The true normal signal can be extracted with the subtraction of the induced signal from the observed voltage signal. The inductive voltage is defined as the product of the local effective inductance value and the value of dI/dt .

There are several ways to estimate the local effective inductance values. We tried a couple of methods to extract the effective inductance values, which are explained in the text. There are always some error signals coming from signal lead wires due to the incomplete twisting, which are estimated.

The corrected voltage signals show a much cleaner quench. The typical quench data of the HFDM-02 are shown in detail. We can also extract the normal resistance data of the cable per meter, and the cable's average temperature. The values are clearly calculated after the magnet quenches. With the clearer voltage data provided by this technique, we are also able to more easily study the data near the quench starting points.

Using this technique, we can see how each part of the HFDM-02 magnet quenches. We can also guess at how the BICC boundary conditions are affecting the initiation of a quench in this magnet.

2. Voltage Signals and Induced Voltages

After a quench starts, the voltage $V(t)$ across two voltage taps of the coil can be expressed as follows,

$$V(t) = R_n(t) \times I + L_{\text{eff}} \times dI/dt \approx R_n(t) \times I + L_{\text{eff}} \Delta I/\Delta t$$

where $R_n(t)$ is the normal resistance of that part of the coil, and L_{eff} is the effective inductance of that part of the coil. The value of L_{eff} is definitely smaller than the inductance value L_0 of the whole magnet and larger than the inductance value of that part of the separated coil because it also includes the mutual inductance. The values of ΔI and Δt are found between successive data points in the quench event data, although it is also possible to use an average of these values if there is too much noise in the raw data (see sections 4 and 5).

In Fig.12, the current shape of the Quench # 36 of the HFDM-02 mirror magnet is shown. At $t = -3$ ms, the magnet starts to quench, and the current starts decaying slightly because some part of the magnet starts showing normal voltage. When the difference voltage grows to the predetermined trigger voltage of 0.5 V, it triggers off the power supply, causing the current to decay in a moderate rate from 3.2×10^4 to 9.7×10^4 A/sec. At $t = 25$ msec, the dump resistor is activated, and the current starts decaying at the very rapid rate of 5.26×10^5 A/sec with the time constant $\tau = L_0 / R(t)$ of the whole magnet system. The decay time constant is made very small to protect the magnet from burning. The value of total resistance $R(t)$ during this period is given by

$$R(t) = R_d + R_n(t),$$

where R_d is the resistance value of the fixed dump resistor, which is 30 m Ω , and $R_n(t)$ is the normal resistance value. The decay curve of the current in Fig. 12 shows a time constant τ value of 26 ms at $t = +25$ ms. The normal resistance of the whole magnet at 25 ms is about 7.2 m Ω , which includes 6 m Ω for the outer coil and 1.2 m Ω for the innermost 3-turn block, as shown in Fig.18. The estimated inductance of the whole magnet L_0 is

$$L_0 = \tau \times R(25 \text{ ms}) = 26 \times 10^{-3} \times (30 + 7.2) \times 10^{-3} = 967 \times 10^{-6} \approx 1 \text{mH}.$$

2.1. Estimation of Error Noise Signal due to Signal Lead Wires

The signal voltage shapes show some electronic noise signals at $t = 0$ ms due to the power supply, and another violent change at $t = +25$ ms due to switching on the dump resistor.

The pair of lead wires, which delivers the electrical signal of the part of the coil or the signal from the short piece of cable, is not completely twisted to cancel the pickup noise. The estimated error voltage $V_n(t)$ due to this is estimated as follows,

$$V_n(t) = d\Phi/dt = S dB/dt.$$

In the case of Fig.12, the current is decaying at maximum rate of 5.3×10^5 A/sec. The value of B_0 is 5 Tesla, and $dB_0/dt = 192$ T/sec. If we assume there is an effective open loop of $S = 1 \text{ cm}^2 = 10^{-4} \text{ m}^2$, then

$$V_n < S dB_0/dt = 192 \times 10^{-4} < 2 \times 10^{-2} = 20 \text{ mV}.$$

On the other hand, if the $L_{eff} = 10 \mu\text{H}$, then the signal voltage V_s is,

$$V_s = L_{eff} \times dI/dt = 10 \times 10^{-6} \times 5.3 \times 10^5 = 5.3 \text{ V}.$$

Thus the signal noise ratio V_s/V_n is quite high.

3. Resistance of Nb_3Sn Cables with Temperature

3.1. Resistance of Regular Nb_3Sn Cable with Temperature and with other Parameters

3.1.1. Nb_3Sn Resistivity

The resistivity of the Nb_3Sn portion of the cable is defined in four parts.

- If the cable is superconducting, the resistivity is 0.
- If the cable is transitioning to the normal state, the resistivity is defined as:

$$\rho_{SC}(j) = \rho_0 \left(\frac{j}{j_c} \right)^n \quad [\Omega \text{ m}],$$

where ρ_0 is $10^{-14} \Omega\cdot\text{m}$, and n is the n -value of the superconductor.

- If the cable is in the normal state, its resistivity is defined as:

$$\rho_{\text{Nb}_3\text{Sn}}(T) = \min \left(7.65 \times 10^{-10} \times T + 2.3 \times 10^{-7}, 2.6 \times 10^{-10} \times T + 3.32 \times 10^{-7} \right) [\Omega \text{ m}].$$

The transition between these two equations takes place at 201.98°K .

3.1.2. Copper Resistivity

The resistivity for the copper with RRR is expressed by,

$$\rho_{Cu} = 1.8 \times 10^{-8} \left(\frac{0.65}{e^{\frac{T_d}{2.3T}} - 1} \left(1 - \frac{1}{RRR} \right) + \frac{1}{RRR} \right) [\Omega \text{ m}],$$

where T_d is the Debye temperature of copper (the constant value 343 was used for this paper), RRR is the RRR of the copper, and T is the temperature [2].

3.1.3. Cable Resistivity

The resistivity of the cable is computed by the following equation:

$$\rho_{cable} = \frac{(1 + \lambda)\rho_{Cu}\rho_{SC}}{\rho_{Cu} + \lambda\rho_{SC}} \quad [\Omega \text{ m}],$$

where λ is the volumetric ratio of copper to the superconducting material (Nb_3Sn), ρ_{Cu} is the resistivity of copper, and ρ_{SC} is the resistivity of the superconducting material.

3.1.4. Cable Resistance

The resistance of the cable is given by the following equation:

$$R_{cable} = \frac{\rho_{cable}}{S_{cable}} [\Omega/m],$$

where ρ_{cable} is the resistivity of the cable, and S_{cable} is the area of the cable cross section ($S_{cable} = 2.2 \times 10^{-5} \text{ m}^2$). The cable resistance R_{cable} and its copper component R_{cu} for a cable with $\lambda = 0.887$, $RRR = 10$, and $n = 50$ are shown in Fig. 13.

4. Data Processing Method

Processing voltage data to correct for the inductive voltage involves four main steps:

1. Retrieve the voltage and current data for the quench event to be studied,
2. Run a customized Excel macro, “VindCorrection”, to read in the data files and set up a spreadsheet for removing inductive voltages,
3. Fill in the inductances for each voltage tap, and
4. Analyze the results.

Each of these steps will be described individually in this section.

4.1. Retrieve the voltage and current data for the quench event to be studied

There are two main ways to handle this step. The first, and recommended, method is loading the Quench Analysis program [3], selecting the quench event to study, selecting the current data and the voltage taps of interest, graphing them, and then writing out the data set to a file. There must be only one voltage tap data set or current data set per file, and the file must be written in the Quench Analysis program’s default format (%16lg %16lg) without imbedding parameters or writing binary data. An example file created from the Quench Analysis program is listed below:

```

@TYPE xy
      -0.99986      0.690413
      -0.99972      0.645387
      -0.99958      0.615368
      -0.99944      0.600359
      -0.9993       0.600359
      -0.99916      0.615368
...
      0.99902      0.281285
      0.99916      0.281285
      0.9993       0.310894
      0.99944      0.266481
      0.99958      0.29609
      0.99972      0.325699
      0.99986      0.29609
      1           0.29609
&

```

Fig. 1: Example data file created from the Quench Analysis program.

Before the file can be read, the first and last lines must be deleted to remove the extra characters. Once this is done, the macro can read in the file and set up the data for analysis.

The second way to input the data into the macro is to create the file manually, either by hand or through another program. In that situation, the file must have the following characteristics:

- The first column must be the time the data was recorded, followed by the current or voltage data.
- The numbers must be right aligned in their columns.
- The data recording times must be the same among all data files. For instance, the time corresponding to row 2 in the voltage tap file(s) must be the exact same as the time corresponding to row 2 of the current file.
- It is recommended that the data be in standard metric units, although it is not required. If the data is in different units, the axes titles on the graphs created by the macro will need to be relabeled.

One particular thing to note is that the VindCorrection macro uses the names of the files containing the data to help name columns and graphs in the worksheet. It is recommended that the filenames for the data files be named to help identify the data contained in the file. This is described further in section 5.

4.2. Run the “VindCorrection” macro to read in the data files and set up the spreadsheet

This step involves simply loading Microsoft Excel and running the VindCorrection macro. The macro itself will be described in a later section.

4.3. Fill in the inductances for the cable portions represented by each voltage tap

This step requires the user to determine the inductance of the cable portions that lie between the voltage taps being studied. Any method can be used, but a recommended method will be described that was also used for the results shown later in this paper.

4.3.1. Methods for finding inductances

To find the inductance between two voltage taps, we can use the graphs created by the VindCorrection macro to “guess and check” the inductances. Since the normal voltage between two voltage taps is found by subtracting the inductive voltage from the raw voltage data (see section 5 for further explanation), an incorrect inductance value will cause the normal voltage curve to show some bias towards the original voltage data or towards the inverse of the inductive voltage. If the inductance value is too low, the inductive voltage would be underestimated. This would cause the normal voltage curve to be biased towards the original voltage data since the inductive voltage in the original data would not have been fully canceled out by the subtraction. If the inductance value is too high, then the inductive voltage would be overestimated. This would cause the normal voltage curve to be biased towards an inverted version of the inductive voltage because too much inductive voltage would have been subtracted from the original voltage data, thereby giving the normal voltage a shape similar to the inverse of the original inductive voltage. By looking at certain locations where the inductive voltage changes, we can adjust the inductance until these two biases are removed. There are 3 main methods that can be used to accomplish this goal.

A. Adjust inductance until the normal voltage has a constant slope around a certain time.

Find a point in time where there is no inductive voltage on one side, some inductive voltage on the other, and the normal voltage is changing at a constant, known rate. In this scenario, a normal voltage curve should have the same slope before and after the chosen time since it should be unaffected by the inductive voltage. However, an incorrect inductance would show a different slope after the selected time because the bias in the normal voltage curve would appear only after the inductive voltage was created. Therefore, we just need to adjust the inductance for the selected pair of voltage taps until the normal voltage curve has a constant slope at the selected time. This method is shown in figures 2a, 2b, and 2c for a non-quenching portion of the coil (so the normal voltage should stay at 0 V) at around $t = 0$ (this is when the power supply is turned off, creating an inductive voltage for $t > 0$, but having little inductive voltage for $t < 0$).

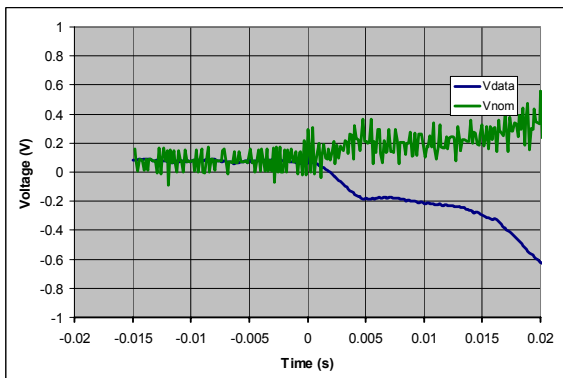


Fig. 2a: Example of too much inductance, which causes the slope of the normal voltage (green) on the right side of $t = 0$ ms to be greater than the slope on the left side.

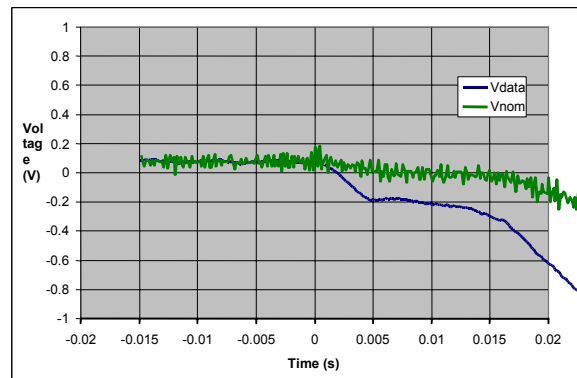


Fig. 2b: Example of too little inductance, which causes the slope of the normal voltage (green) on the right side of $t = 0$ to be less than the slope on the left side.

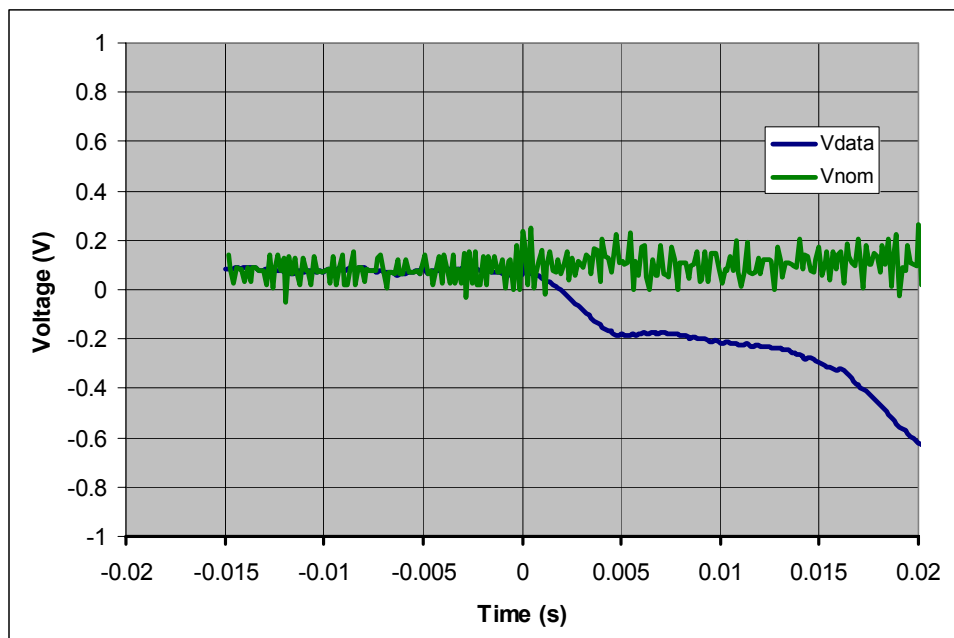


Fig. 2c: Example of correct inductance. Notice the similar slopes before and after the power supply is shut off at $t = 0$.

B. Match peaks around the noise of the dump resistor

If the quench in a voltage tap occurs too early to find a point where the normal voltage has a constant slope, but the normal voltage peak occurs just when the dump resistor is fired, then we use the two normal voltage “peaks” on both sides of the dump resistor noise to find the inductance. If we assume the peak occurs in the middle of the dump resistor noise, then the two peaks around the noise should be near the same voltage. However, an incorrect inductance value will cause the second peak to be higher or lower than the first peak due to the fact that the large change in the inductive voltage after the dump resistor is fired will cause the any small inductive voltage biases to affect the second peak more than the first peak. Therefore, the correct inductance can be found by adjusting the inductance until the peaks on both sides of the dump resistor noise are at the same voltage. This would guarantee that there are no voltage biases since both peaks are at the same voltage despite the fact that inductive voltages affect each peak differently from the other. Examples of this method are shown in figures 3a, 3b, and 3c. This method’s assumption makes it less accurate than other methods, but it gives a good approximation of the actual inductance.

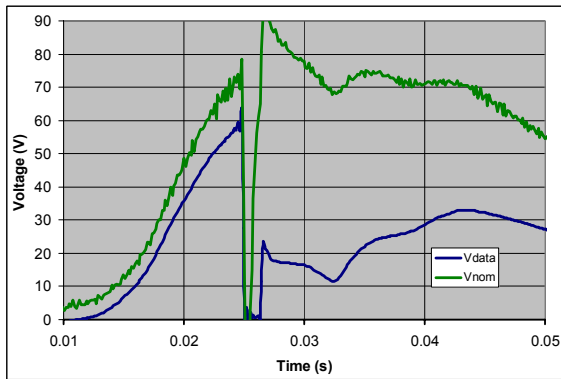


Fig. 3a: Example of too much inductance causing a higher normal voltage peak (green) after the dump resistor noise.

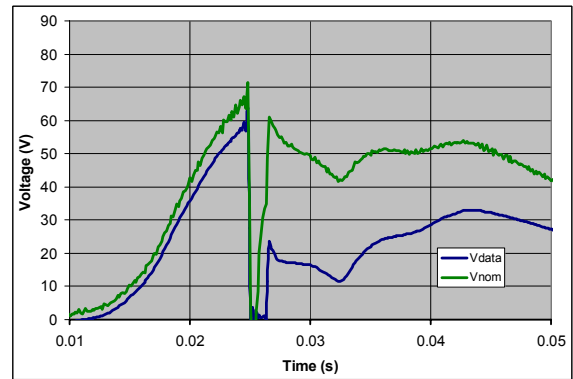


Fig. 3b: Example of too little inductance causing a lower peak (green) after the dump resistor noise.

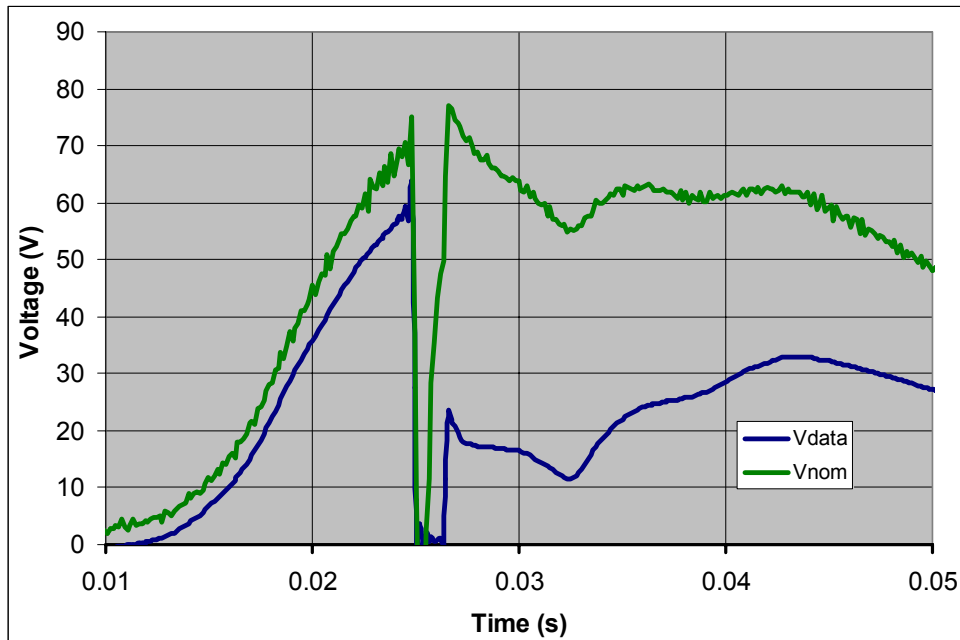


Fig. 3c: Example of correct inductance since both peaks are at about the same voltage.

C. Match slopes in voltage rise/decline

If the quench in a voltage tap occurs too early to find a point where the normal voltage has a constant slope, and the normal voltage peak for a voltage tap occurs before or after the dump resistor fires, then the best method for finding the inductance is to match the slope of the normal voltage curve across the dump resistor noise. If it can be assumed the normal voltage is changing at a constant rate when the dump resistor fires, then the normal voltage slope should be constant through the dump resistor noise. However, incorrect inductance values will cause the slope through the noise to be too high or too low due for the same reason as the previous method (large changes in the inductive voltage due to the dump resistor cause biases to more greatly affect the normal voltage after the dump resistor is fired). Therefore, the inductance is changed until the normal voltages on both sides of the dump resistor noise show a fairly constant slope before, during, and after the noise. This method is shown in figures 4a, 4b, and 4c. This method suffers from the assumption of a constant slope through the dump resistor noise, but gives a general idea of the correct inductance.

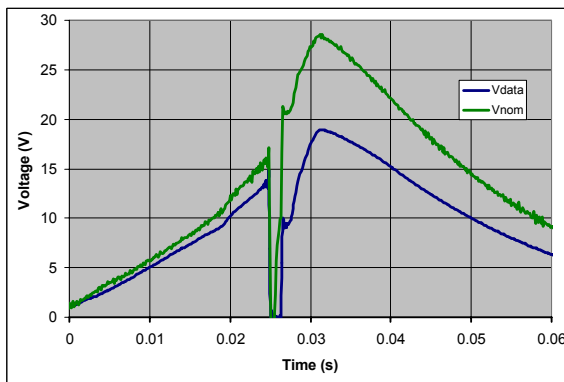


Fig. 4a: Example of too much inductance causing a higher slope in the normal voltage (green) across the dump resistor noise.

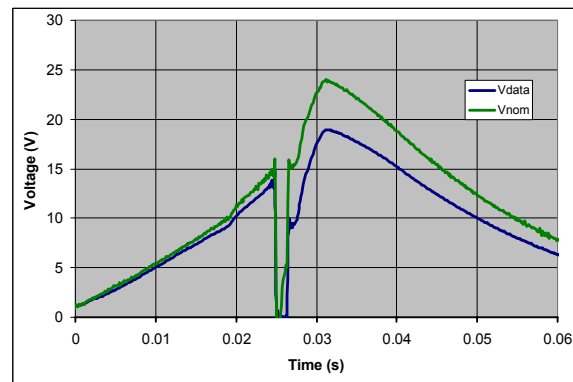


Fig. 4b: Example of too little inductance causing a lower slope in the normal voltage across the dump resistor noise.

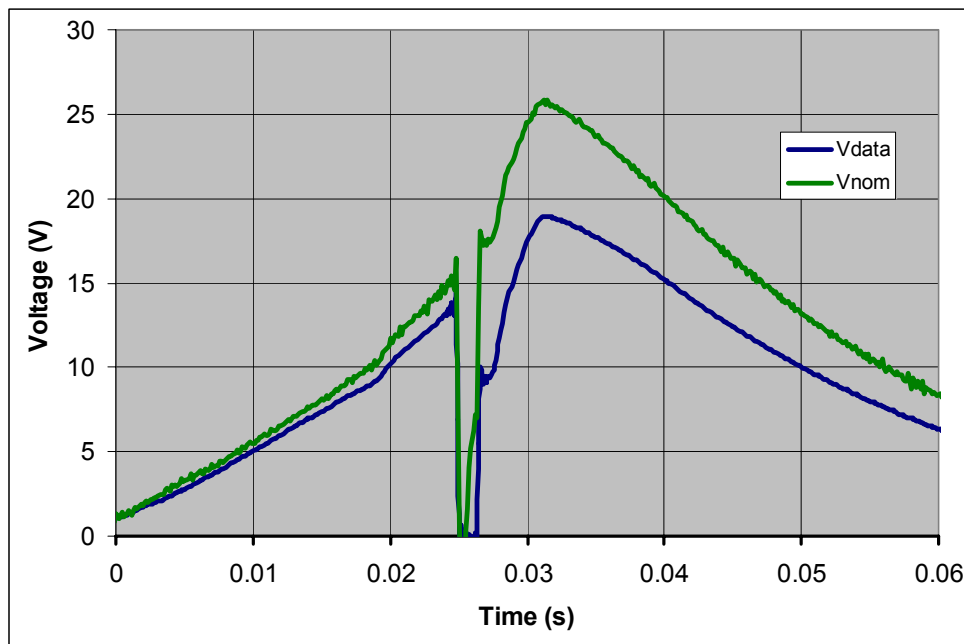


Fig. 4c: Example of correct inductance. Notice the slope before the dump resistor fires continues through the noise and meets up with the normal voltage curve on the other side.

4.4. Analyze the results

After the previous 3 steps are complete, the data should be accurate and ready to be analyzed.

5. Macro Program “VindCorrection”

The VindCorrection Excel macro can be used to quickly and easily set up an Excel spreadsheet and graphs for analysis of voltage data. It reads in current and voltage files, inputs spreadsheet formulas needed to compute the inductive voltage information, and creates labeled graphs for each pair of voltage taps being studied. It had been tested on Microsoft Excel 2000, but it should work for most versions.

To use the macro, follow these steps:

- Select and run the macro while in Microsoft Excel.**
- Select the current data file using the first file selection window.**
- Select the voltage data file(s) using the second file selection window.** Multiple voltage files can be selected by either highlighting many files at once by clicking and holding the left mouse button, or holding down **Ctrl** and individually clicking on each file.
- Input the desired minimum and maximum time to be used for the graphs at the prompts.** This does not effect how the data is stored in the spreadsheet, but it effects what range of data is displayed initially on all the graphs.

Once these steps are complete, the macro automatically creates the necessary formulas and graphs for each voltage tap file.

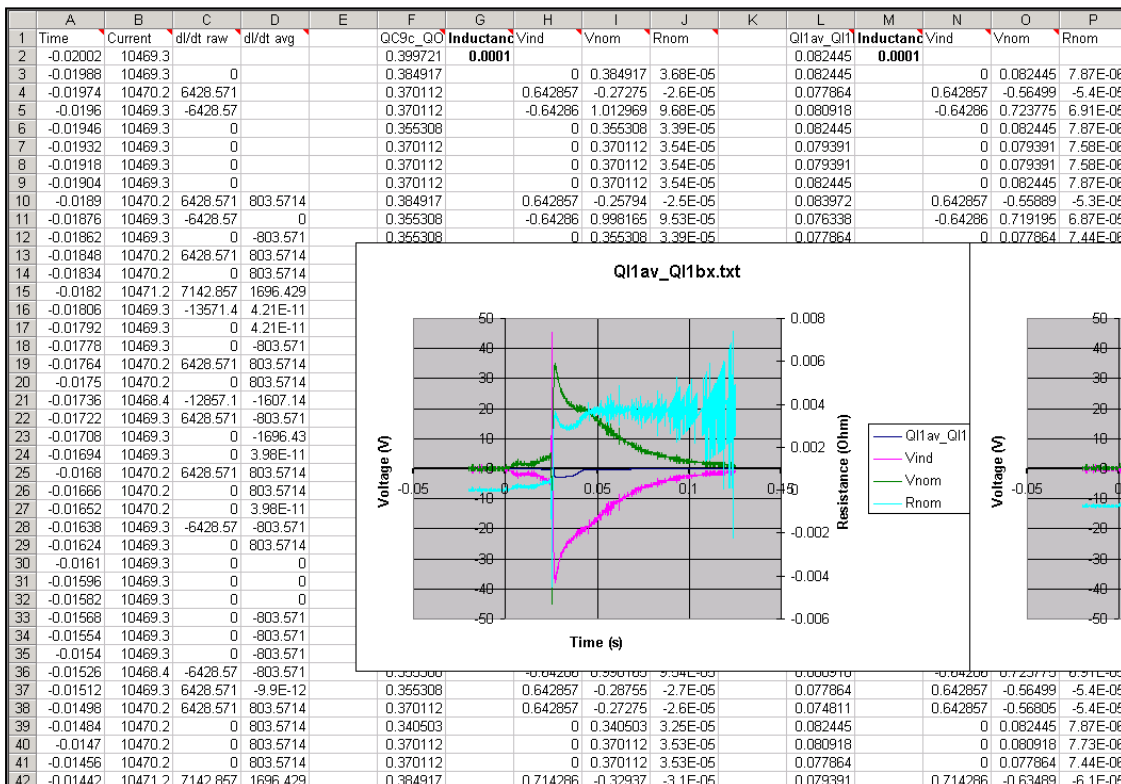


Fig. 5: Example worksheet created through the “VindCorrection” macro.

5.1. Worksheet

The worksheet contains all the time, current, and voltage data needed to remove the inductive voltages from the voltage taps and analyze the results. The general structure is as follows:

There 4 columns at the left end of the spreadsheet that hold the time and current data. The columns store (in order):

- The time, in seconds, that the data in that row was taken (named “Time”). The Quench Analysis program records data every 0.14 ms.
- The current in amps (named “Current”)
- The change in current over the change in time since the previous data point in amps per second (named “dI/dt raw”). This value may cause lots of noise in the inductive voltage if the resolution of the current data is not small enough for the time step.
- The change in current over the change in time in amps per second averaged over the past 8 time steps (named “dI/dt avg”). When using data from the Quench Analysis program, this corresponds to averaging over about 1 ms. This column is not used for any calculations by default, but it is included in case a user wants to use a smoother value for dI/dt. This value is used for the calculations in Fig. 37 (see section 7).

	A	B	C	D
1	Time	Current	dI/dt raw	dI/dt avg
2	-0.02002	12352.7		
3	-0.01988	12351.8	-6428.57	
4	-0.01974	12352.7	6428.571	
5	-0.0196	12351.8	-6428.57	
6	-0.01946	12352.7	6423.983	
7	-0.01932	12352.7	0	
8	-0.01918	12351.8	-6428.57	
9	-0.01904	12351.8	0	
10	-0.0189	12350.9	-6428.57	-1607.72
11	-0.01876	12351.8	6428.571	-0.57357
12	-0.01862	12351.8	0	-804.145
13	-0.01848	12352.7	6428.571	802.9979
14	-0.01834	12351.8	-6428.57	-803.571
15	-0.0182	12351.8	0	-803.571
16	-0.01806	12351.8	0	2E-11

Fig. 6: Leftmost four columns on a worksheet created by the macro.

To the right of these four columns is the voltage tap data. Each voltage tap will have 5 columns to hold its data. Each voltage tap column group is separated from other groups by a blank column on both sides. The columns store (in order):

- Raw voltage data in Volts (named as the portion of the voltage tap’s filename that comes before the file type extension; i.e. a filename of “QI1av_QI1Bx.txt” will have a column name of “QI1av_QI1Bx”).
- Inductance value for the voltage tap in Henry (named “Inductance”). The value and the column name are bolded to signify that the user should change the inductance.
- Inductive voltage in Volts (named “Vind”). This is found by multiplying dI/dt by the inductance L.
- Resistive/normal voltage in Volts (named “Vnom”), found by subtracting Vind from the raw voltage data.
- Resistance in Ohms (named “Rnom”), found dividing Vnom by the current.

L	M	N	O	P
QI1av_QI1Bx	Inductance	Vind	Vnom	Rnom
0.0824447	0.0001			
0.0839715		-0.64286	0.726829	4.97E-05
0.0809179		0	0.080918	5.54E-06
0.0809179		0.642398	-0.56148	-3.8E-05
0.087025		0	0.087025	5.96E-06
0.0824447		0	0.082445	5.64E-06
0.0854982		0	0.085498	5.85E-06
0.0916052		0.642857	-0.55125	-3.8E-05
0.0916052		0	0.091605	6.27E-06
0.087025		0.642398	-0.55537	-3.8E-05
0.0885517		0	0.088552	6.06E-06
0.0885517		0	0.088552	6.06E-06
0.0778644		0	0.077864	5.33E-06
0.0778644		0	0.077864	5.33E-06
0.0778644		0	0.077864	5.33E-06

Fig. 7: Voltage tap data columns on a worksheet created by the macro.

Comments in the column titles describe the data contained in that column. If the data in the column came from a file, they also list the filename containing that data. Plus, all of the columns that store derived voltage data (such as Vind or Vnom) also state the file that contained their raw voltage data.

The formulas in the worksheet are set up so that changing one cell will automatically change the values that reference that cell. In other words, changing the voltage data for a particular voltage tap will also change the normal voltage and resistance for that voltage tap automatically. This feature extends to the inductances for each voltage tap, allowing the user to easily change the inductances without worrying about changing other values.

5.2. Graphs

One graph is created for each voltage tap file. It contains the curves for:

- The raw voltage data in dark blue (named “Vdata”, not corresponding to any cell)
- The inductive voltage in pink (named “Vind”, corresponding to the column name for that voltage tap’s inductive voltage column)
- The normal voltage in green (named “Vnom”, corresponding to the column name for that voltage tap’s normal voltage column)
- The resistance in light blue (named “Rnom”, to the column name for that voltage tap’s resistance column)

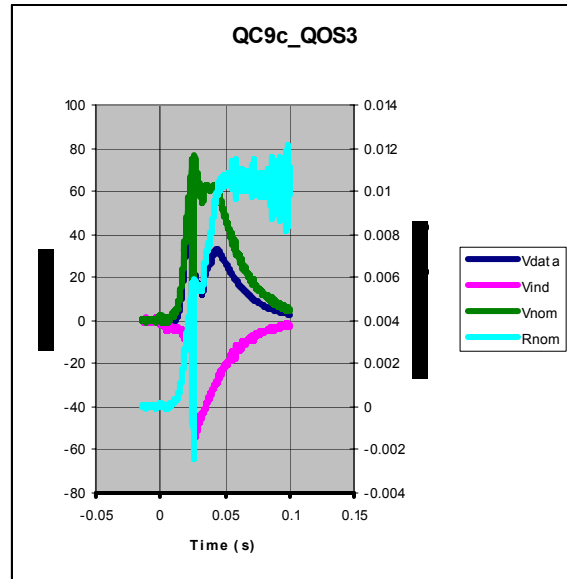


Fig. 8: Graph created by the macro.

The name of each graph is based on the filename that contained the graph’s voltage data. Specifically, the name of each graph corresponds to the portion of the filename before the file extension (this is exactly the same as the column name of the raw voltage data).

Every graph has the same axes. Time is along the x-axis, voltage is along the left y-axis, and resistance along the right y-axis. The axes are automatically labeled for metric units (seconds, Volts, and Ohms).

The graphs are made without markers on the data points, and have the thickest line possible.

5.3. General notes and known bugs

After the macro completes, some of the graphs may be hidden behind other graphs. If you can’t find a certain graph, try moving some of the graphs near the location of the missing graph’s data.

The macro has no known bugs when run normally, but certain actions might cause strange behaviors. Canceling out of some dialog windows might cause “Type mismatch” or “Method ‘[some name]’ of Object ‘[another name]’ Failed” errors. These are due to the Visual

Basic customizations, and can be safely ignored. If these errors occur, just press the “End” button, close the worksheet created by the macro (if any), and rerun the macro.

A more serious problem arises if the macro is run once, then run again while selecting the same current data without closing the first macro’s worksheet. This scenario will cause a dialog box to pop up asking if you want to reopen the current data file and discard all changes (this occurs because the macro opens the current data file first, then copies all the voltage data onto that worksheet). Selecting to reopen the file might cause Excel to crash. It is highly recommended that the user save the first worksheet (if desired) and close it before rerunning the macro on the same current data.

6. HFDM-02

The HFDM-02 magnet is a mirror magnet, made with a half coil and a semicircular iron piece. It was assembled with a stainless steel yoke. Its construction report is given in another report [4], and its general test data will be reported in another report [5]. Its voltage tap layout is shown in Fig. 9 for its inner and outer coils. Its field distribution in the cross section of the magnet is shown in Fig.10 [6], and its load lines are shown in Fig. 11. In our test configuration, only two lines, the line marked as “B0 no yoke” and the line marked as “Bpeak no yoke”, are used. Due to the stainless steel yoke, it has a field distribution different from the previous mirror magnet HFDA-03A [7]. Both mirror magnets have quite different field distributions from the regular dipole magnet HFDA-04 [8,9], especially with the high reduction in the vertical field component into the med-plane cable. This causes very different boundary conditions for any BICC, and we can expect different quench patterns in the HFDM-02 magnet.

The HFDM-02 magnet was tested at 4.5° K and at lower temperatures down to 2.16° K, and at ramp rates from 4 A/sec, corresponding to 0.00094 Tesla/sec, to 301 A/sec, corresponding to 0.07 Tesla/sec. At 4.5° K, all of the 26 Quench events started at the outer splice, QOS3_QOS2, and in the outer coil, QC9c_QOS3, except for Quench event #12. Its quench started in the inner middle 5-turn coil block, QI4au_QI9au, and had an exceptionally higher MIITs value of 42.5, while all other quench events had MIITs values around 7, or up to 16.

At lower temperature tests with the ramp rate of 20 A/sec, the quenches started mostly at the innermost 3-turn coil block of the inner coil. However, one started in the inner middle 5-turn block, and another one at the outer splice and outer coil. At a ramp rate of 300 A/sec, two events started quenching at the outer splice and outer coil. These two Quenches show strong evidence of being caused by the higher ramp rate inducing greater supercurrents which are dissipated in the splice, heating up that area and causing a quench.

6.1. Results using Corrected Data of Quench # 36 of HFDM-02

Quench #36 was done at 2.16 K with 20 A/sec. It had the highest current value of 14,558 A for this magnet. From Fig.11, we can see the “Bpeak no yoke” is 5.85 Tesla, and the “B0 no yoke” is 4.6 Tesla. The maximum current of this magnet when tested at 4.54 K with 20 A/sec ramp rate was 12,321 A (Quench # 4). That shows the maximum quench current is increased by 2,237 A (18 %) when the temperature is lowered by 2.38 K.

Experimentally observed voltage tap waveforms are shown in Fig.14 (also in Fig. 16 and Fig. 19). The connected voltage waveforms are shown in Fig.15 (also in Fig. 17 and Fig. 20) together with the current form. The current is gradually decreasing after $t = -2.5$ ms when the coil starts quenching. Then it starts moderately decreasing at $t = 0$ ms when the power supply is

tripped off due to the setting of 0.5 V in the difference voltage detection. At $t = +25$ ms, the dump resistor is activated, and the current starts decaying drastically.

In Fig. 15, it is clearly shown that the innermost 3-turn block of the inner coil, QI9au_QC9c, started quenching at $t = -2.5$ ms. The outer coil, QC9c_QOS3, followed the innermost 3-turn block, and started quenching at $t = +5$ ms. The remaining part of the inner coil does not show any quench before the dump resistor is activated at $t = +25$ ms. This means the quench starting point in the innermost 3-turn block is close to the center of the magnet.

With the corrected waveforms in Fig.15, it is clearly seen that all remaining inner coil blocks started quenching around 28 ms. This may be due to the quench back effect caused by the very rapid decrease of the current starting at 25 ms. This quench back effect takes only 2 to 3 ms at this level of current.

The outer coil shows a peak at 25 ms, which is split into two peaks due to the activation noise of the dump resistor. There are two more small peaks at 35 and 43 ms. These peaks are due to a similar quench back effect, but the peak at 43 ms may be due to the heating of the protection heaters, which are activated at $t = 0$ ms together with the dump resistor. The protection heater is mounted only on the outer surface of the coil, and it will take about 35-43 ms to warm up the outer coil.

To see the initial stage of the quench, the early parts of the Fig.14 and 15 are expanded and shown in Fig.16 and 17. They are further magnified and shown in Fig. 19 and 20 respectively. The corrected shape of the outer coil shows noise due to the calculation of dI/dt , which is taken at the unit interval of 0.14 ms, but we can see the general tendency.

The resistance values of each segment coil block and splices are shown in Fig. 18, together with the current waveform. The resistance of the innermost 3-turn block starts rising at $t = -2.5$ ms, and continues rising though the dump resistor time at 25 ms, finally leveling off at 50 ms (Fig.23). The outer coil starts heating slowly at 5ms, and picks up speed around 13 ms. At 25 ms, it stops growing, but it starts growing again from 32 ms 43 ms. This later increase may be due to the heating by the fired heater strip (Fig.22). Also interesting is the very similar voltage and resistance waveforms are observed in the outer splice, QOS3_QOS2, when compared to the outer coil (although the magnitude is 400 times less) (Fig.21).

The other parts of the inner coil are showing rising resistances between 28 to 35 ms. The inner splice shows an increase in resistance at 40 ms.

From Fig. 18, we can judge that the coil part of the magnet is adiabatic up to 80 ms after the current is tripped off.

The summary of the corrected voltage data of Quench #36 is shown in Table I. Using the temperature data of the coil segment together with the resistance vs. temperature graph of Nb3Sn cable (Fig.13), we can estimate the average temperature of short cables. The resulting average temperatures of the component coil at 80 ms are also shown in Table I. In general, the temperature range is around 90 to 130 K, but the quench-starting innermost 3-turn block went up to 170 K. The temperature of the inner splice is high, which needs more study.

The corrected voltage data together with the resistance value for each component of the coil are shown from Fig. 21 to Fig. 30, starting from the outer splice down to the inner splice along the cable.

7. Quench # 39 of HFDM-02

This quench event was run at 2.16K with a ramp rate of 300A/sec. Its quench current was 10,431A. This was surprisingly less than the current in Quench #11, which was run at 4.4K at the ramp rate of 301A/sec and reached 10,967A. Both of them had the quench starting point at the outer coil, QC9c_QOS3, and at the outer splice, QOS3_QOS2.

7.1. Results of Quench #39 of HFDM-02

This Quench #39 is a premature quench, showing recovery. It could have been prevented by setting the quench protection trigger to a higher voltage, such as 1 V instead of 0.5 V.

The original voltage data are shown in Fig. 31 (also in Fig. 33 and Fig. 36). The outer coil voltage tap, QC9c_QOS3, shows a voltage rise starting at $t = -7$ ms, growing up to +0.5 V, and triggering off the power supply. However, its voltage signal goes down and the quench recovers. At around $t = +6$ ms, the system loses control due to the power supply being triggered off at $t = 0$ ms. The outer coil starts quenching again around $t = +15$ ms.

This phenomenon is clearly seen in Fig. 32 (also in Fig. 34 and Fig. 37) with the inductive voltages removed. The outer coil can be seen with a small voltage rise followed by recovery at around $t = 0$ ms. In this figure, it is also clear that the other coil blocks do not quench before $t = +25$ ms, and then start quenching after +34 ms due to quench back. We also can see the outer coil has another peak at around +48ms due to the heating of the Heater Strips.

To check the start of the initial quench, the early stages of Fig. 31 and 32 are expanded around $t = 0$ ms, and are shown in Fig. 33 and 34.

The resistances of each of the coil components are shown in Fig. 35. The summary of the data is shown in Table II, and the estimated temperatures of each of the coil block elements at $t = +80$ ms are also listed.

In Fig. 36 (original data) and Fig. 37 (corrected data), the early voltage signals, which start the whole magnet quench, are shown for the outer splice and outer coil for comparison. They are almost exactly the same shape, suggesting the quench started in the outer splice. Due to high amounts of noise from the dI/dt value in the corrected voltages in Fig. 37, we used a value for dI/dt that was averaged over the previous 1 ms. (see section 5). This resulted in the smoother lines seen in the figure.

As in the Quench #36, the voltage shape at the outer splice (Fig.38) is similar in shape as that in the outer coil (Fig.39) except its magnitude is much less by a factor of 400. In both figures they show a bump due to Heater Strip Heating at $t = 58$ ms.

From Fig. 38 to Fig. 47, the voltage variation from the outer splice to the other end of the inner splice is displayed. Before the dump resistor is activated at $t = +25$ ms, only the outer splice and outer coil go through quenching. The remaining parts of the coil start quenching from $t = +33$ ms to +40 ms possibly due to the quench back. In Quench #39, we adjusted the inductance so that the voltage does not become negative after $t = +25$ ms, in addition to the regular adjustment. We see some rounding in the voltage curves, which may need more study. In the inner splice, we observe some voltage rise at $t = +73$ ms in Fig. 47, which may be related to NbTi cable in the splice.

The summary of data is shown together with the estimated temperature at 80 ms of each component. The adjusted inductances are similar to the previous case, but those in the inner coil tend to be bigger.

8. Quench # 40 of HFDM-02

This quench was run in the same way as the Quench #39 at 2.16 K with a ramp rate of 300A/sec. However, it was precycled from 0A to 9,000A, back to 0A, and went up to the quench. Its quench current was 12,308A, which was 1,923A higher than the quench current of Quench #39 without pre-cycling. This increase might be related to BICC. Next time, we should repeat the operation with similar cycling but with a slow ramp rate beyond 11,000A.

8.1. Results of Quench # 40 of HFDM-02

The original voltage forms of every component are shown in Fig. 48 (also in Fig. 50). The corrected voltage forms are shown in Fig. 49 (also in Fig. 51). We can now clearly see how the quench is propagating in every part of the coil. In this case, the outer coil is quenching smoothly from the beginning of $t = -2.8$ ms. All other parts start quenching from 29 ms to 34 ms from the quench back effect. The outer coil is heated by the heater strip, and its voltage shows a peak at 40 ms.

Fig. 52 shows the resistance development in each of the components. The effect of the heater warming up the outer coil can be seen starting $t = +37$ ms.

The close-up of Fig. 48 and Fig. 49 are shown in Fig. 50 and Fig. 51. We clearly see the quench development of the outer coil before $t = 0$ ms.

The detailed description of the voltage rises in the Outer Splice and the Outer Coil are shown in Fig. 53 (original data) and in Fig. 54 (corrected data). We can see the clear correlation between them in the figure at the high ramp rate of 300 A/sec.

From Fig. 55 to Fig. 64, we can see the quench propagation in each component. Compared with Quench #39, Quench #40 has a higher current, and therefore the effect of the quench back is happening sooner. In Fig. 64, the voltage and resistance of the inner splice are shown, with an effect starting at $t = +50$ ms. This may be due to the NbTi cable.

The summary of the data is shown in Table III, together with the list of temperatures at 80 ms.

9. Quench #4 and Quench #11 at 4.5° K

Both Quench #4 and Quench #11 were run at 4.5° K. Quench # 4 is the highest current case at a ramp rate of 20 A/sec at this temperature, with $I_q = 12,321$ A. Quench #11 is the highest current case at the ramp rate at 301 A/sec. Both cases started quenching at the outer coil QC9c_QOS3. Their original data and corrected data are shown in Fig 65 and Fig.66 for the Quench # 4, and in Fig. 67 and Fig. 68 for the Quench #11. In both cases, the corresponding signals of the outer splice QOS3_QOS2 are shown. Although the signal of the outer splice is 400 times smaller, they both show the exact same pattern. From these facts, we can judge the quench started from the splice and the Nb₃Sn cable next to it, meaning the BICC current heated up the splice and adjoining cable enough to start quenches in the splice region in both Quench cases.

10. Conclusions

Experimental magnet data, especially with short superconducting magnets, suffer from large noises due to inductive voltage. By correcting for these inductive voltages, we can see much clearer pictures of the quench behaviors for each component of the coil, as was shown in this report. First, we can see the general overview of what, which, and when each component goes through the quench process. This is true over the entire period from when the coil starts to quench, through the triggering off the power supply, and even going through the activation of the dump resistor. Also, the average temperature variation of each component during the quench can be clearly estimated.

This process is also essential to clearly judge if the quenching portion of the coil is going through a premature quench or not, as shown in the case of the Quench #39 of HFDM-02. We also can observe the correlation between the quenching at the splice and the quenching at the cable as shown in the Quench #39 and #40, both at slow and fast ramp rates in those runs. We think this will lead to the understanding of the BICC effect around the splices, even at a slow ramp rate. We believe this technique will be used widely in the future to help enhance our understanding of the quenches in high field magnets.

11. Conclusion about HMDM-02 with Consideration Towards BICCs

During **4.4 to 4.5° K** operation, the HMDM-02 magnet quenched in almost all cases **around the outer splice**, regardless of the ramp rate, in the quench current range from **10,604 to 12,321 A**. However, at lower temperature operation from **3.9 to 2.16° K**, and with lower ramp rates of 20 A/sec, the magnet **quenched mostly at the innermost 3-turn block**. It also quenched once at the outer splice area under these conditions. At this temperature, the quench current values went **up by 2,200 A**, ranging from **12,674 to 14,558 A**. This data shows that cooler temperatures lead to higher quench currents.

These facts show that, with better cooling at lower temperature, the cooling of the outer splice improved, and the quenching at that location stopped. Instead, the next weakest point in the coil from the standpoint of BICC, the innermost 3-turn of the inner coil, started to quench. **This means that, with better cooling, the quench starting point moved to the next weakest point, thus causing an increase in the quench current.**

With 2.14 K operation, and the higher ramp rate of 300 A/sec, the splice region got hotter than the innermost 3-turn block of the inner coil, and once again started to quench before the rest of the coil. This could be caused by the splice region having more resistive loss due to the eddy current effect as well as BICC effect at the splice.

The combination of all these facts shows that **the quenching around the splice is not due to mechanical damage. It is due to the heating of the splice from BICC.**

12. Recommendation for Improvements of Cosine Theta Design Magnet

Probably the splice structure of the HFDM-02 has improved over the previous one, but it still needs better cooling, as was proven above. To make the splice easier for mechanical construction, the splice region should be brought further away from the coil region than compared to its current location. The Nb₃Sn cable should be sandwiched with two NbTi cables to decrease the resistance and increase the heat capacitance, and a copper cover block should cover the splice to work as a heat sink.

The aluminum spacers should have spiral grooves on the inside surface so that there will definitely be good liquid He cooling channels to cool the splice region as well as the whole outer surface of the coil.

We also need more cooling for the innermost 3-turn inner layer block. This can be done by making a cooling hole through the center wedge.

With 14,558 A, the Bpeak at the conductor where the quench is starting is 5.85 Tesla. This is in the high field region away from flux jumping region. This current is the highest for the cosine series magnets, but it is not the highest Bpeak record due to the stainless steel yoke of the magnet HFDM-02. The highest Bpeak we have achieved is 7.56 Tesla with HFDA-04 with a current of 12,199A.

Due to the mirror magnet structure and the stainless steel core, the field distribution on the conductor cables is quite different from that of the regular cosine theta magnets, as well as in the end field region. This complicates the testing of the mirror magnet, and thus we have to go back to the testing of the regular magnet at some point soon.

We are still far away from the short sample data values. With the very low RR value of 5 to 10, and with the very low n-value around 15, the cable is still not stable [4]. We suspect, due to the extremely bad non-uniformity values of these parameters, the next weak spot from the standpoint of BICC can be anywhere in the coil. The magnet end region is especially suspect because it has the smallest bending radius, and the RRR value might be the worst in that location. Plus, the end field distribution gives it a very poor boundary condition. The stability of the cables needs to be improved before we can reach the short sample data values.

Reference:

- [1] Ryuji Yamada, "Quench Study on HFDA-03A, (TC-1 & TC-2), with Consideration on Possible Relation to Boundary Induced Coupling Currents, TD-03-024, May 30, 2003.
- [2] S. S. Kozub, Ya. V. Shpakovich, A. V. Zlobin, "Thermal Conductivity and Electrical Resistance of Composite Wires based on HT-50." Cyrogenics 1992, Vol. 32, ICEC Supplement, p. 295. And M. Wake, private communication.
- [3] Quench Analysis program :
<http://sdsg.fnal.gov/dmcsweb/dcms/gui/quenchanalysis/quenchanalysis.htm>
- [4] D.R. Chichili et al., "Nb3Sn Cos(θ) Dipole Magnet, HFDM-02 Production Report", TD-03-029, June 16, 2003.
- [5] S. Feher et. al., "HFDM-02 Test Summary", TD-03-xx, 2003.
- [6] D. Chichili, "Mechanical Analysis of Mirror Magnet for Shell-Type HFM Dipole Coils" TD-03-xx, 2003.
- [7] V. V. Kashikhin, A.V. Zlobin, "Magnetic analysis of the splice fields in HFDA magnets." TD-03-010, March 27, 2003.
- [8] D.R. Chichili et al., "Nb3Sn Cos(θ) Dipole Magnet, HFDA-04 Production Report", TD-02-025, May 15, 2002.
- [9] S. Feher et. al., "HFDA-04 Test Summary", TD-02-45, 2002, August 2, 2002.

Table I. Summary Table of Quench #36 of HFDM-02.

Iq = 14558 A 20 A/sec 2.22 K Quench starts at I9qu_C9c									
Outer Coil		Length	Quench	Leff	Vpeak	Rnom at 80 ms	Rnom / m	Temp	
		(m)	start time	(micro H)	(V)	(mΩ)	(Ω / m)	(K)	
Outer Splice	QOS3_QOS2	15.2 cm	0.1524	+5 ms	0.27	0.185	0.03	0.00020	48.9
Outer Coil	QC9c_QOS3	13 turns	20.48	+5 ms	100	77	11	0.00054	142.9
Inner Coil									
Innnermost	QI9au_QC9c	3 turns	3.834	-2.5 ms	15	26	2.75	0.00072	177.4
mid	QI4au_QI9au	5 turns	8.0077	+27 ms	42	27.5	2.8	0.00035	102.0
bottom	QI1bv_QI4au	2.2 turns	3.6621	+30 ms	20	12.5	1.6	0.00044	123.5
midplane	QI1bz_QI1bv	0.03 turn	0.05	+30 ms	0.065	0.2	0.023	0.00046	128.3
midplane	QI1bx_QI1bz	0.03 turn	0.0482	+30 ms	0.065	0.185	0.0217	0.00045	126.3
midplane	QI1av_QI1bx	0.5 turn	1.5499	+29 ms	9	4.3	0.43	0.00028	79.1
midplane	QIS3_QI1av	0.13 turn	0.2997	+29 ms	0.21	0.88	0.11	0.00037	106.8
Inner Splice	QIS2_QIS3	15.2 cm	0.152	+40 ms	0.7	0.88	0.175	0.00115	270.0

Table II. Summary Table of Quench #39 of HFDM-02.

Iq = 10431 A 300 A/sec 2.22 K Quench starts at I9au_OS3									
Outer Coil		Length	Quench	Leff	Vpeak	Rnom at 80 ms	Rnom / m	Temp	
		(m)	start time	(micro H)	(V)	(mΩ)	(Ω / m)	(K)	
Outer Splice	QOS3_QOS2	15.2 cm	0.1524	+5 ms	0.27	0.098	0.013	0.00009	10.1
Outer Coil	QC9c_QOS3	13 turns	20.48	-7 ms	100	40	4.5	0.00022	57.8
Inner Coil									
Innnermost	QI9au_QC9c	3 turns	3.834	+34 ms	17	6.8	1.5	0.00039	113.0
mid	QI4au_QI9au	5 turns	8.0077	+34 ms	54	13	2.5	0.00031	90.7
bottom	QI1bv_QI4au	2.2 turns	3.6621	+36 ms	25	5.5	1.3	0.00035	103.5
midplane	QI1bz_QI1bv	0.03 turn	0.05	+37 ms	0.15	0.1	0.02	0.00040	115.1
midplane	QI1bx_QI1bz	0.03 turn	0.0482	+37 ms	0.14	0.1	0.019	0.00039	113.7
midplane	QI1av_QI1bx	0.5 turn	1.5499	+36 ms	11	1.8	0.34	0.00022	57.6
midplane	QIS3_QI1av	0.13 turn	0.2997	+36 ms	0.45	0.36	0.085	0.00028	81.2
Inner Splice	QIS2_QIS3	15.2 cm	0.1524	+32 ms	0.7	0.16	0.12	0.00079	193.3

Table III. Summary Table of Quench #40 of HFDM-02.

Iq = 12308 A 300 A/sec 2.22 K Quench starts at I9au_OS3									
Outer Coil		Length	Quench	Leff	Vpeak	Rnom at 80 ms	Rnom / m	Temp	
		(m)	start time	(micro H)	(V)	(mΩ)	(Ω / m)	(K)	
Outer Splice	QOS3_QOS2	15.2 cm	0.1524	-2 ms	0.27	0.17	0.024	0.00016	33.7
Outer Coil	QC9c_QOS3	13 turns	20.48	-2.5 ms	100	70	9.3	0.00045	127.1
Inner Coil									
Innnermost	QI9au_QC9c	3 turns	3.834	+30 ms	16	11.5	1.7	0.00044	124.9
mid	QI4au_QI9au	5 turns	8.0077	+30 ms	49	20	2.5	0.00031	90.7
bottom	QI1bv_QI4au	2.2 turns	3.6621	+33 ms	23	8.4	1.4	0.00038	110.7
midplane	QI1bz_QI1bv	0.03 turn	0.05	+33 ms	0.1	0.14	0.02	0.00040	115.1
midplane	QI1bx_QI1bz	0.03 turn	0.0482	+33 ms	0.1	0.13	0.019	0.00039	113.7
midplane	QI1av_QI1bx	0.5 turn	1.5499	+33 ms	9.6	2.7	0.34	0.00022	57.6
midplane	QIS3_QI1av	0.13 turn	0.2997	+32 ms	0.32	0.55	0.09	0.00030	86.8
Inner Splice	QIS2_QIS3	15.2 cm	0.1524	+25 ms	0.85	0.47	0.17	0.00112	263.8

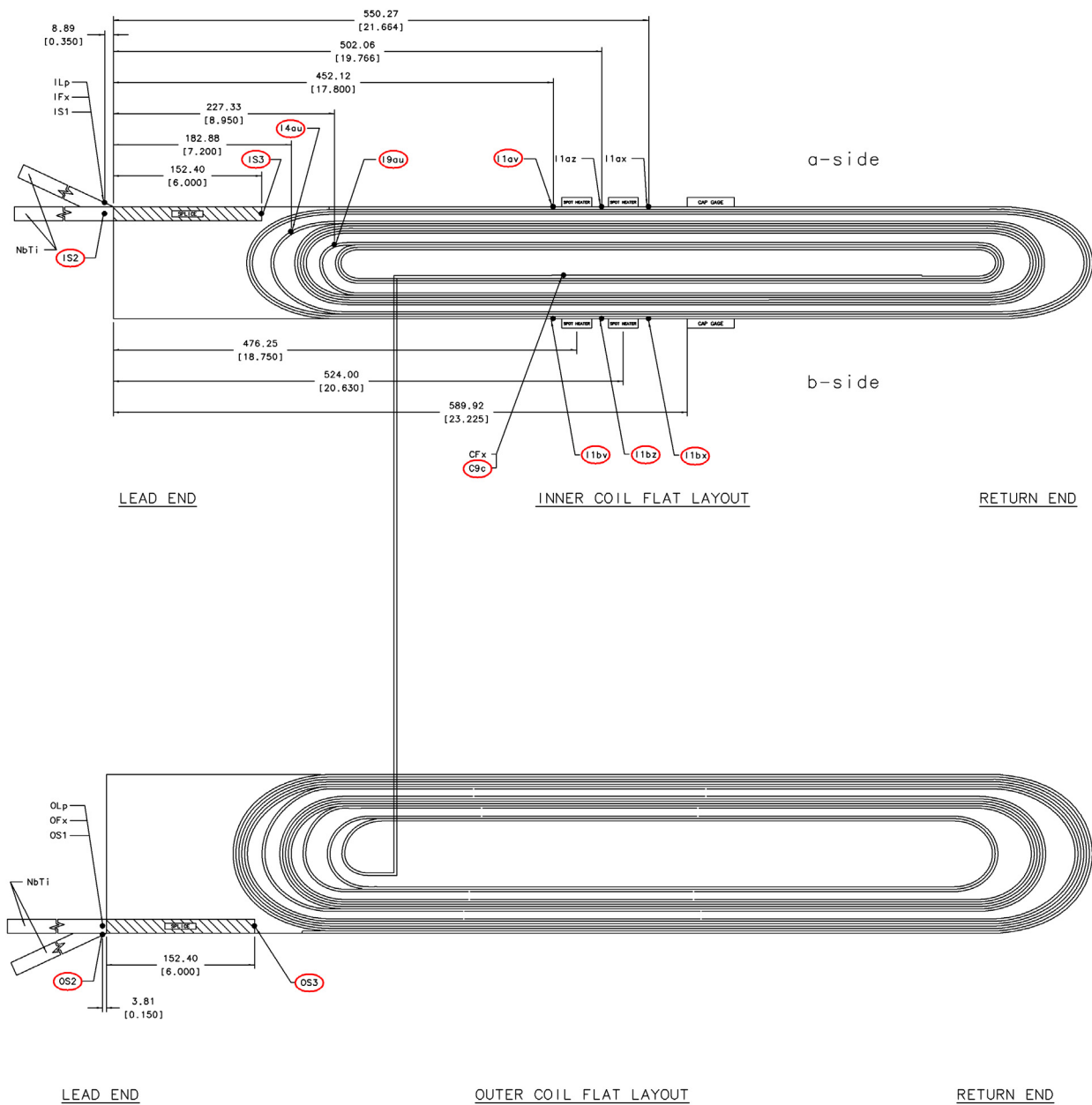


Fig. 9 Voltage Tap Layout of the Magnet HFDM-02 for Inner and Outer Coils

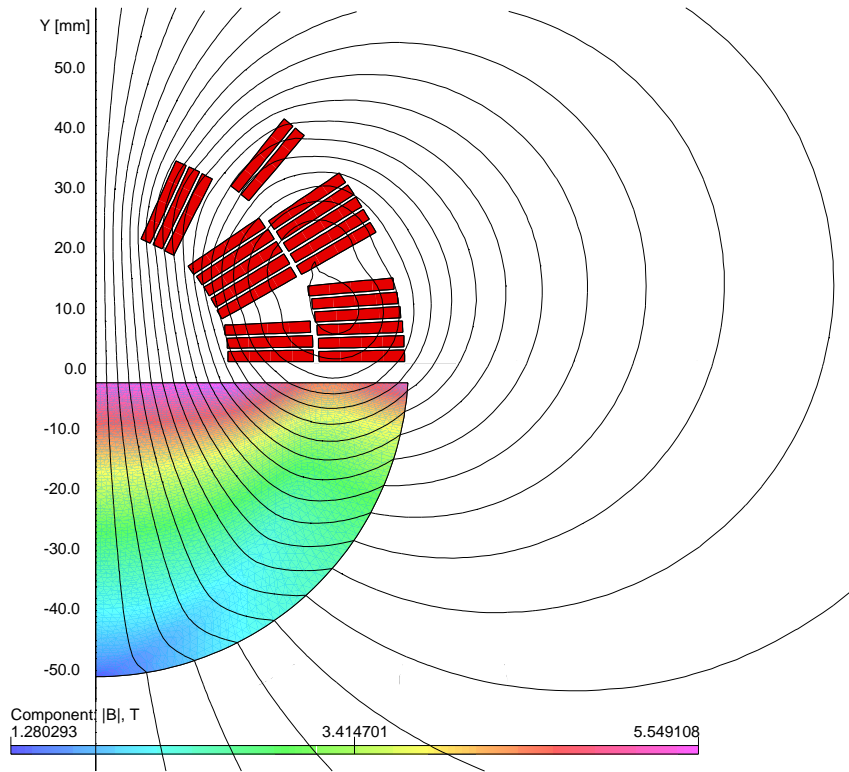


Fig. 10: Field in HFDM02 without iron yoke.

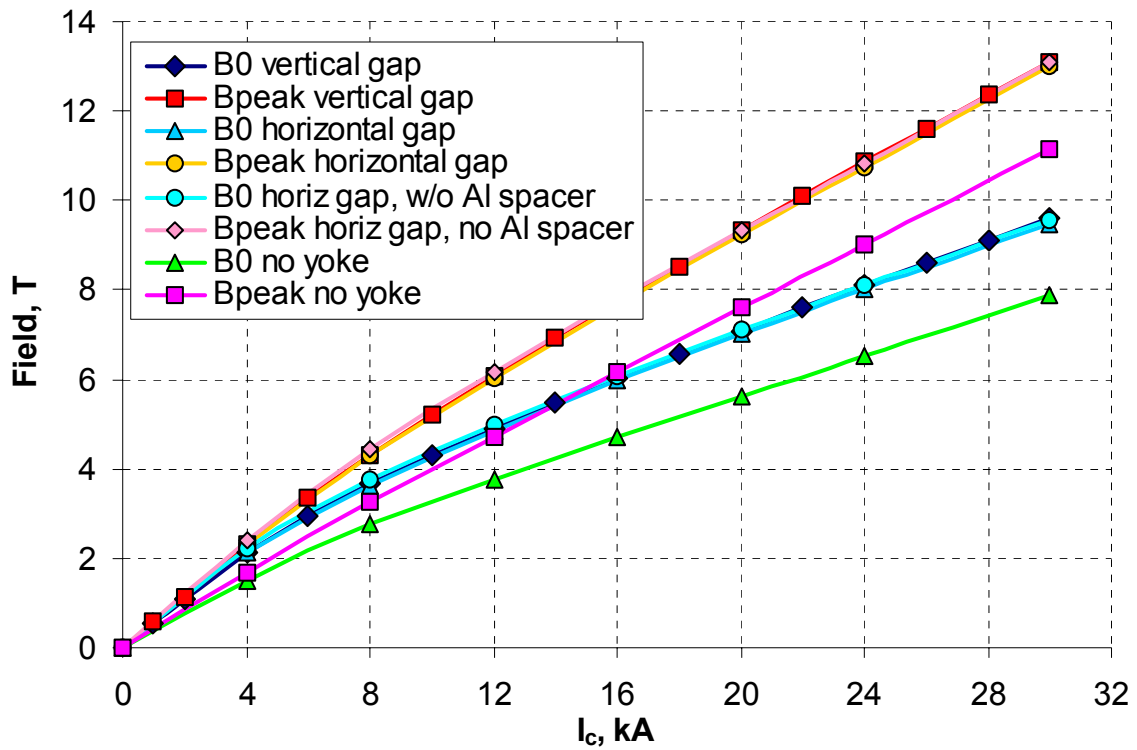


Fig. 11: Load lines on HFDM02.

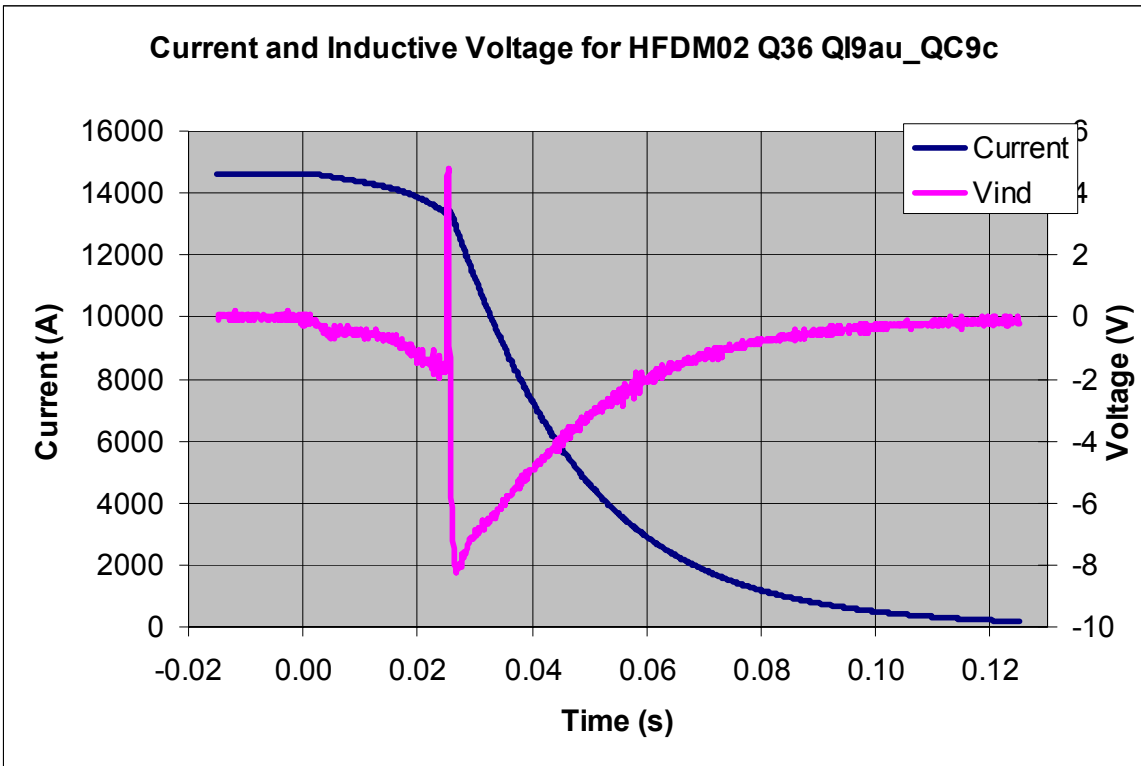


Fig. 12: Magnet current of the HFDM02 and the inductive voltage across the innermost three turn coil are shown for the Quench event #36. Quench started at -3 ms.

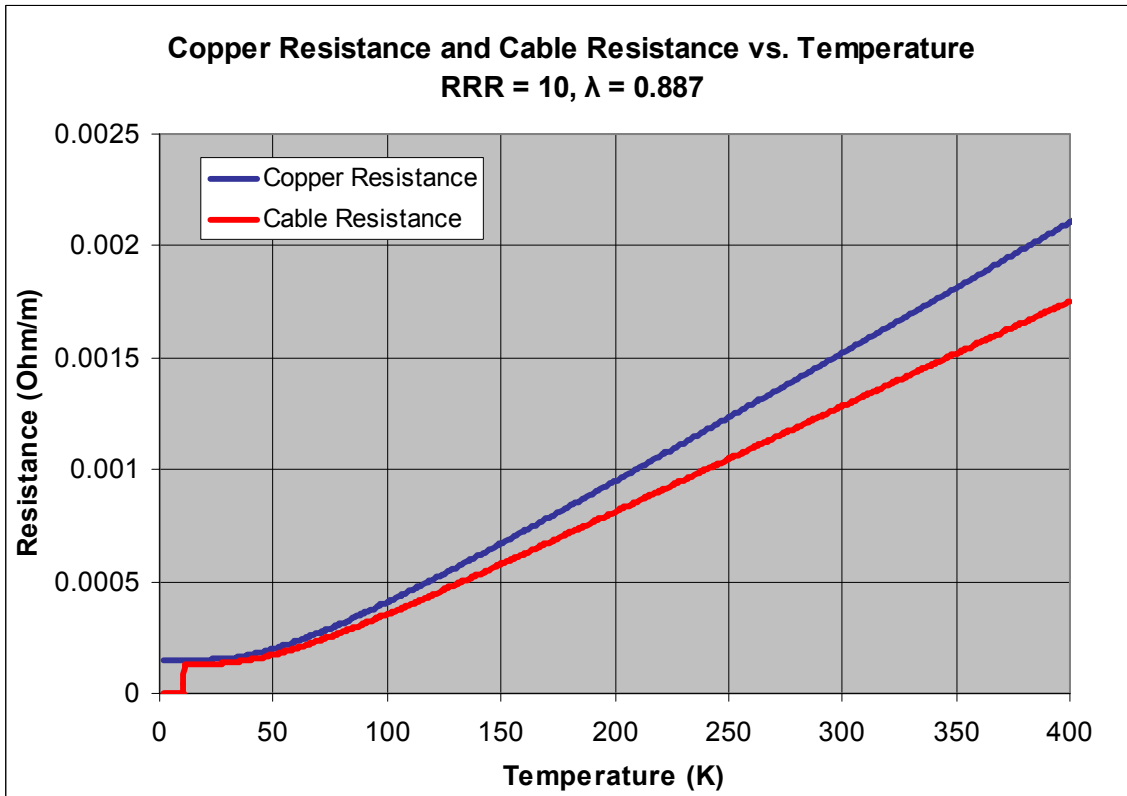


Fig. 13: Resistance of copper and resistance of the Nb₃Sn cable per meter vs. temperature.

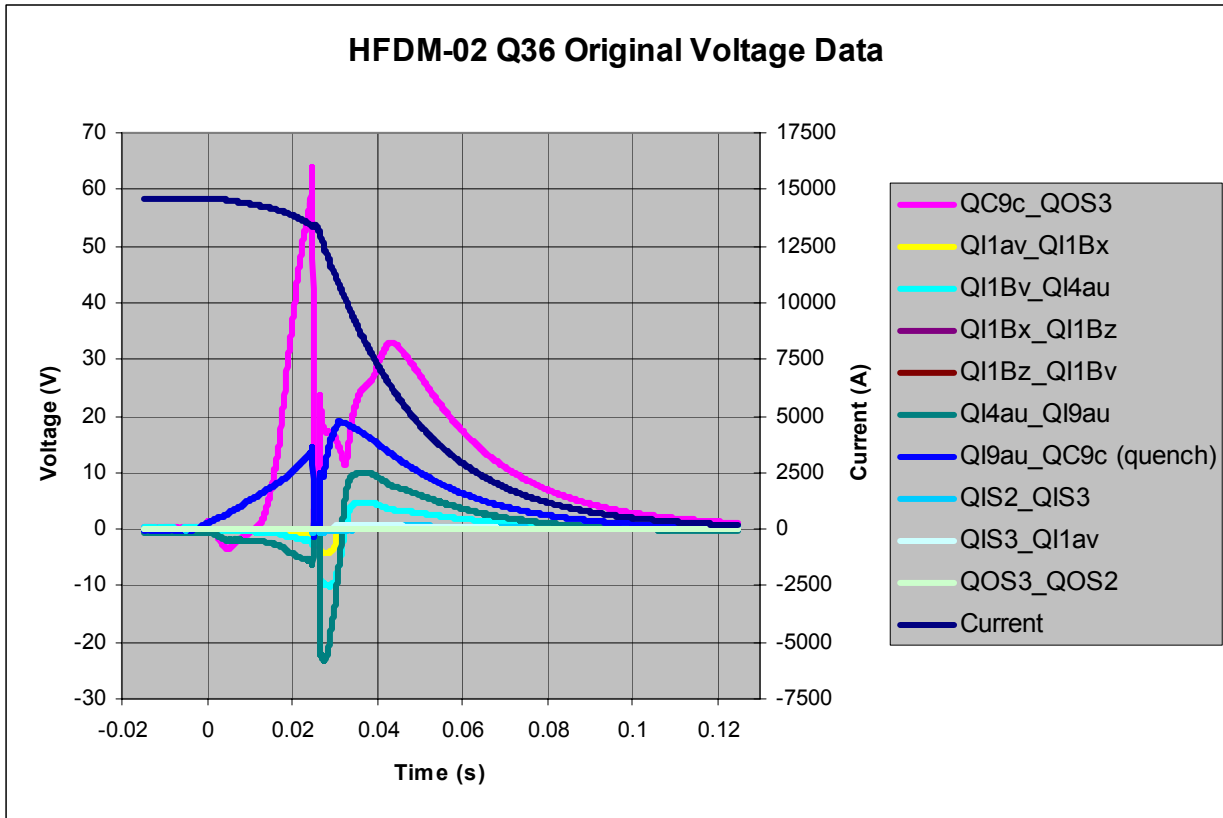


Fig. 14

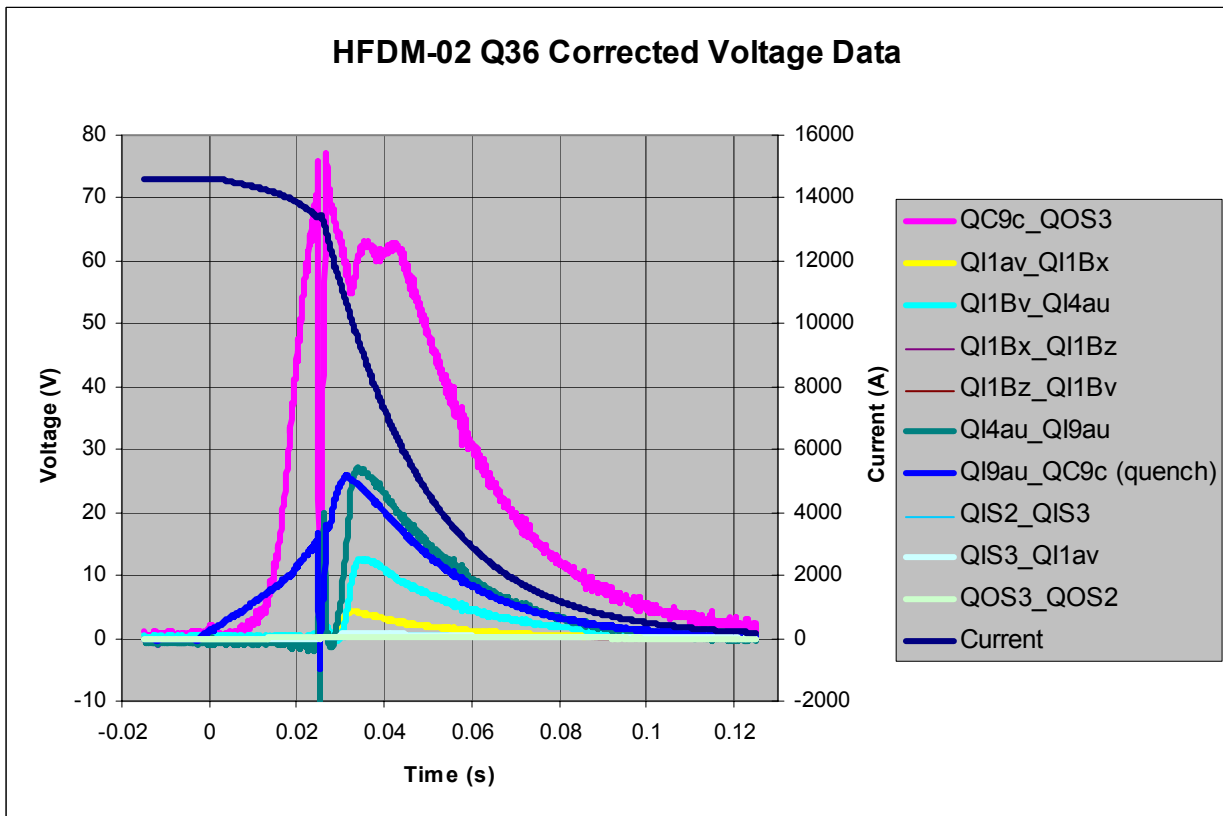


Fig. 15

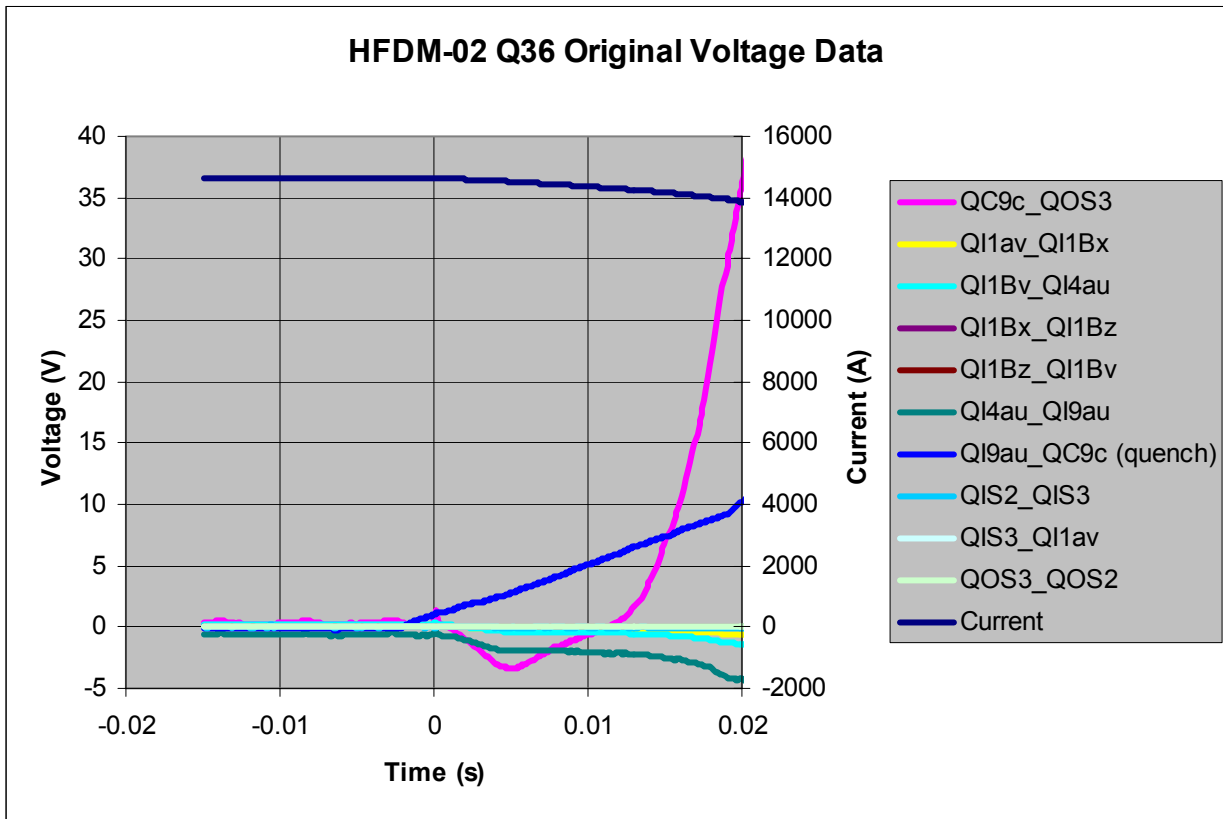


Fig. 16

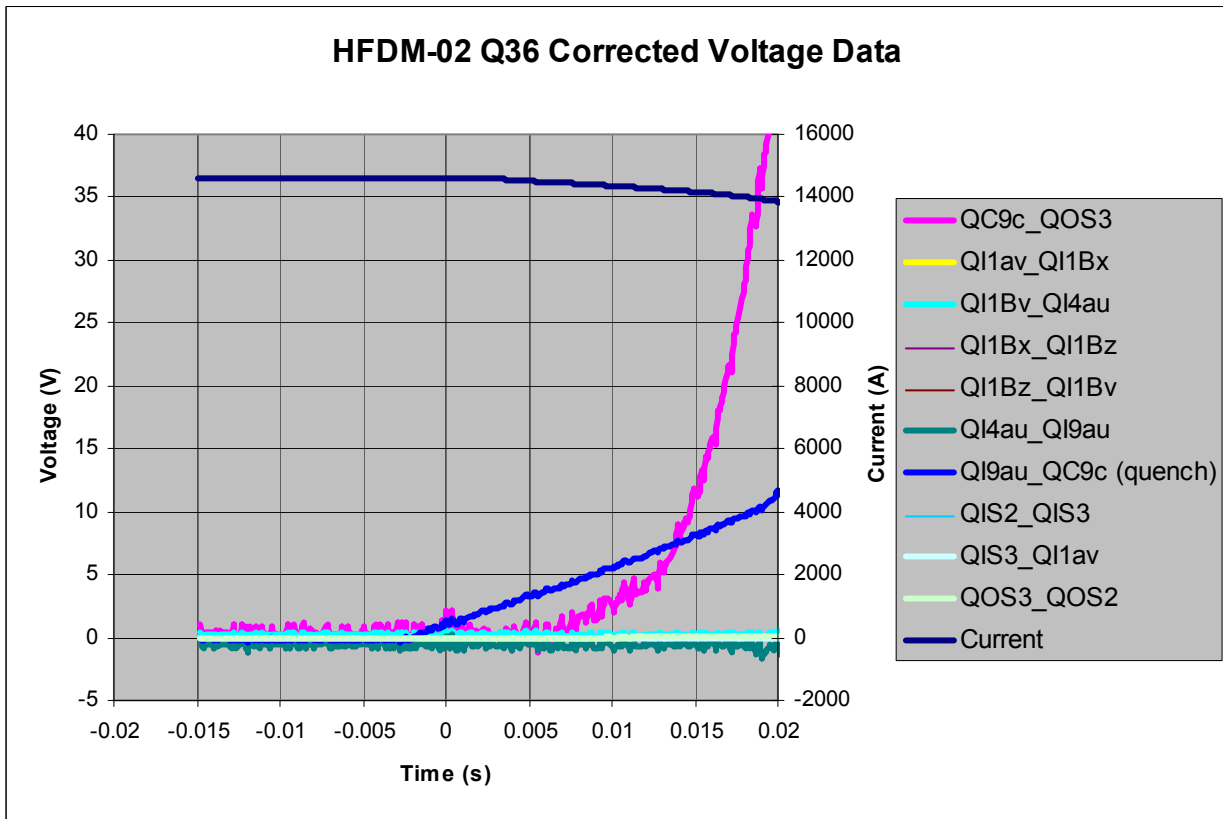


Fig. 17

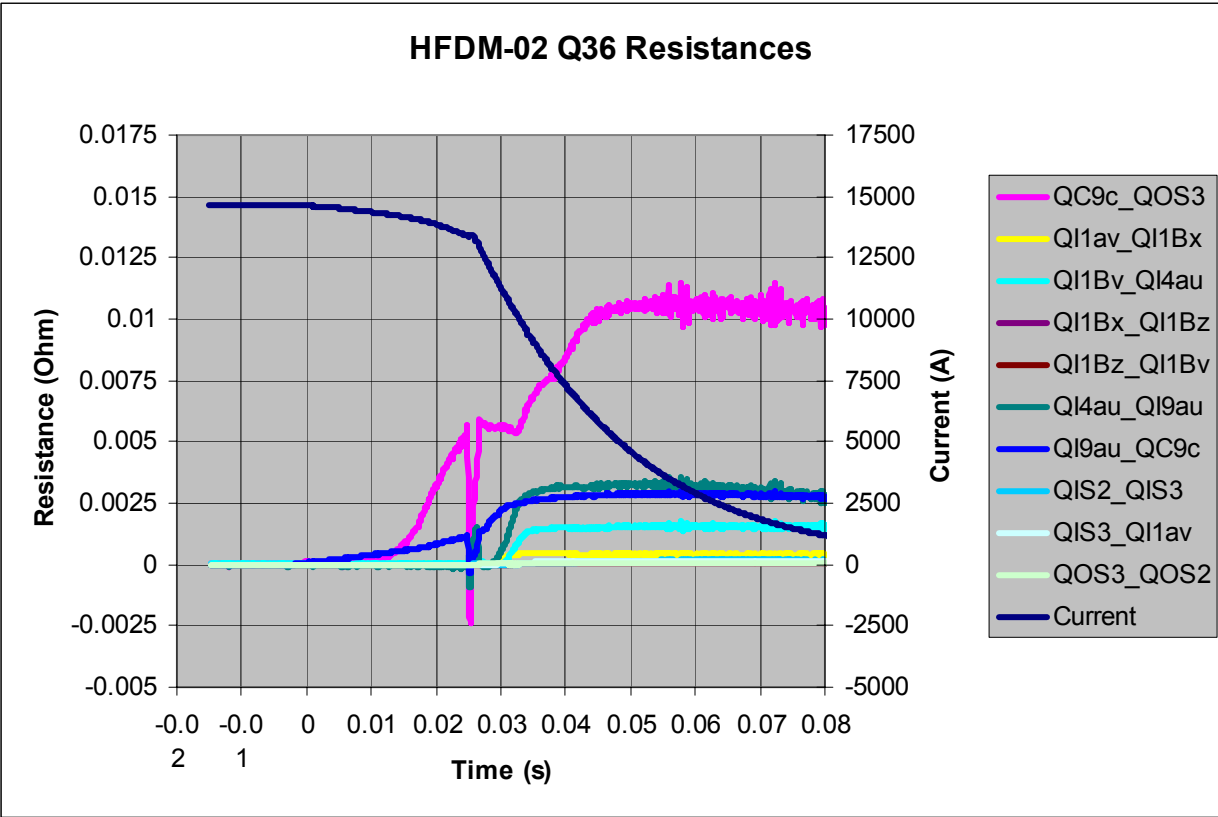


Fig. 18

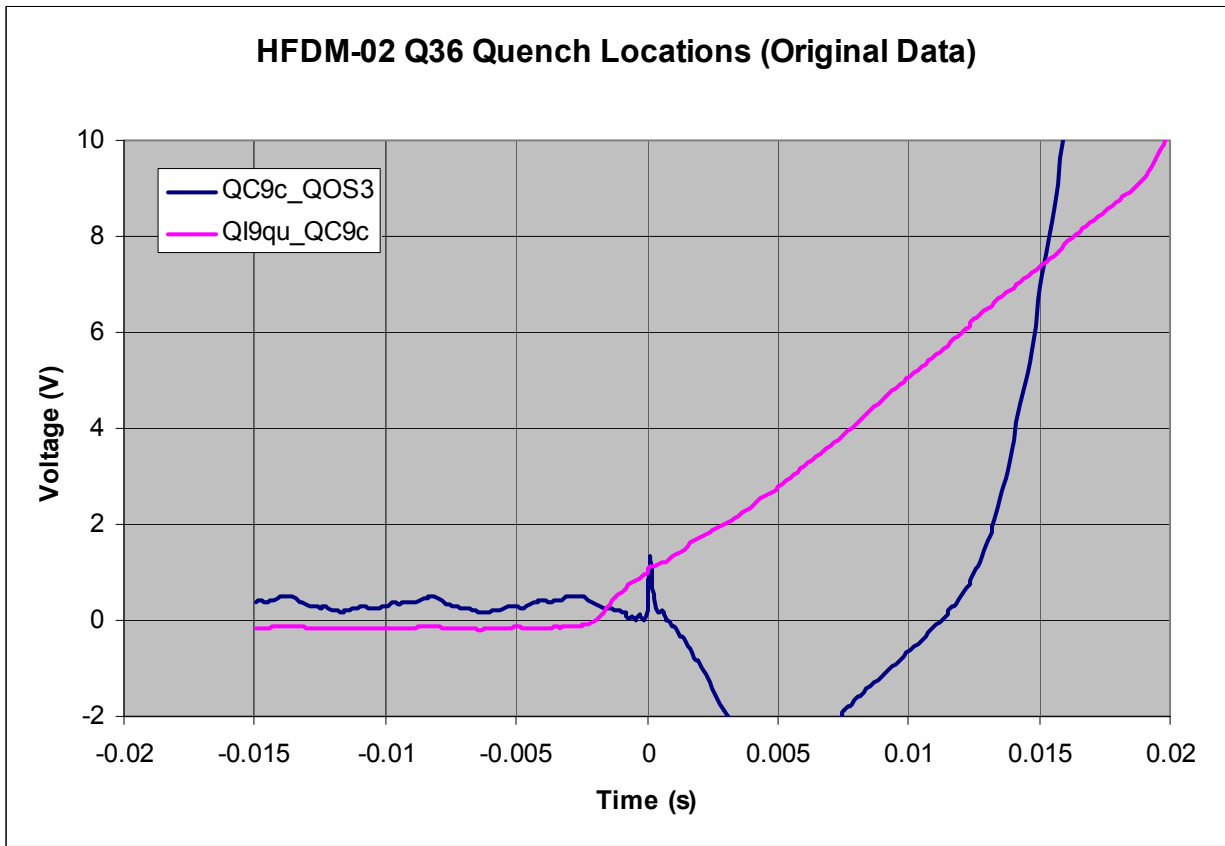


Fig. 19

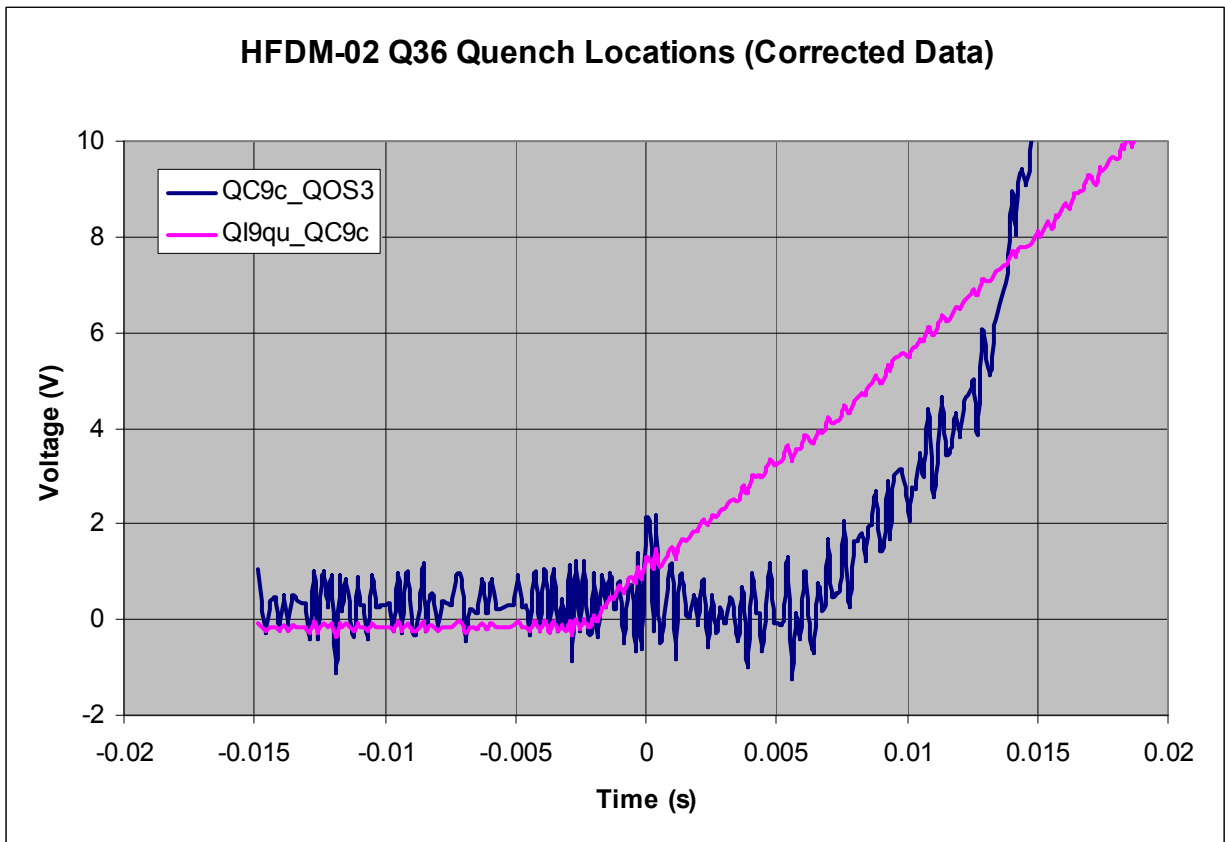


Fig. 20

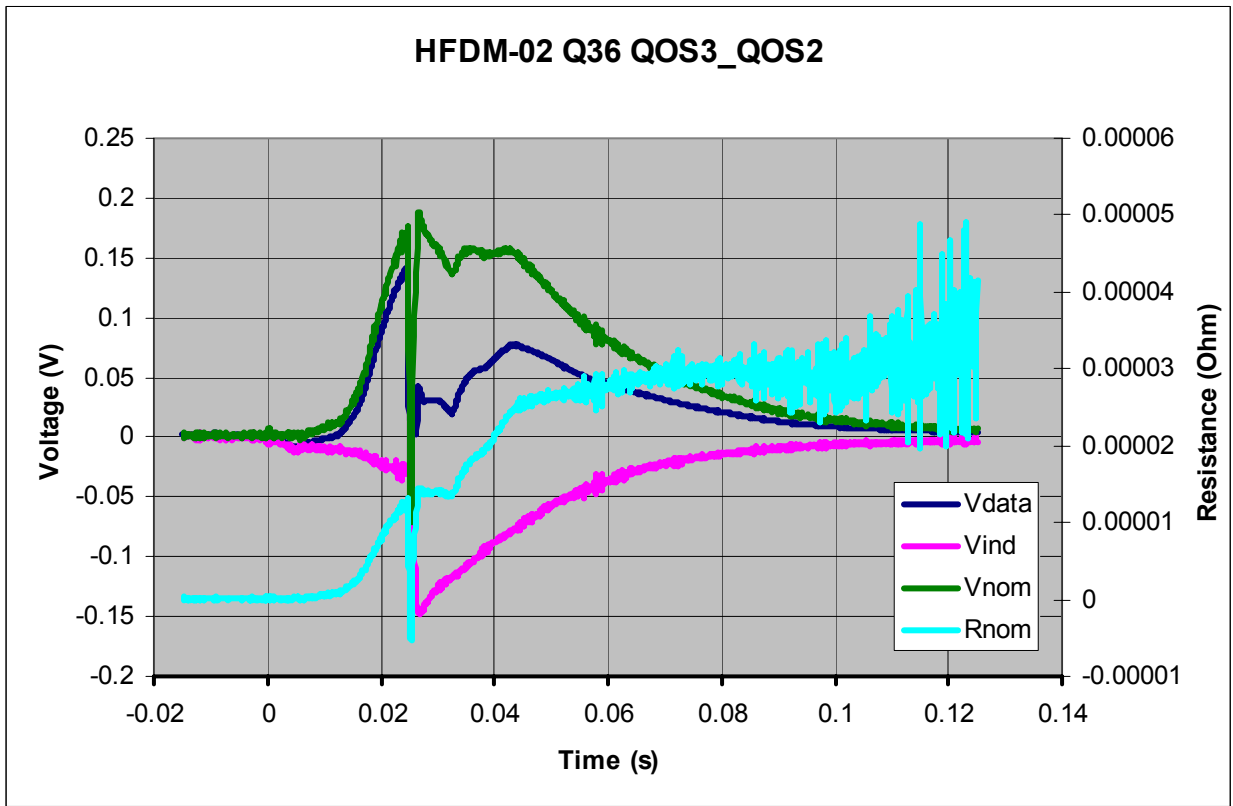


Fig. 21

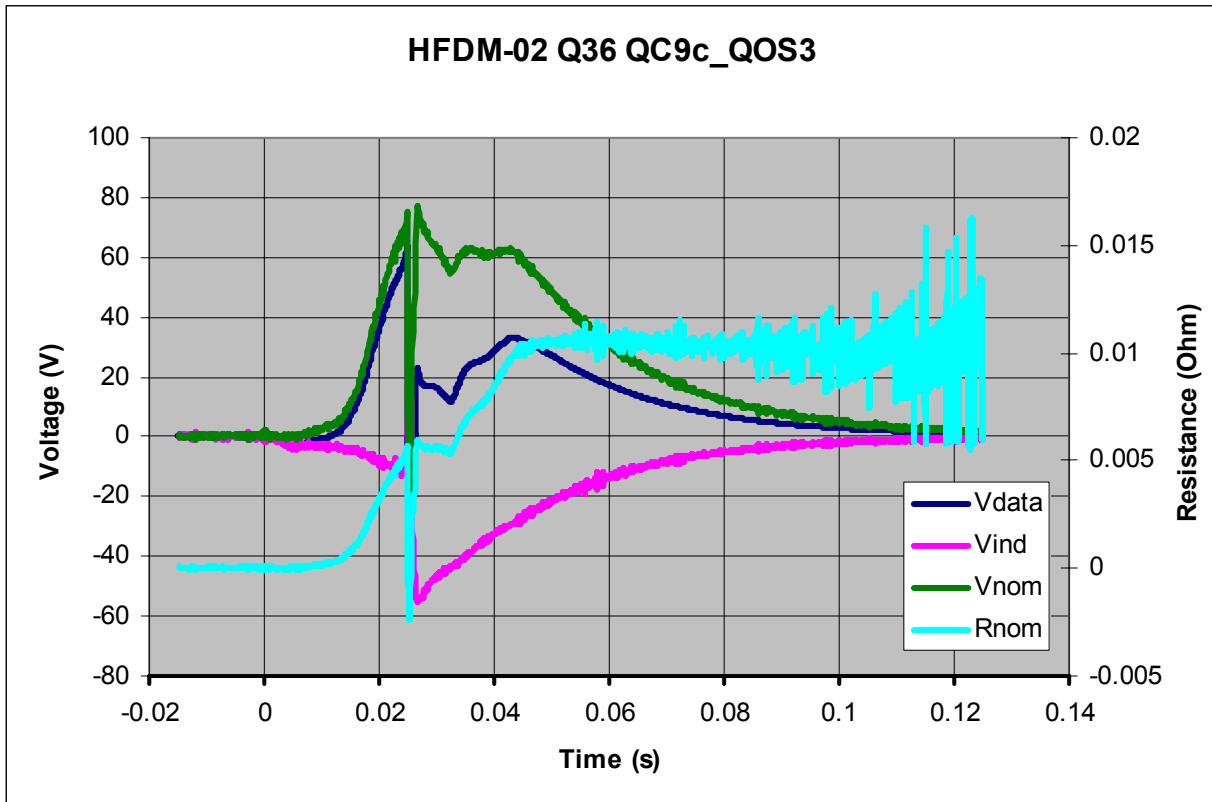


Fig. 22

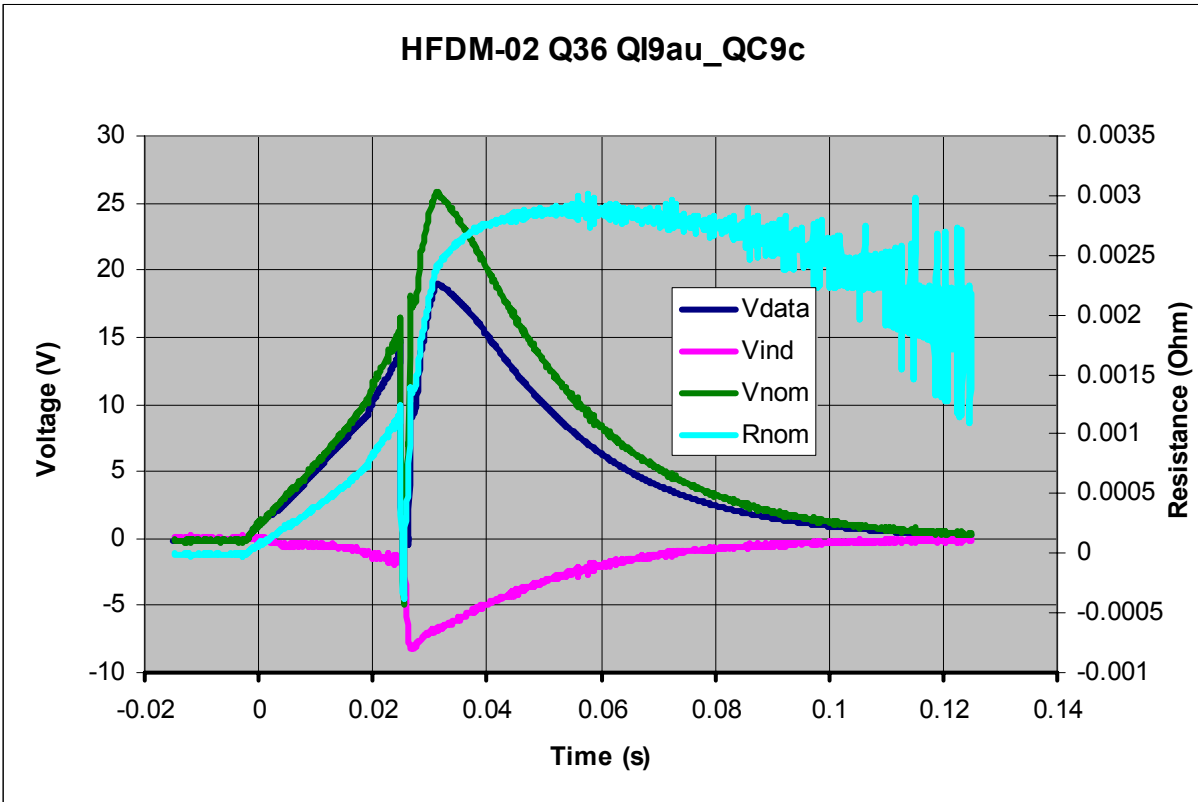


Fig. 23

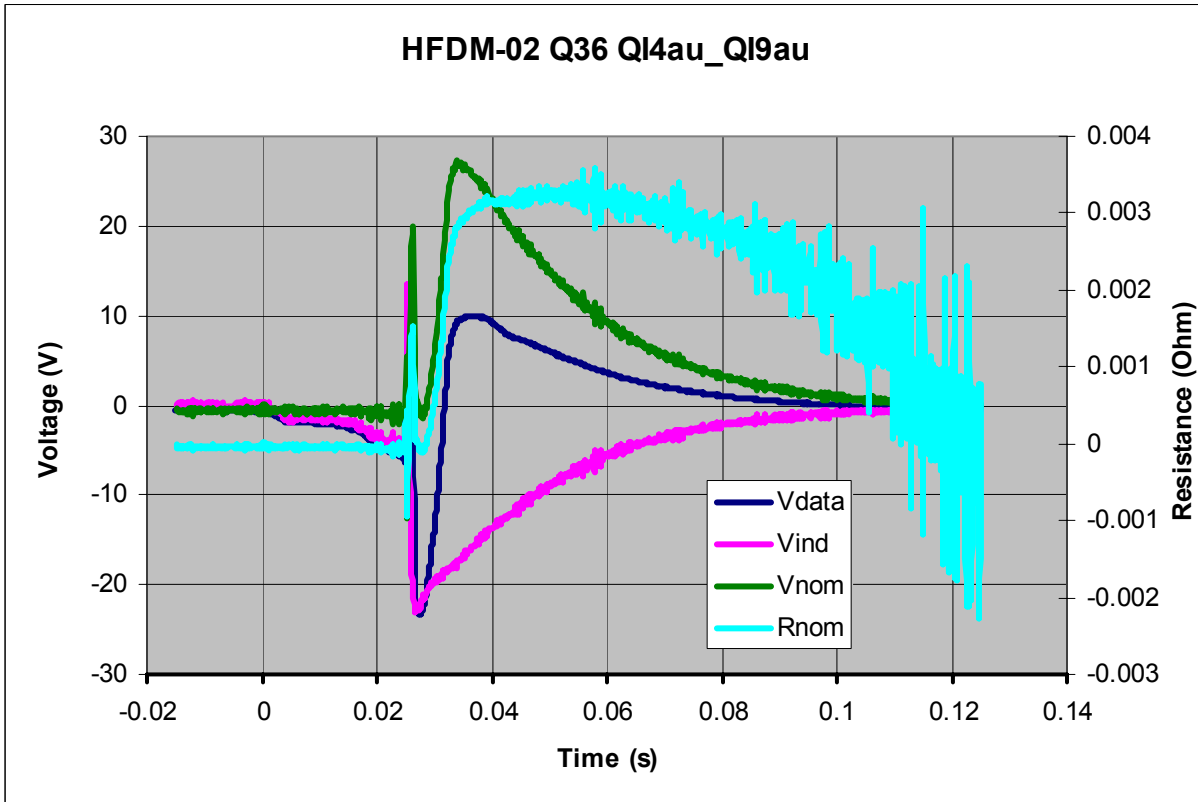


Fig. 24

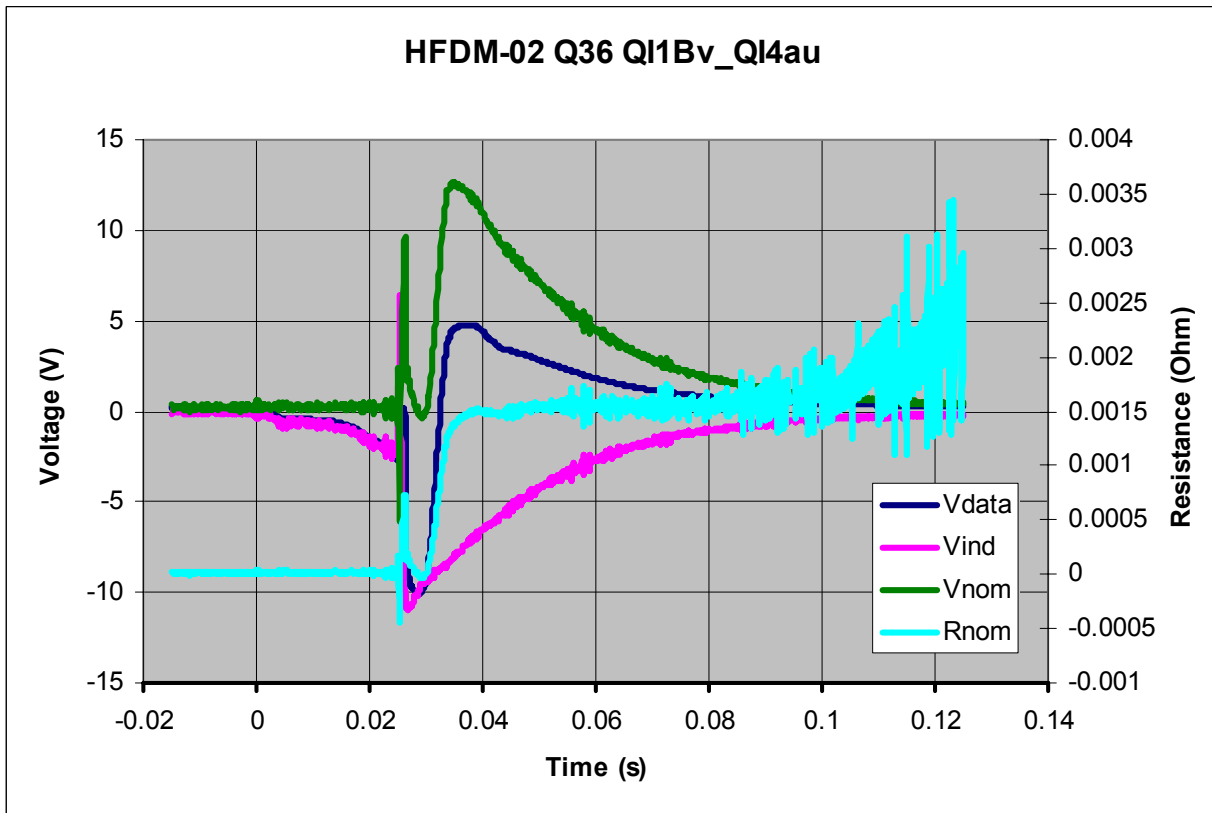


Fig. 25

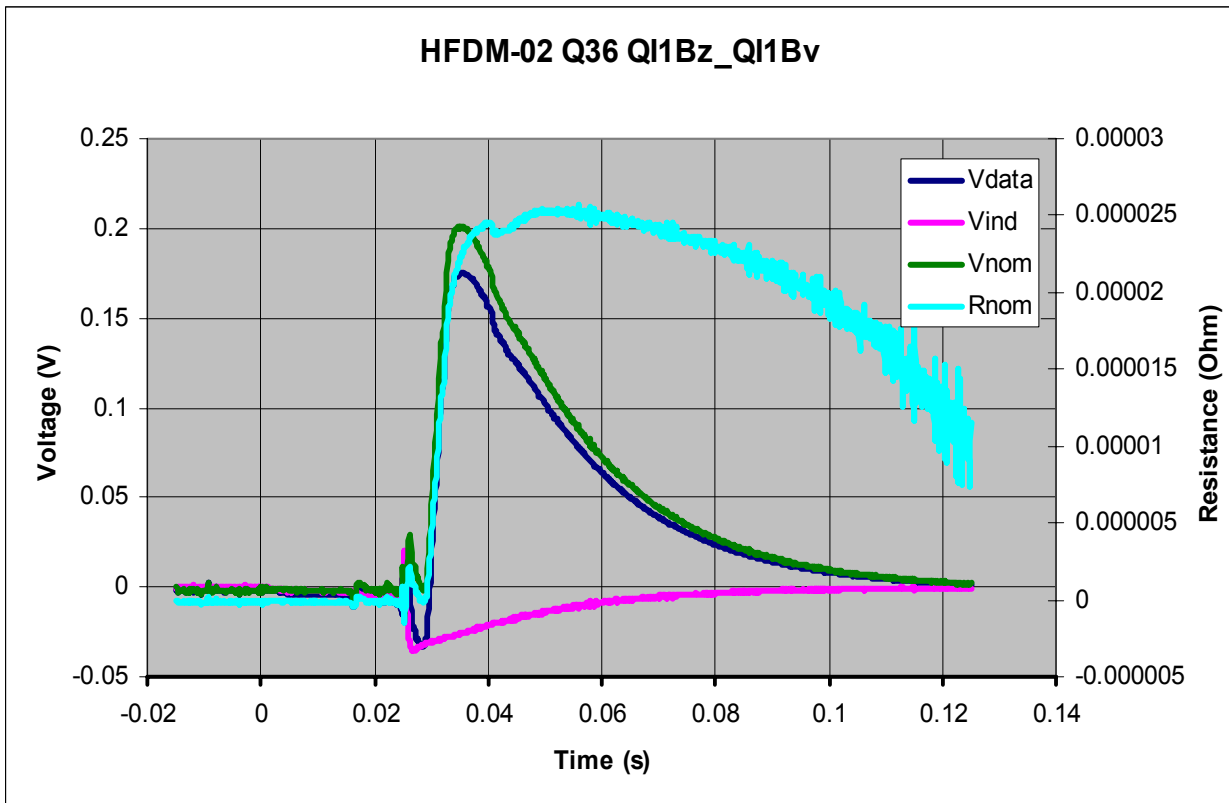


Fig. 26

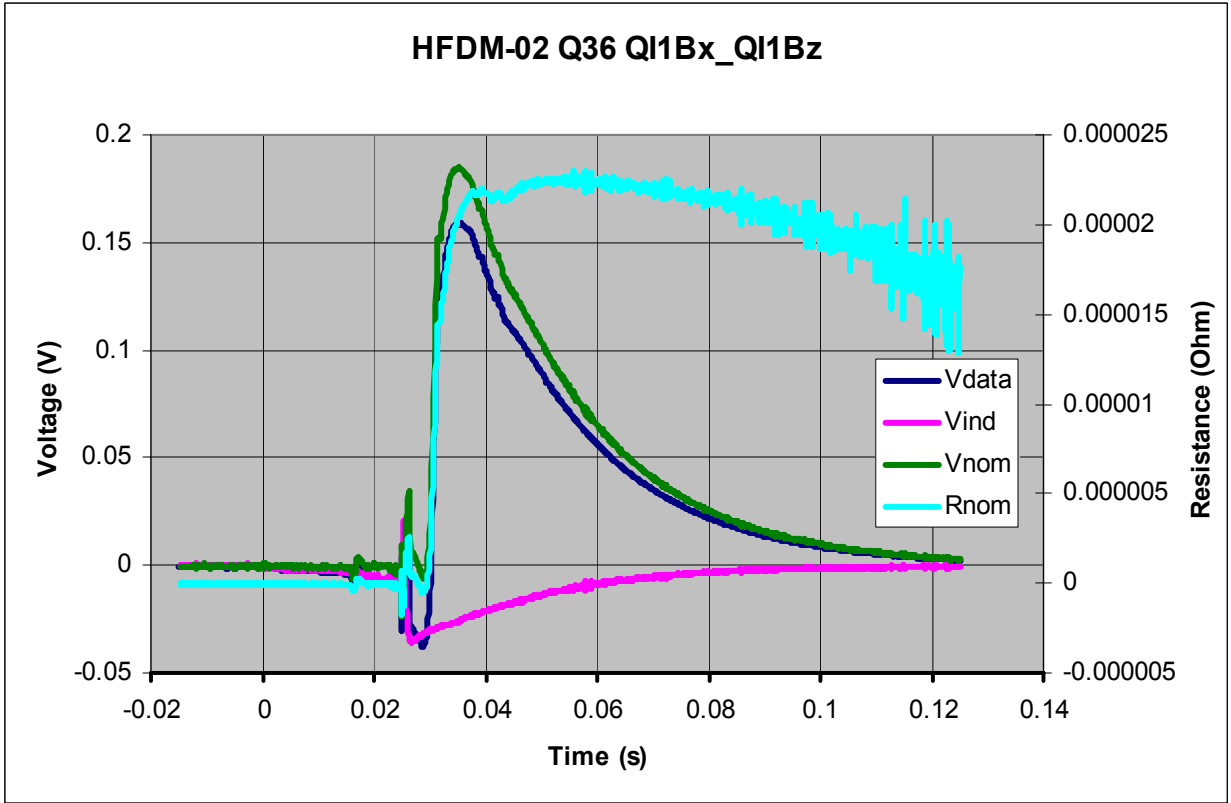


Fig. 27

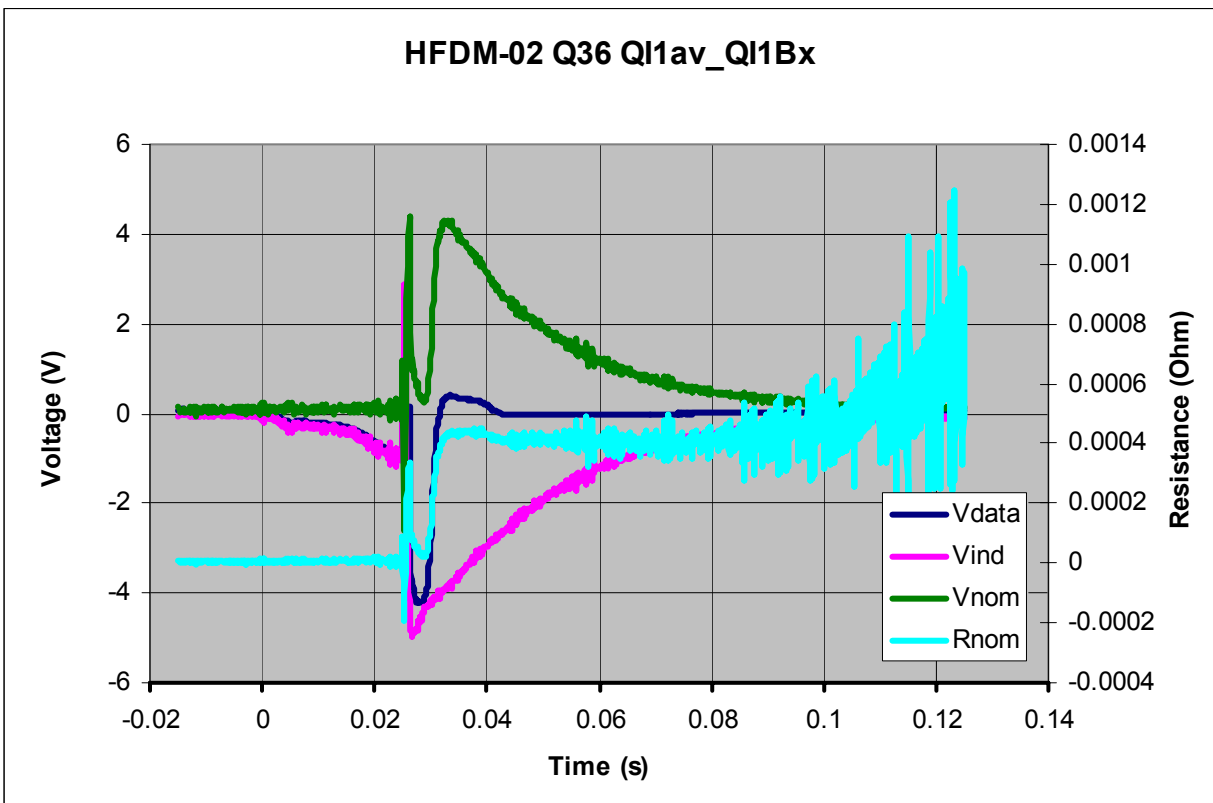


Fig. 28

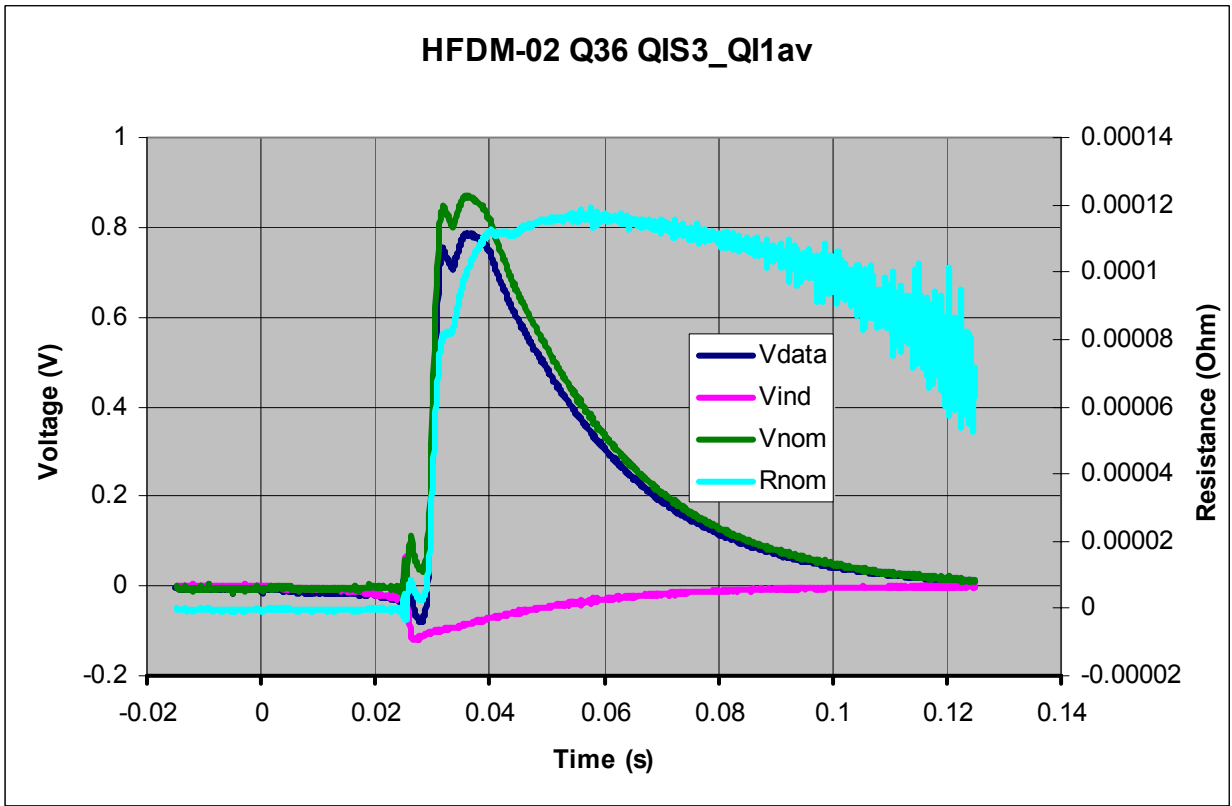


Fig. 29

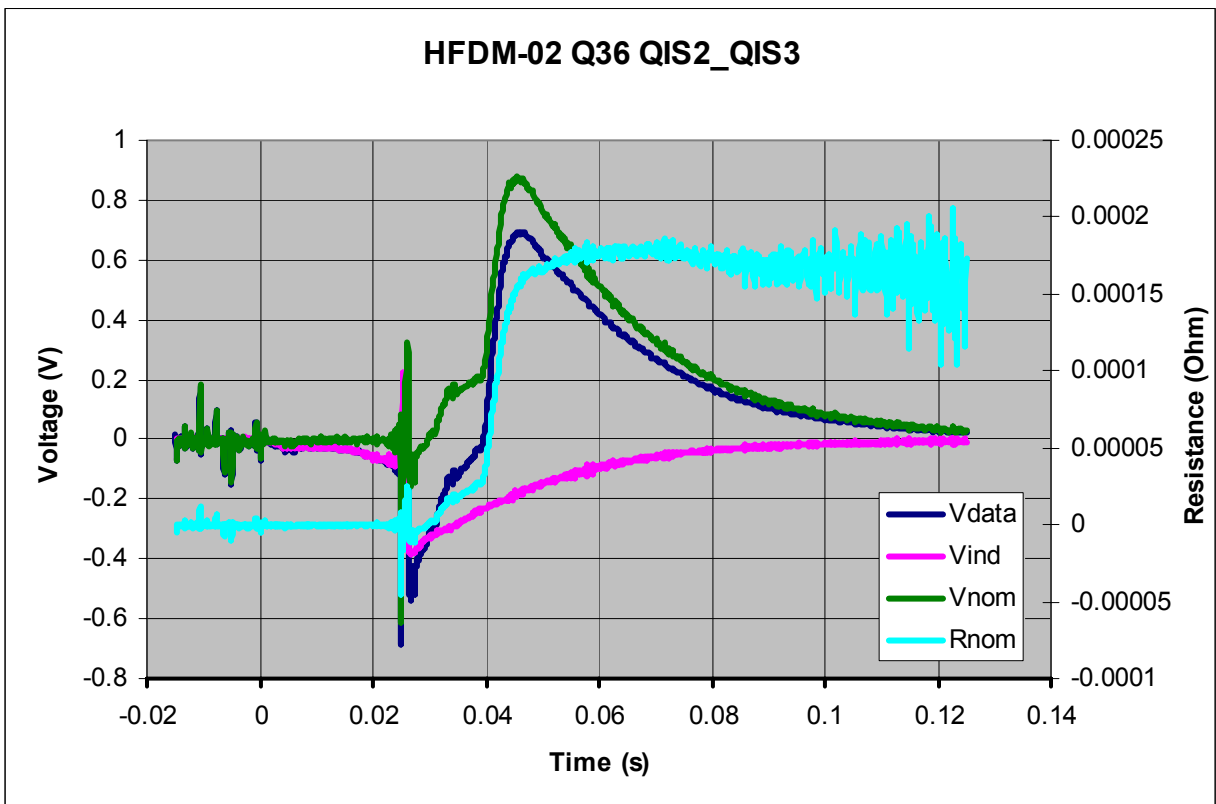


Fig. 30

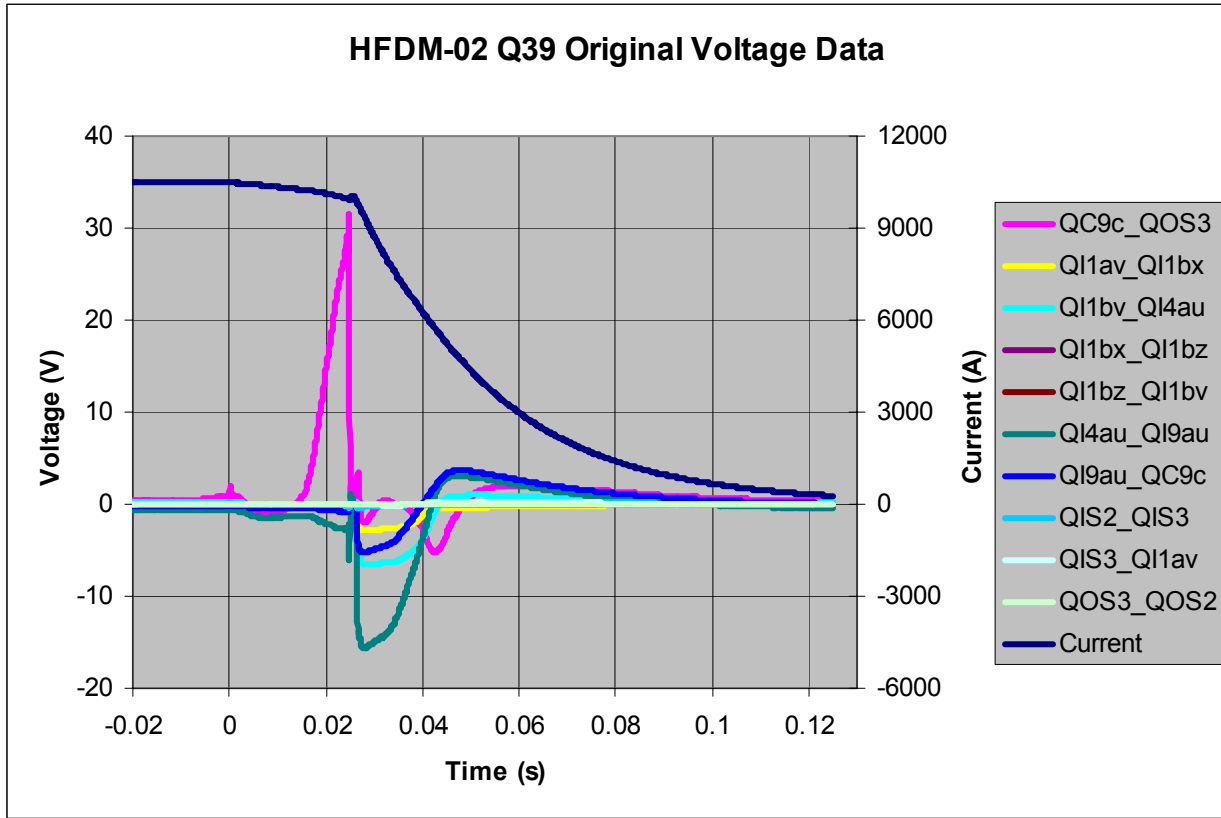


Fig. 31

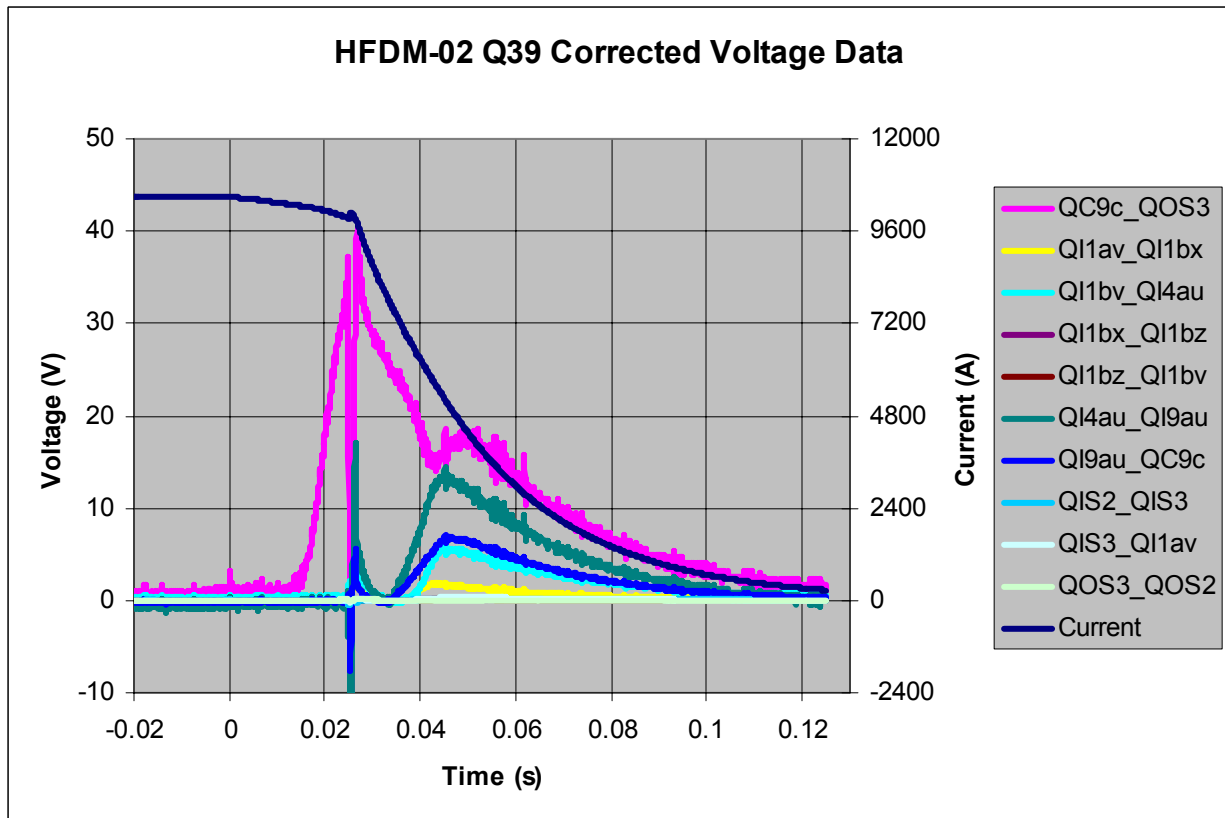


Fig. 32

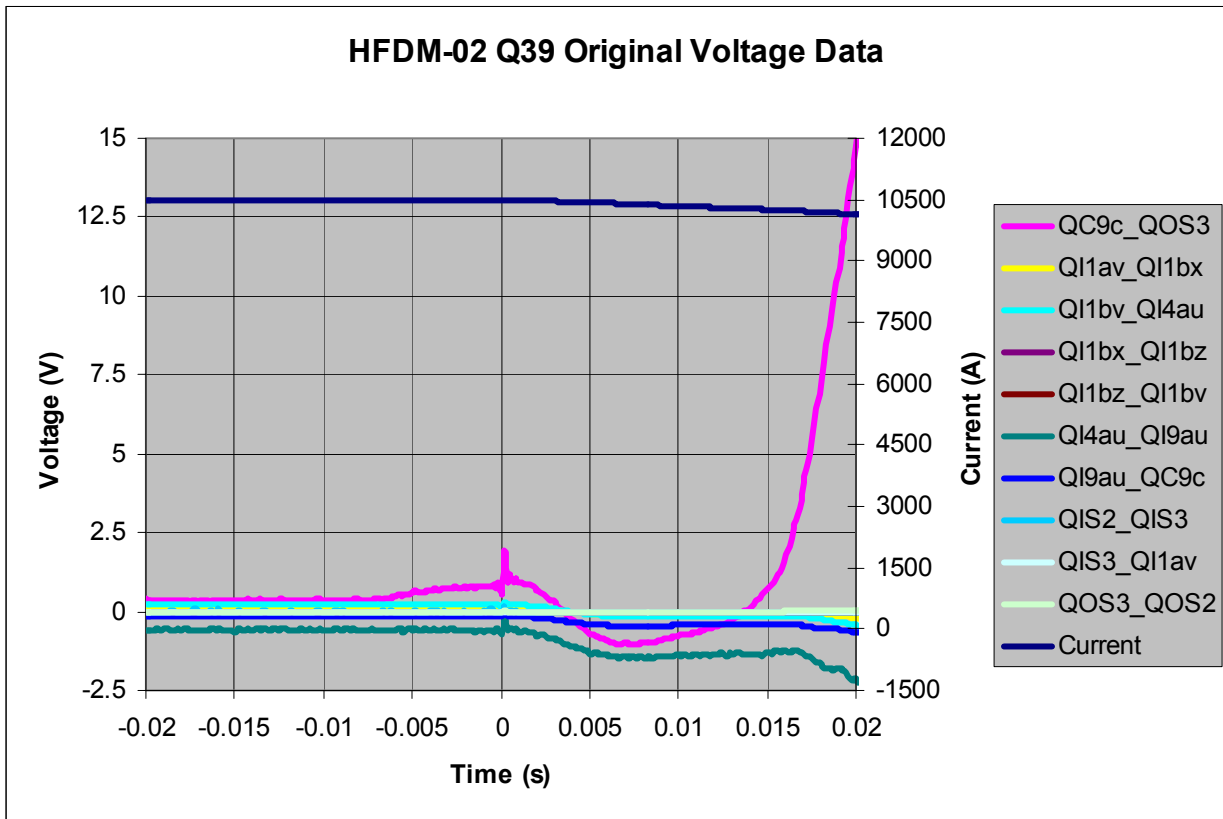


Fig. 33

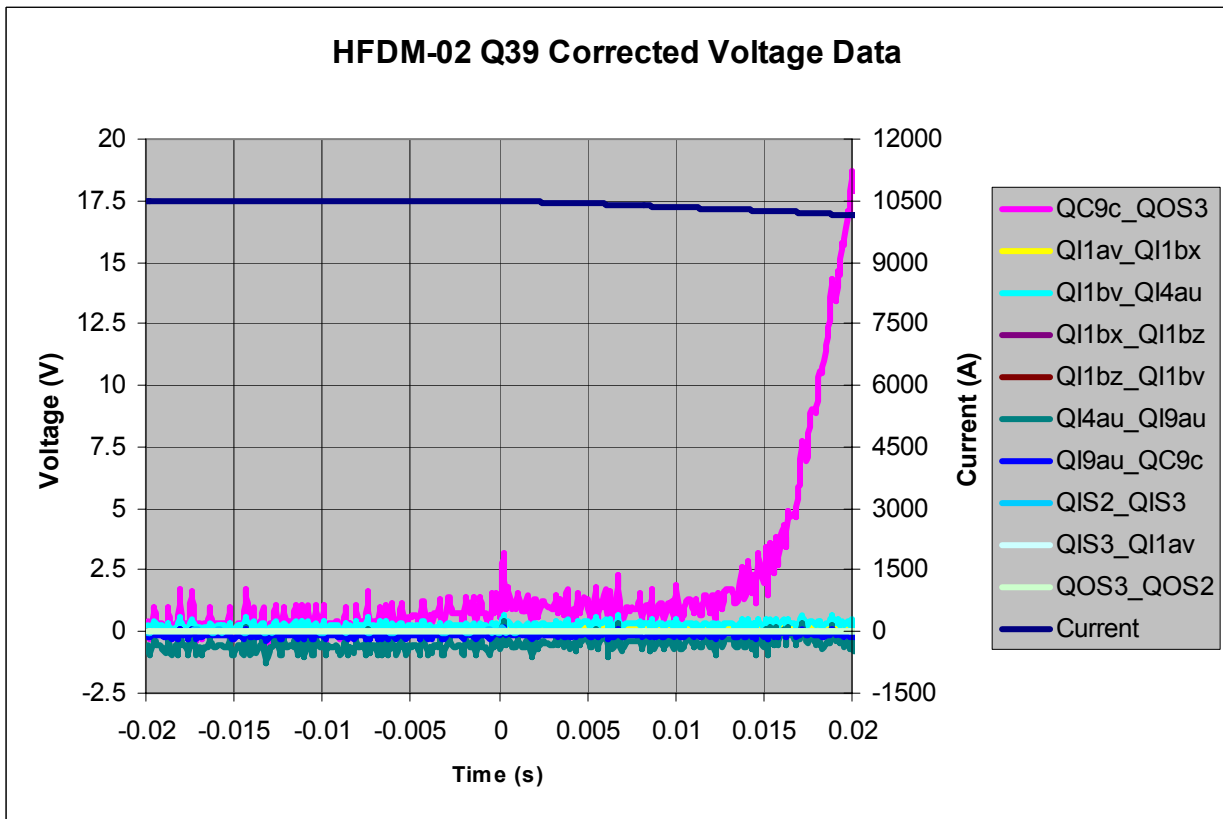


Fig. 34

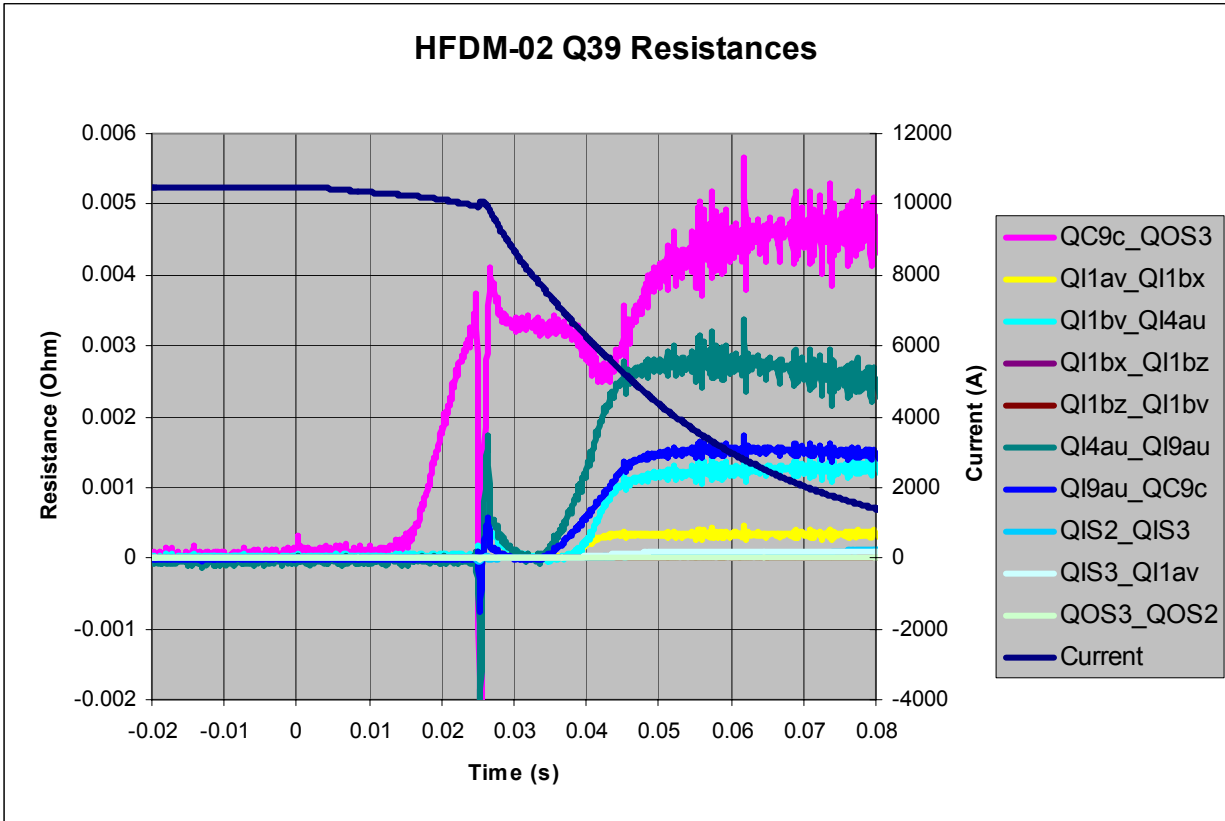


Fig. 35

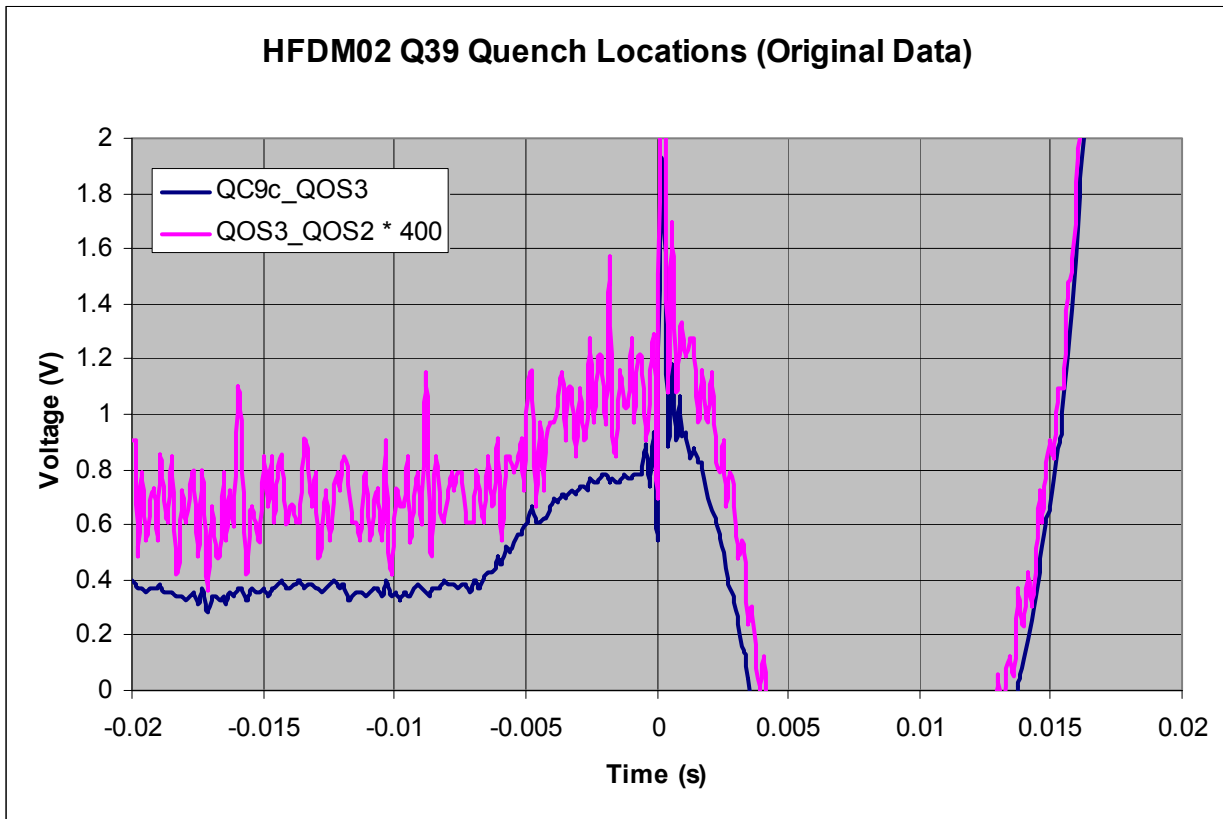


Fig. 36

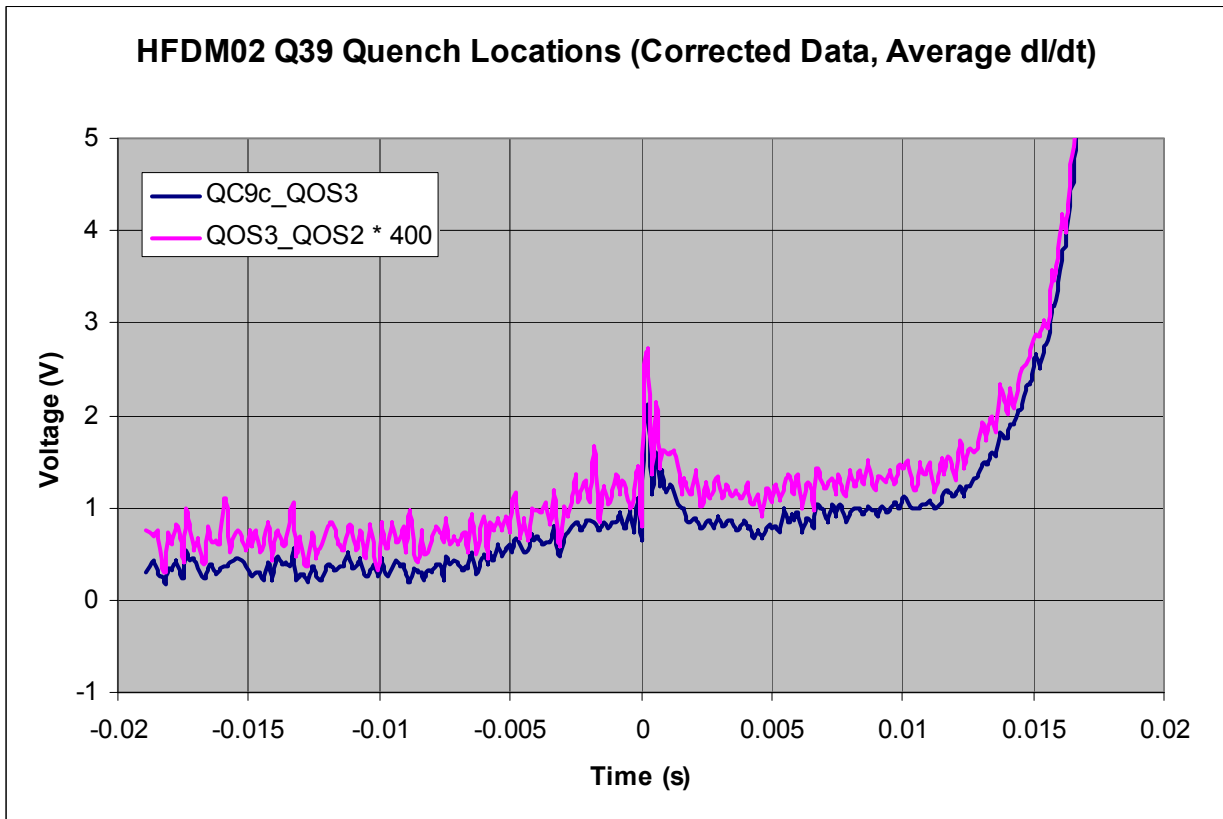


Fig. 37

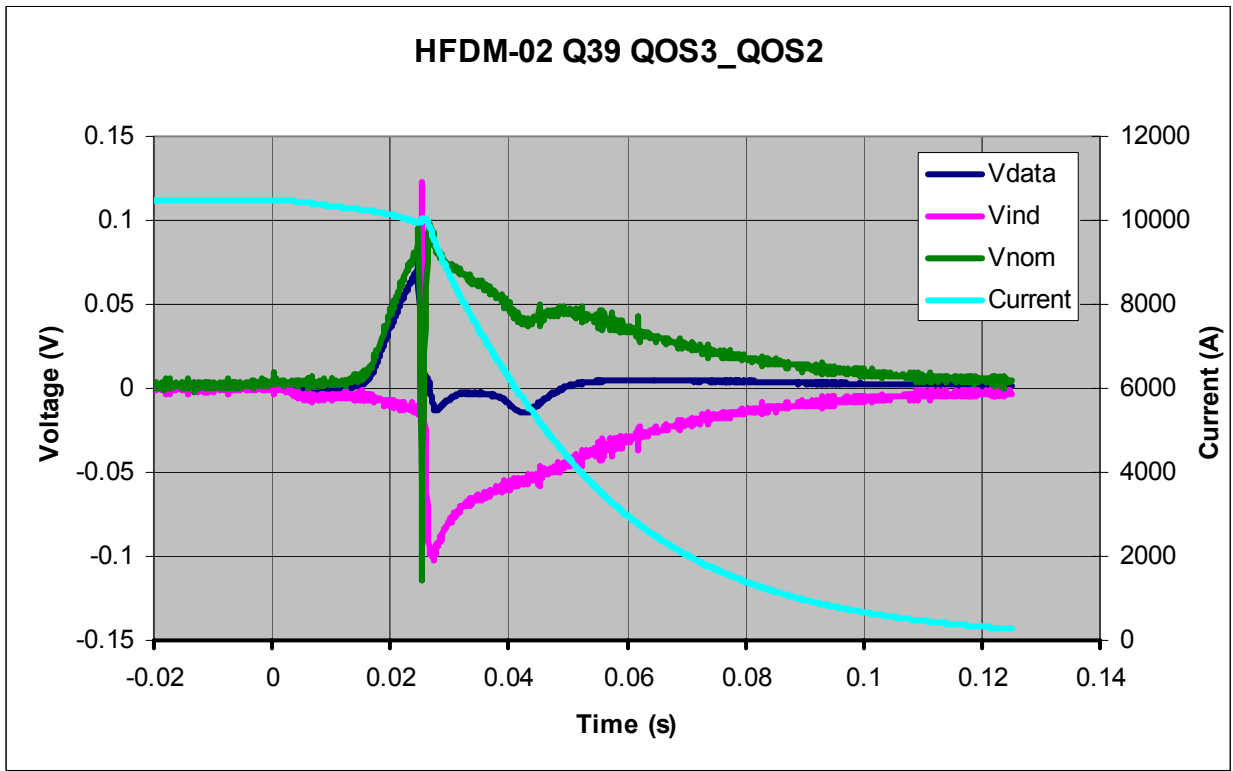


Fig. 38

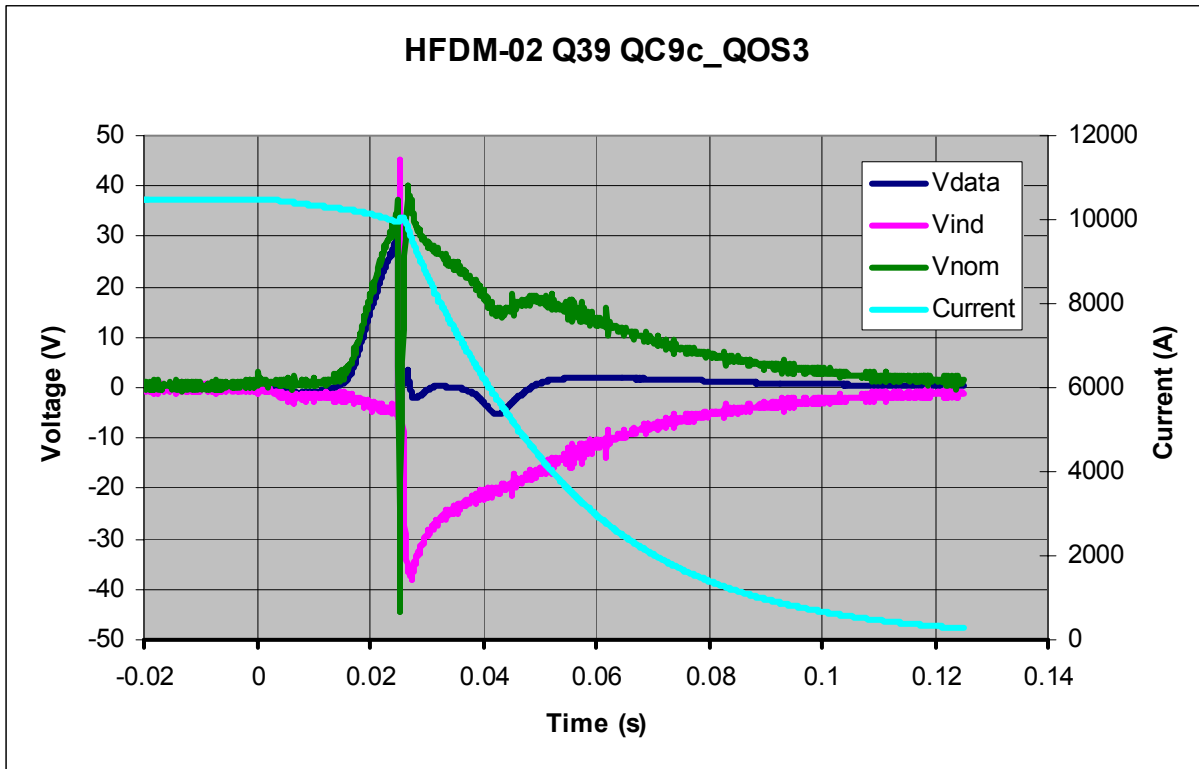


Fig. 39

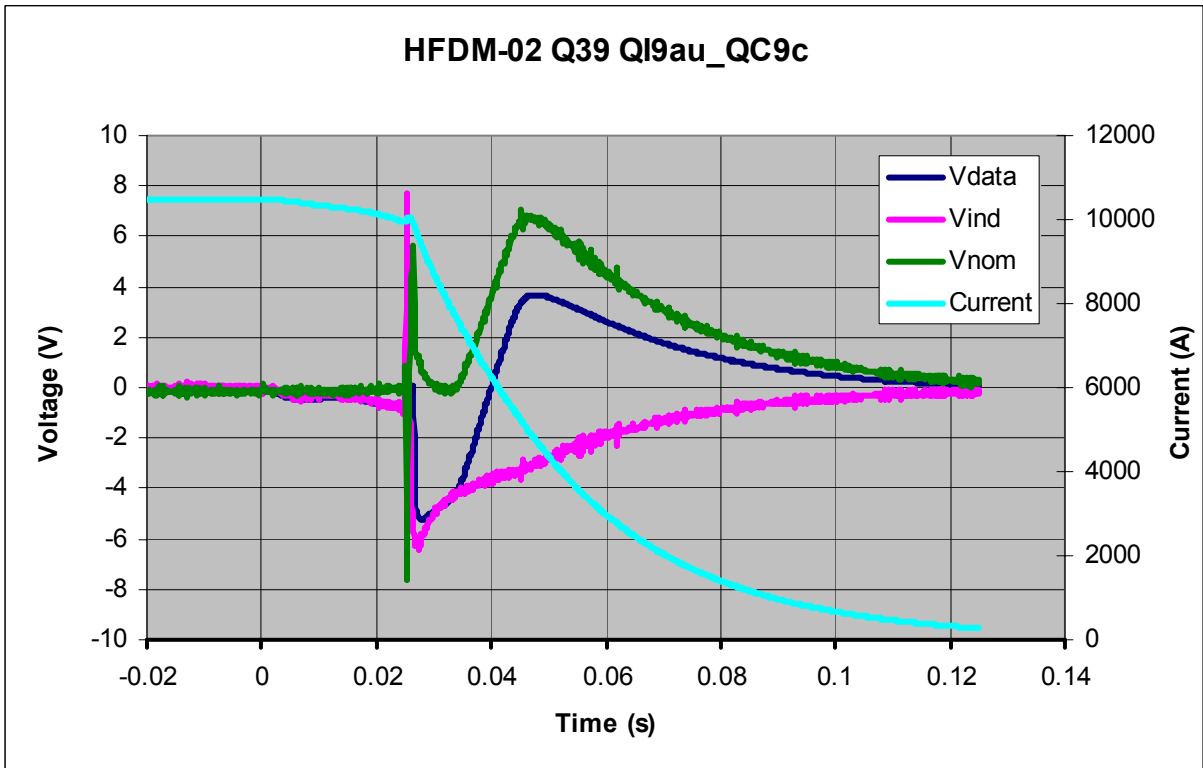


Fig. 40

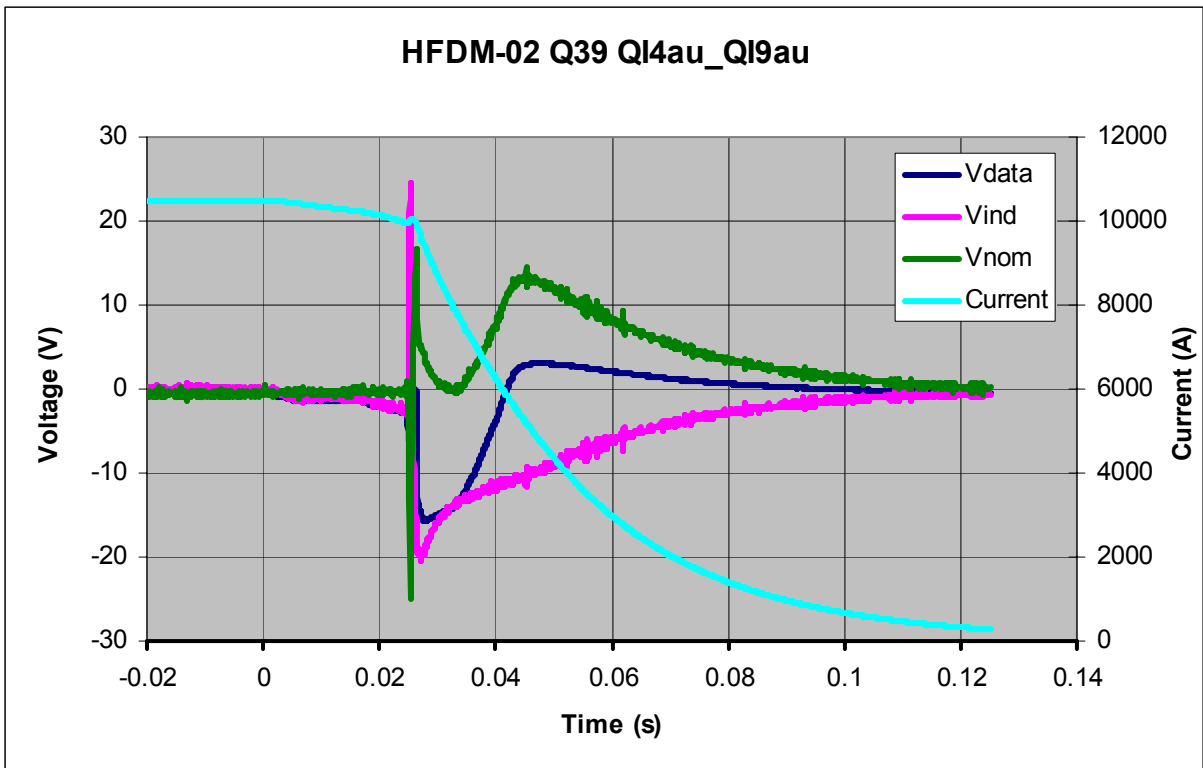


Fig. 41

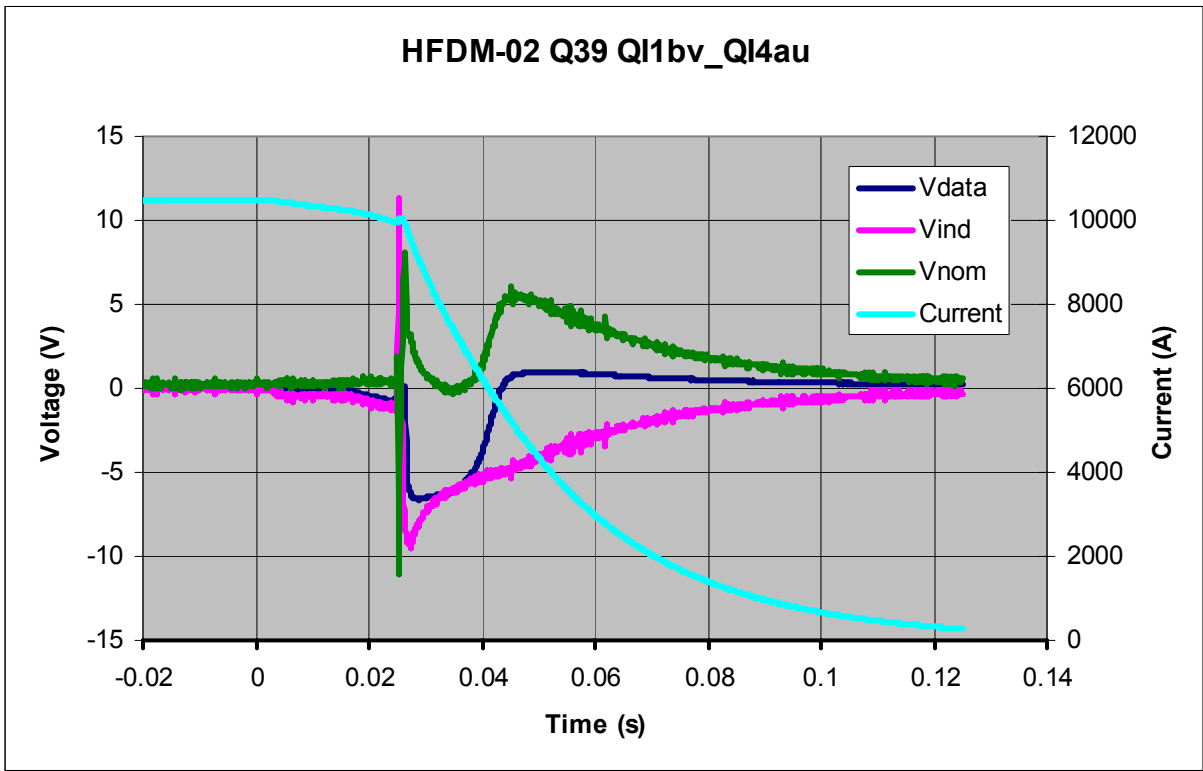


Fig. 42

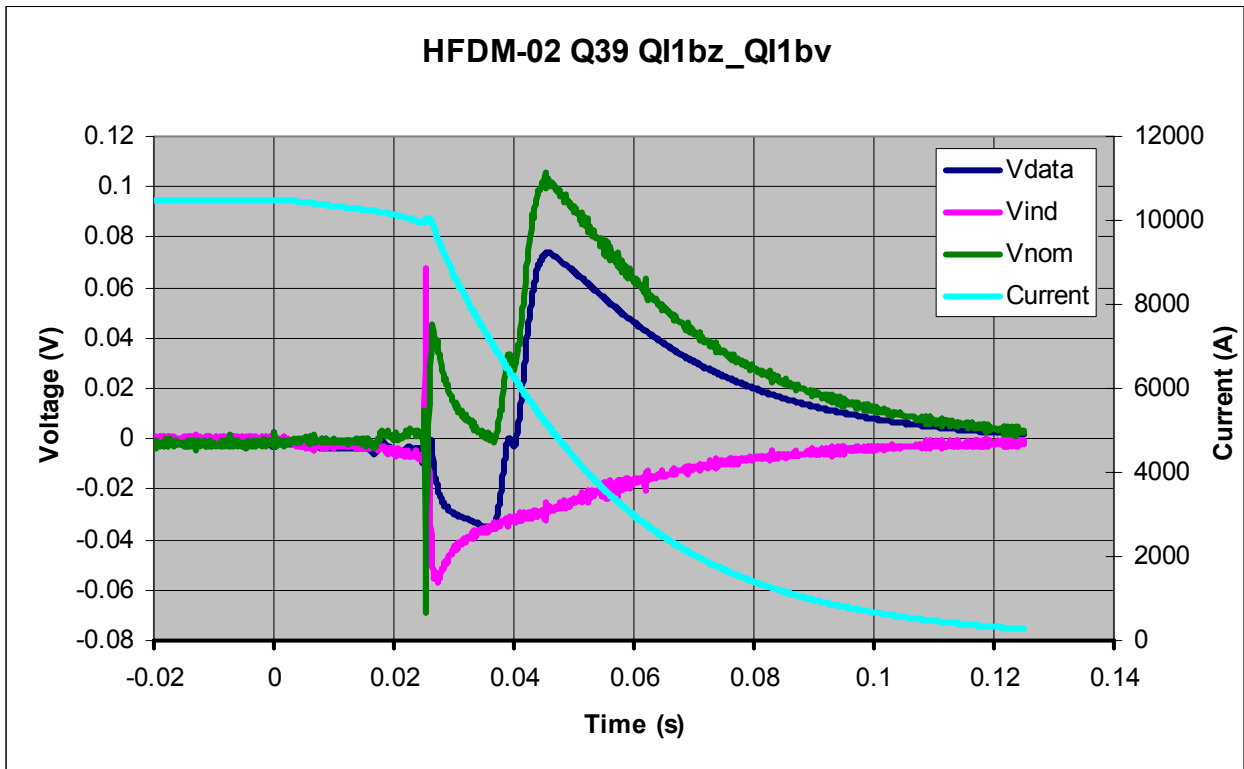


Fig. 43

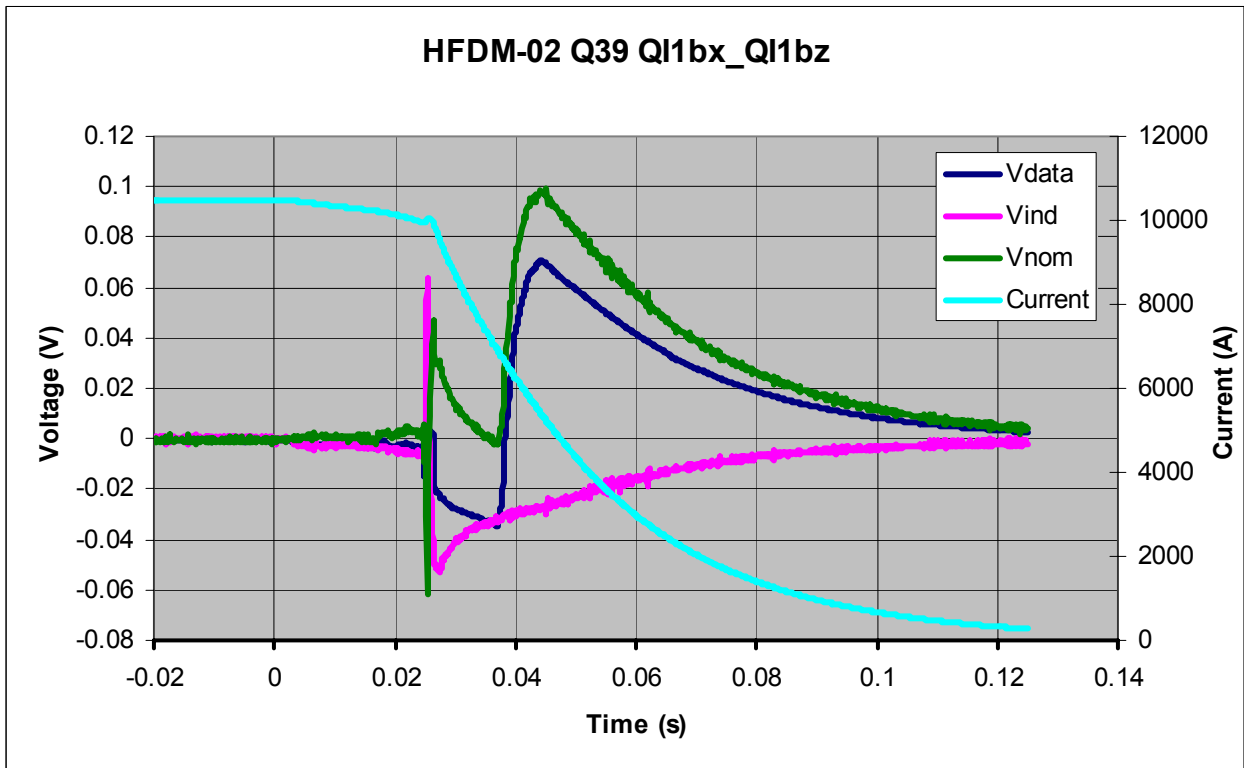


Fig. 44

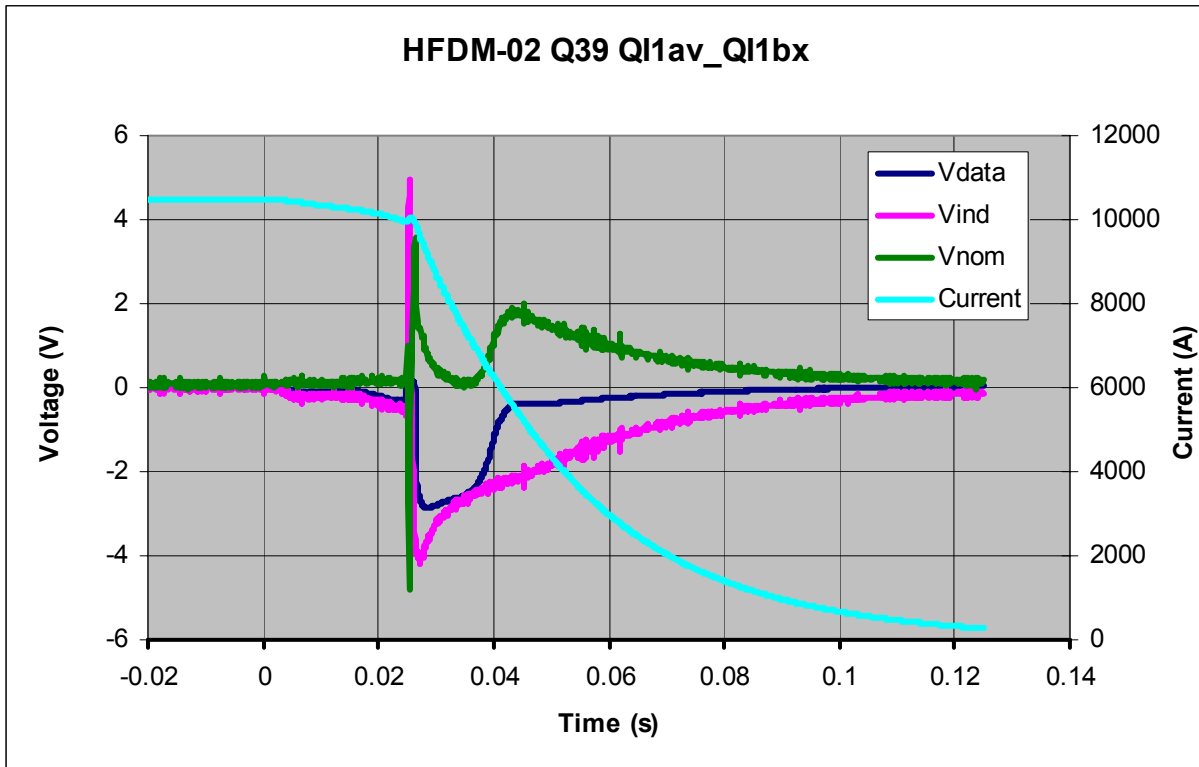


Fig. 45

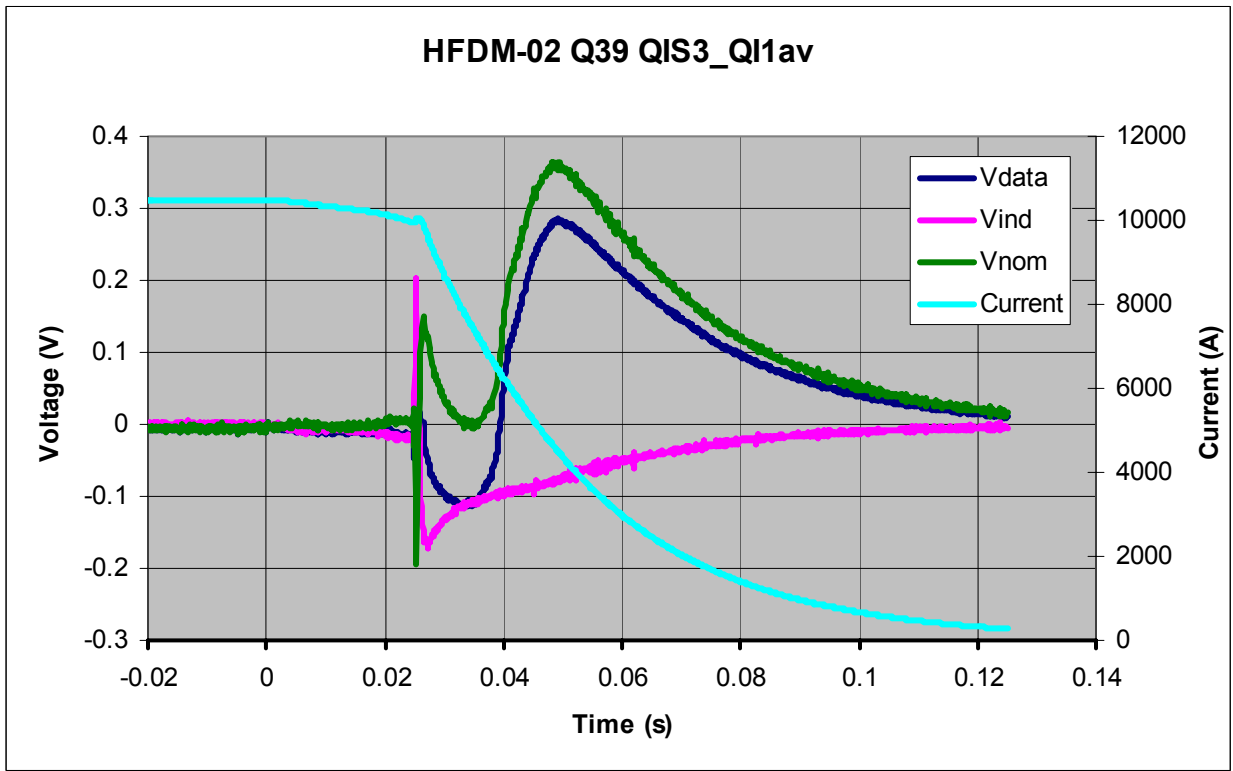


Fig. 46

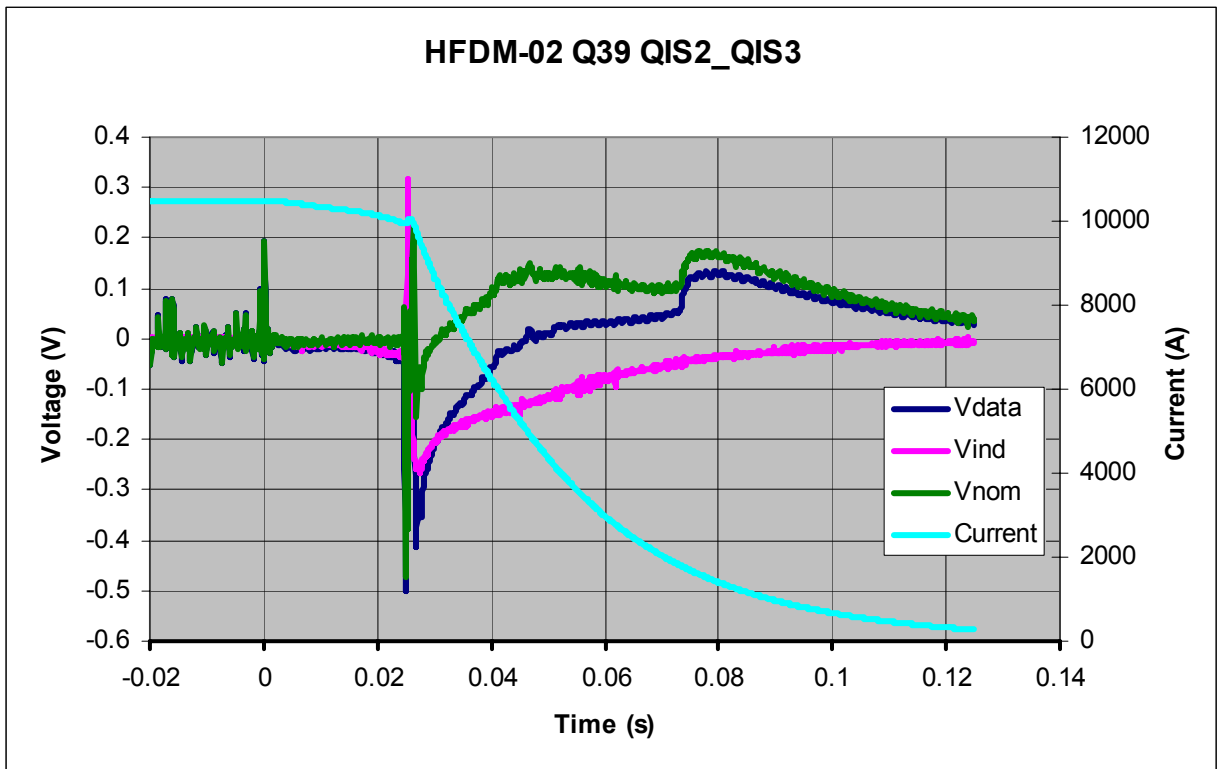


Fig. 47

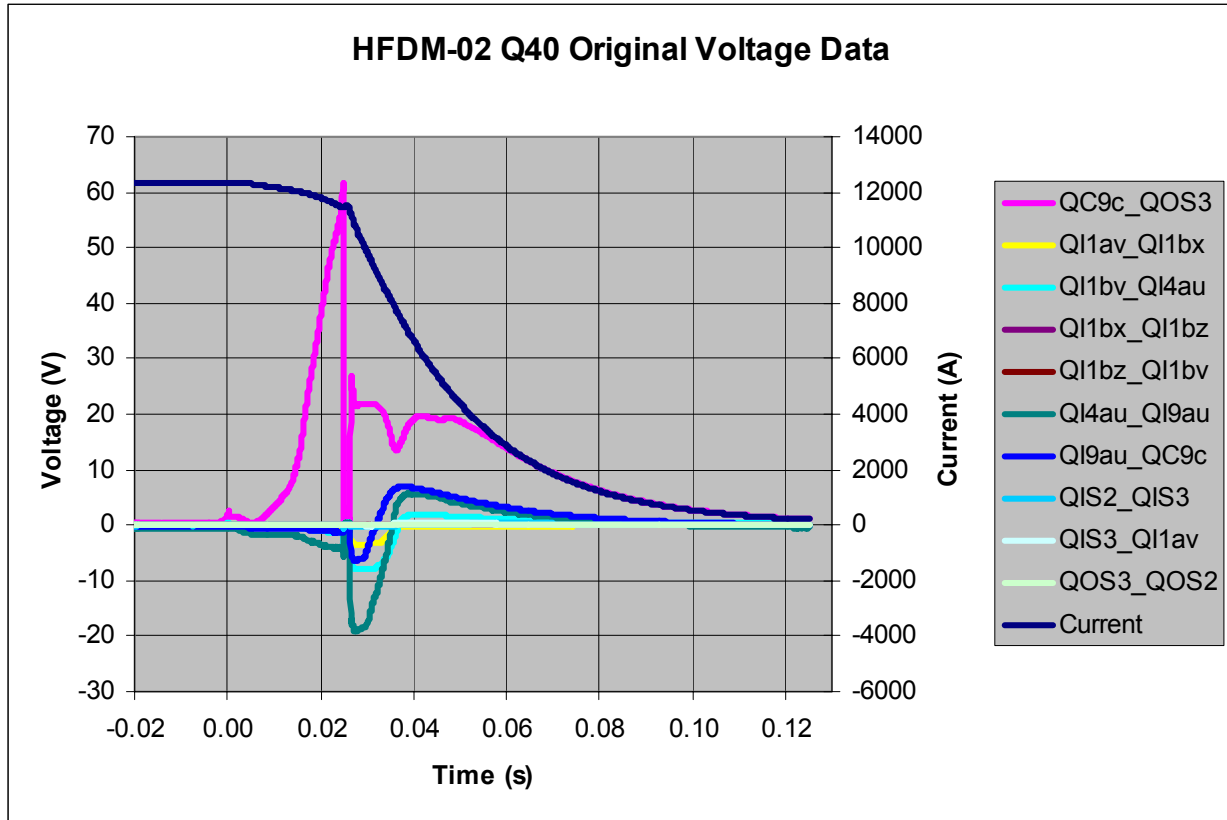


Fig. 48

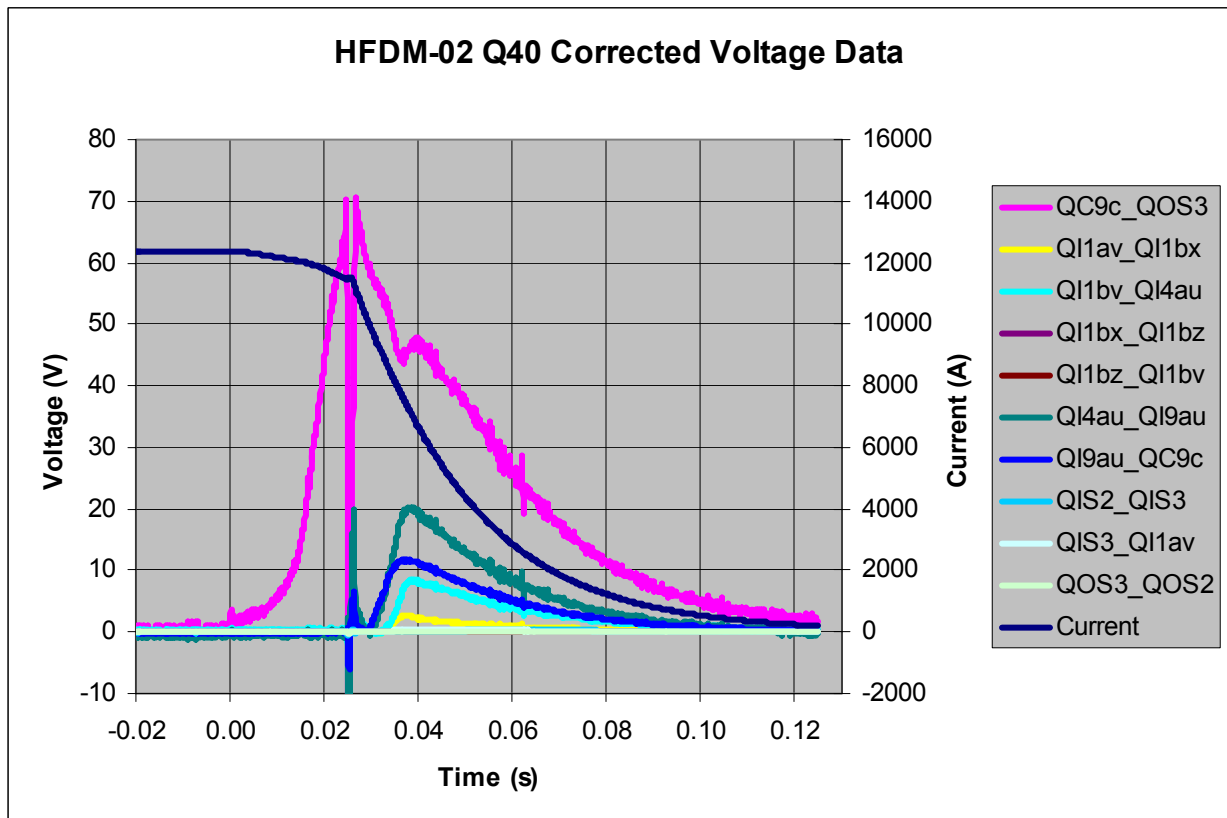


Fig. 49

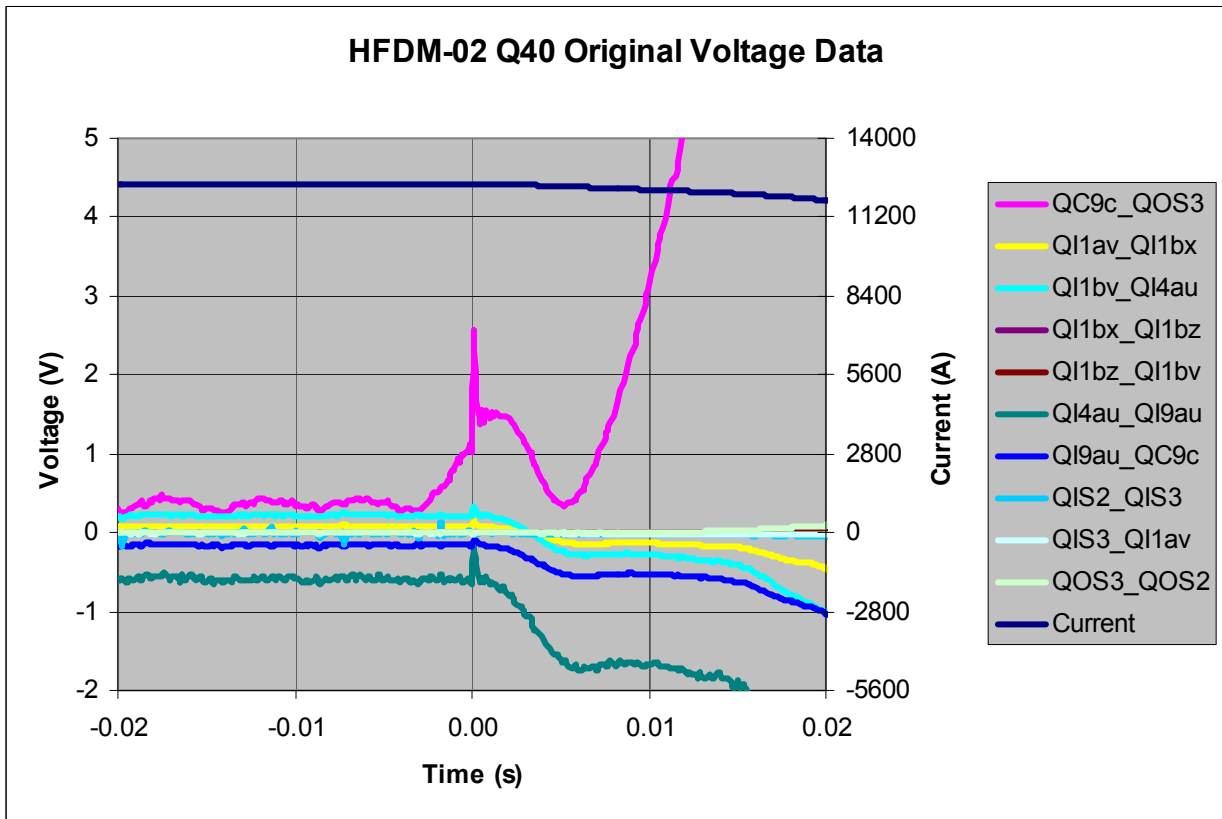


Fig. 50

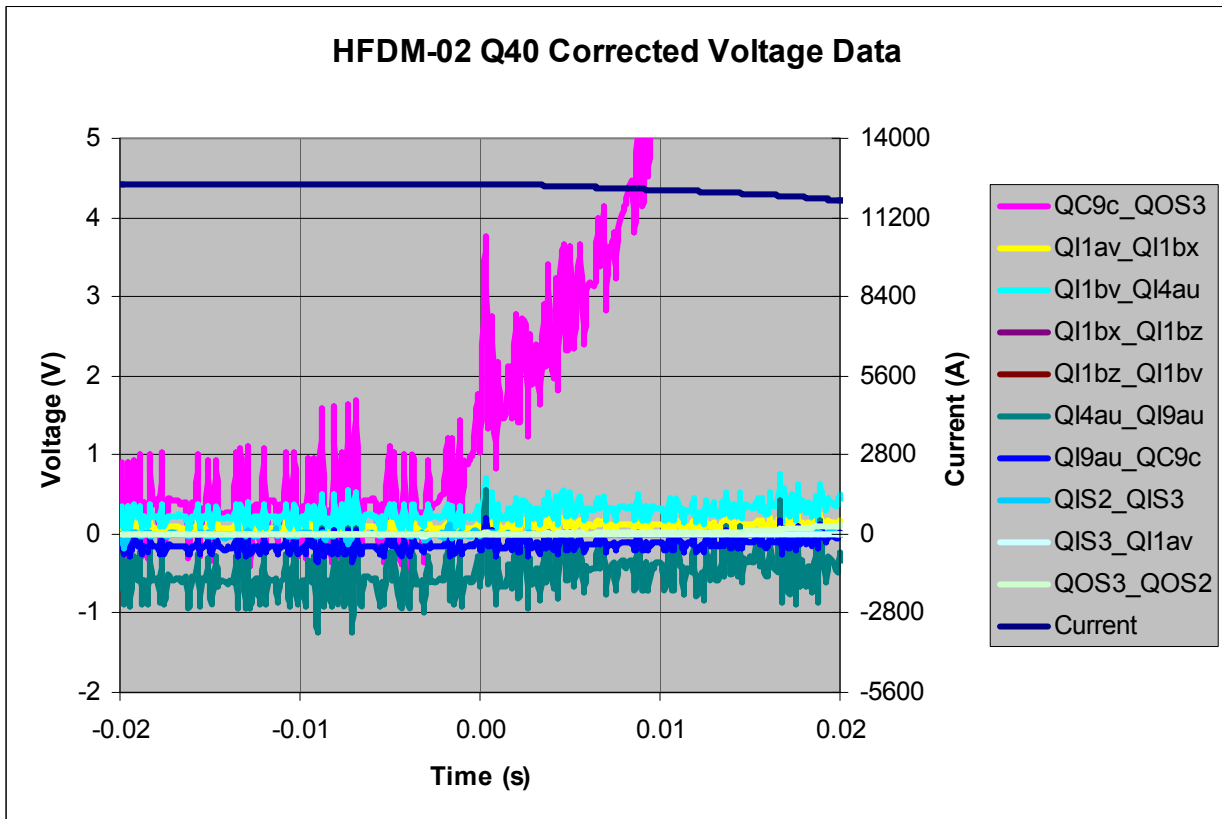


Fig. 51

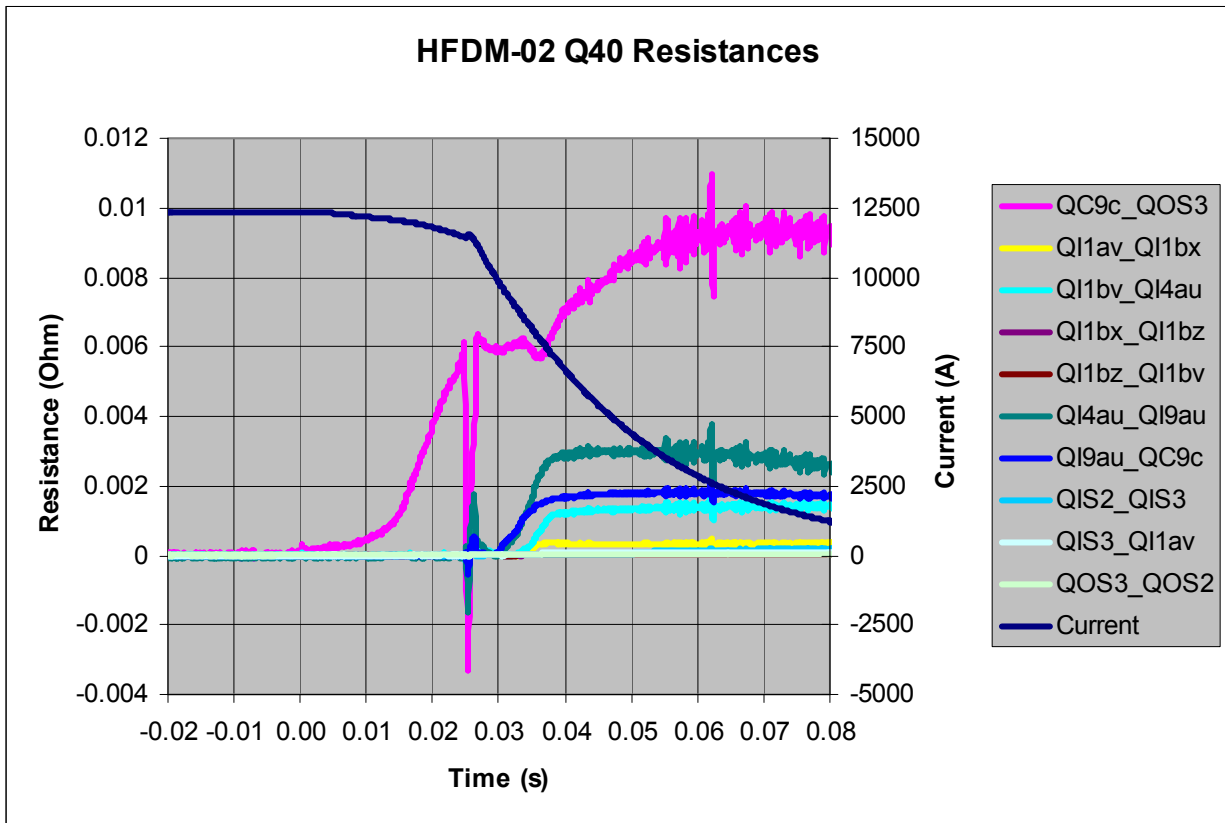


Fig. 52

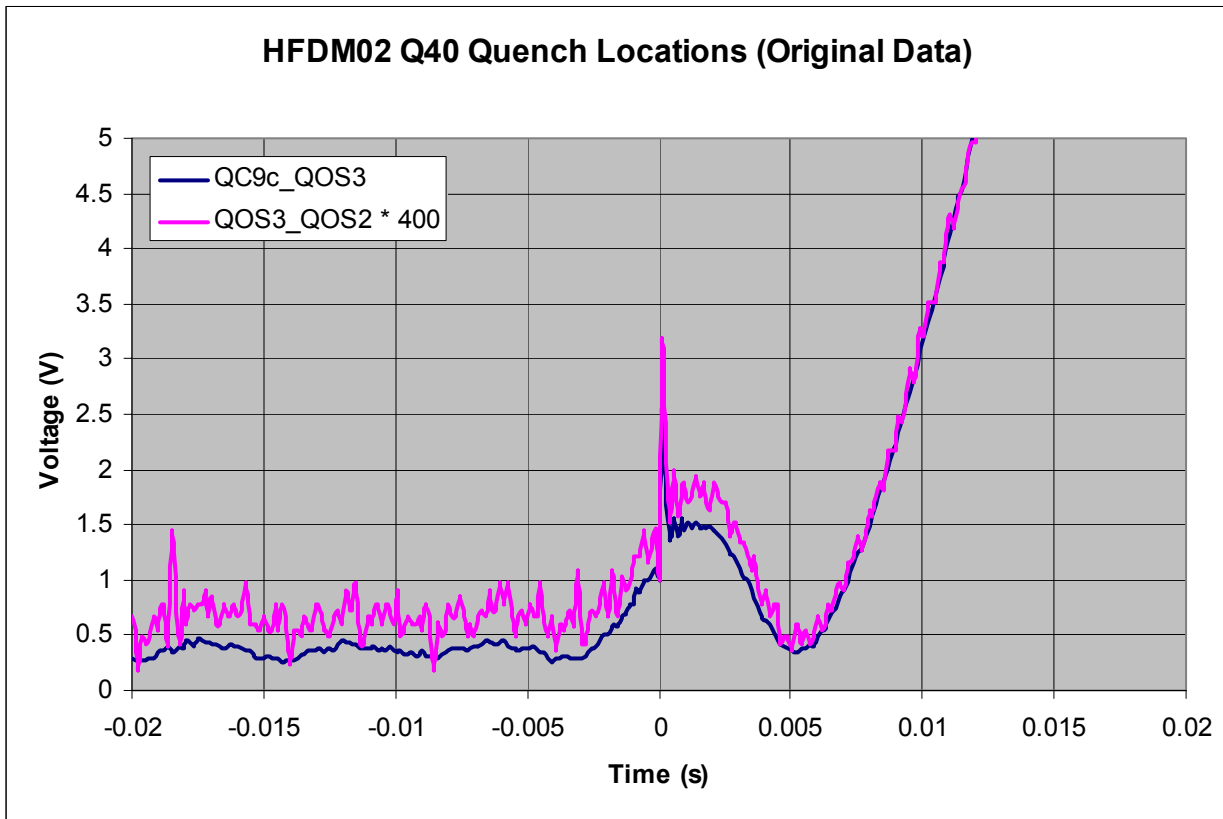


Fig. 53

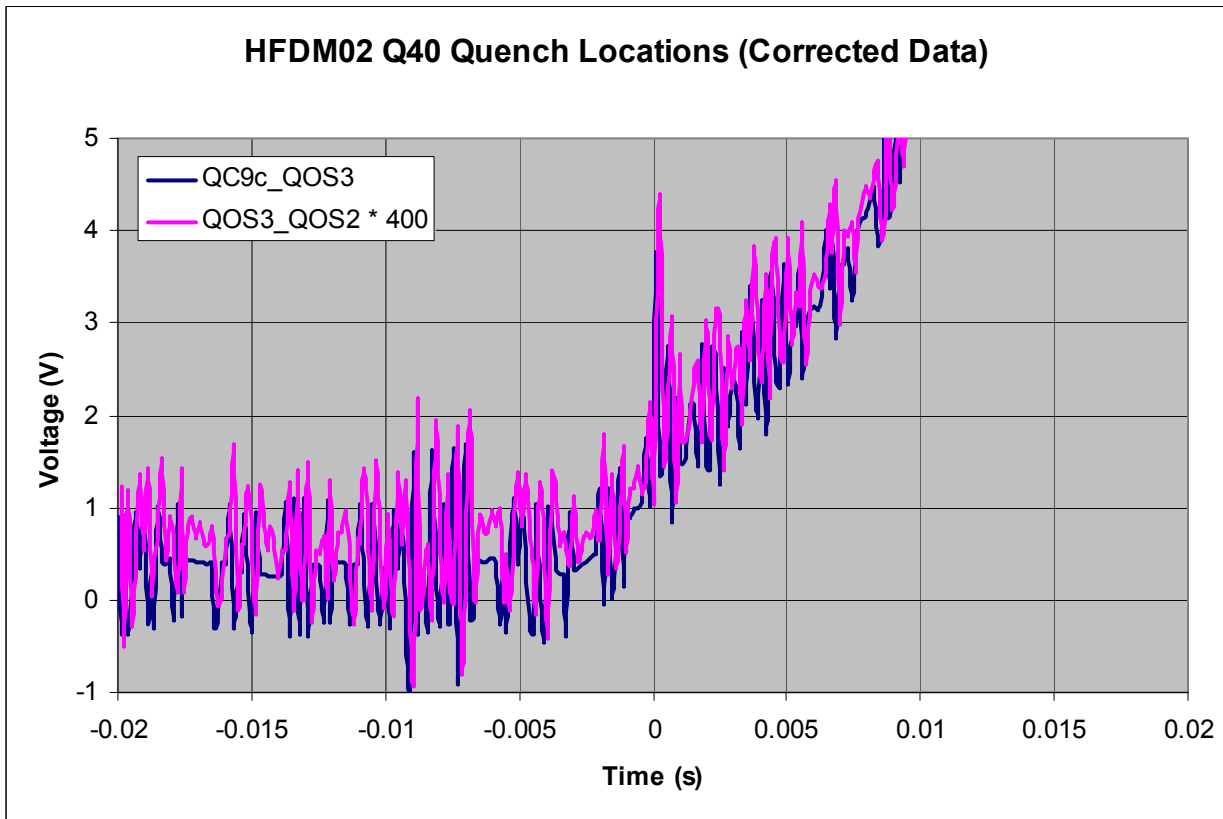


Fig. 54

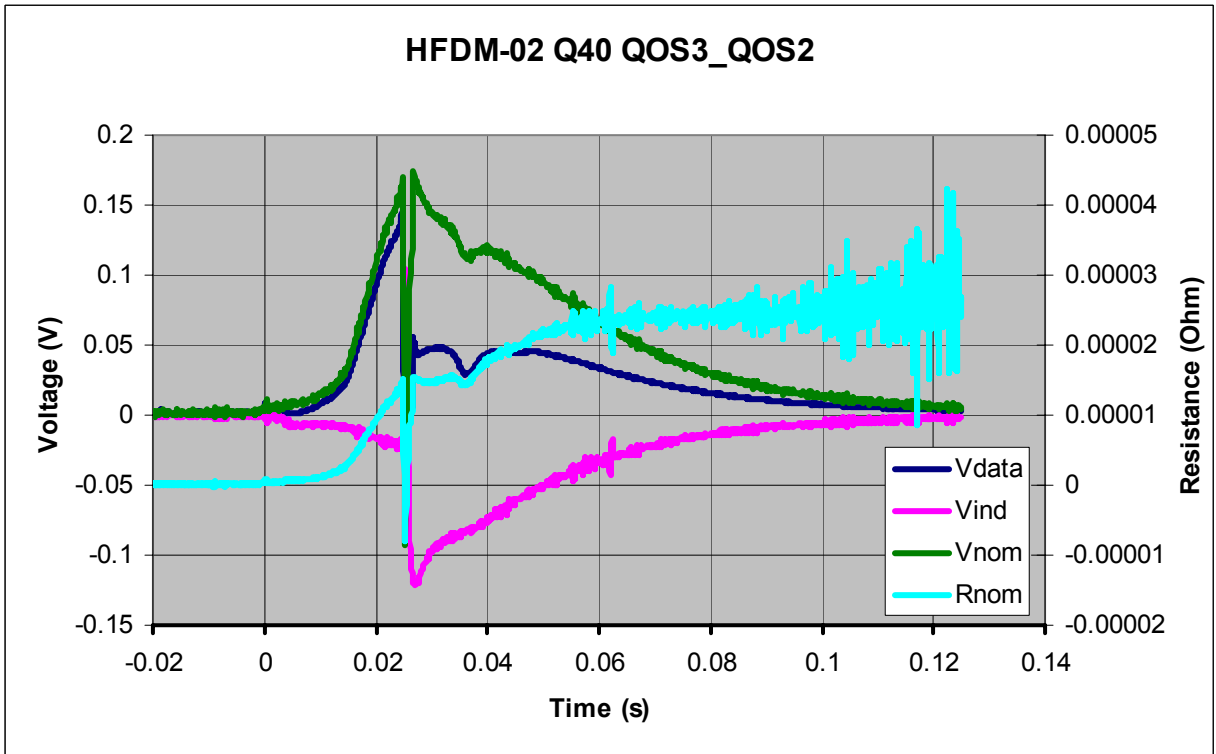


Fig. 55

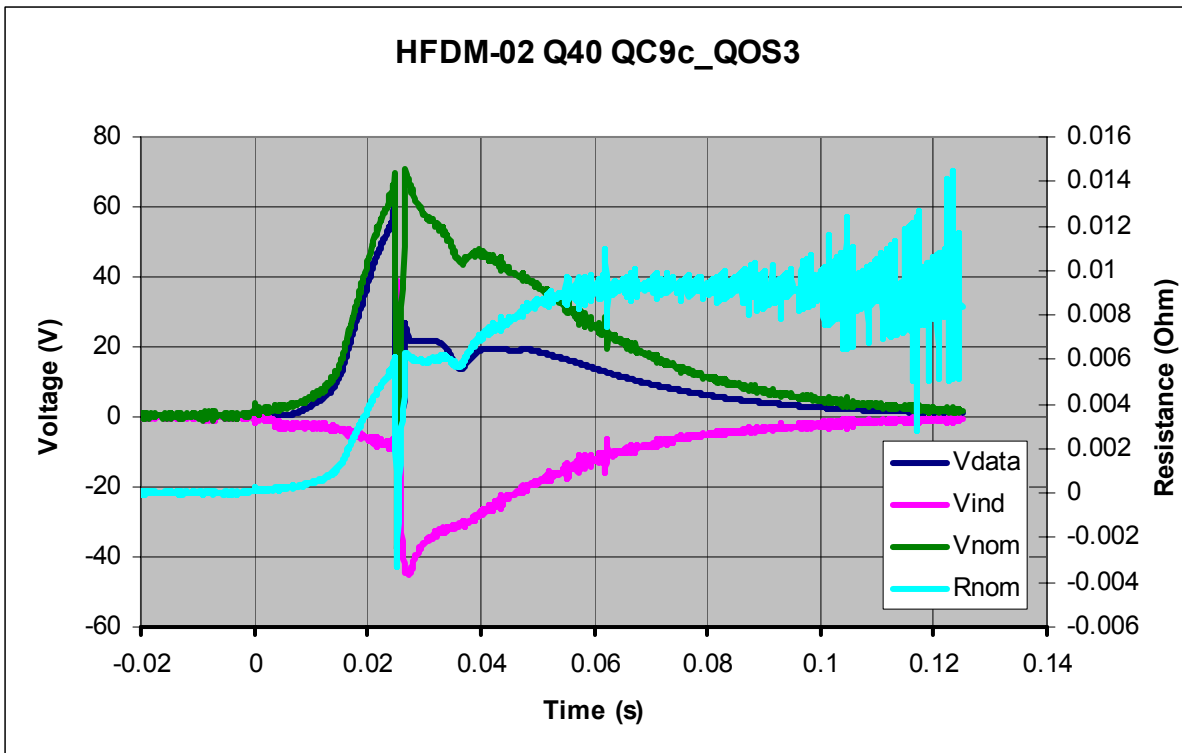


Fig. 56

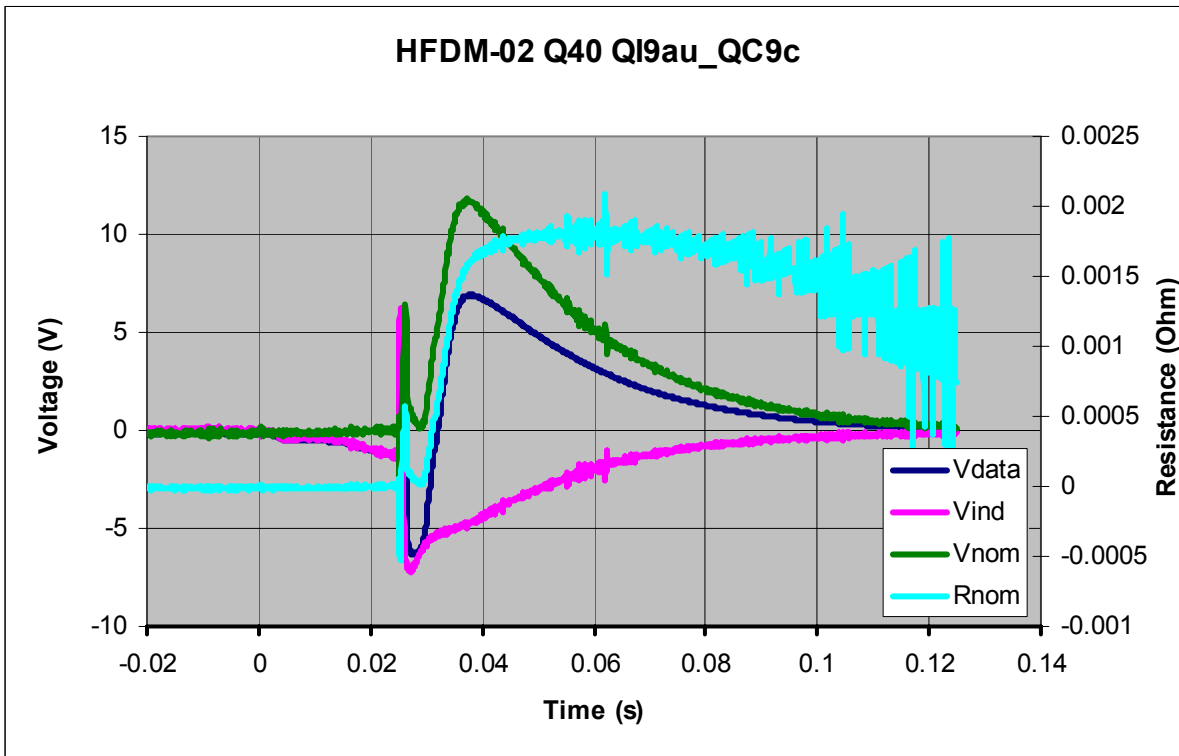


Fig. 57

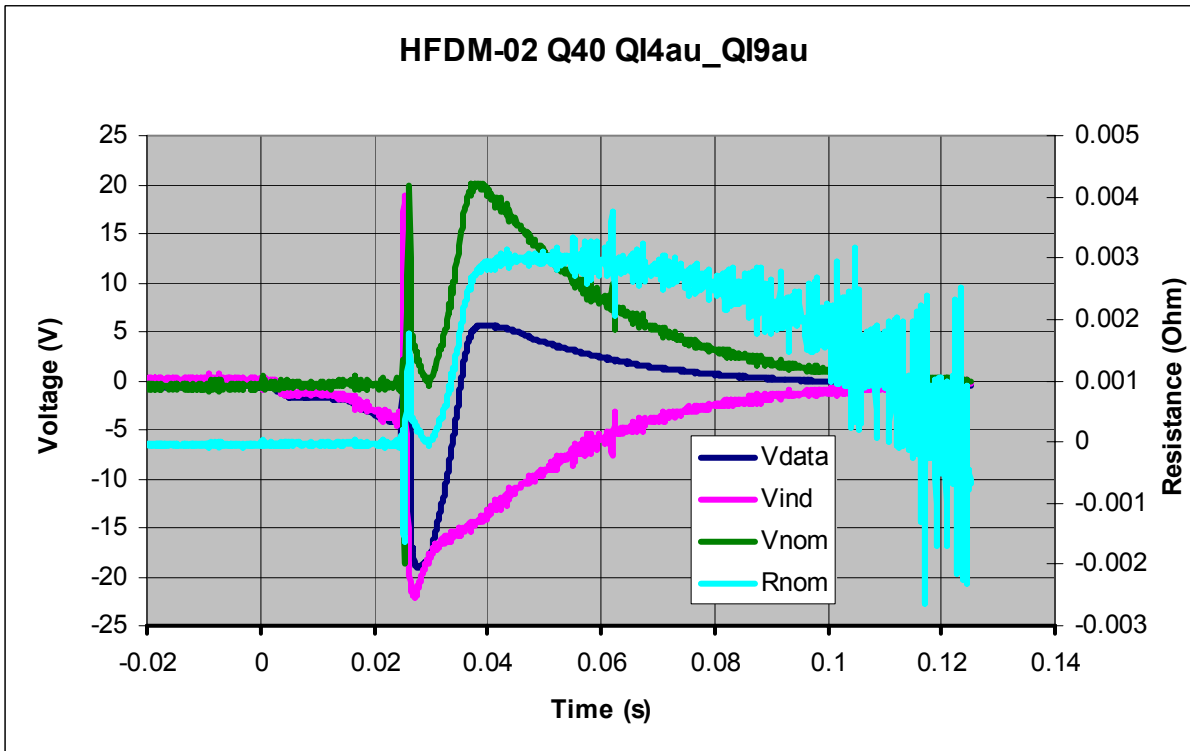


Fig. 58

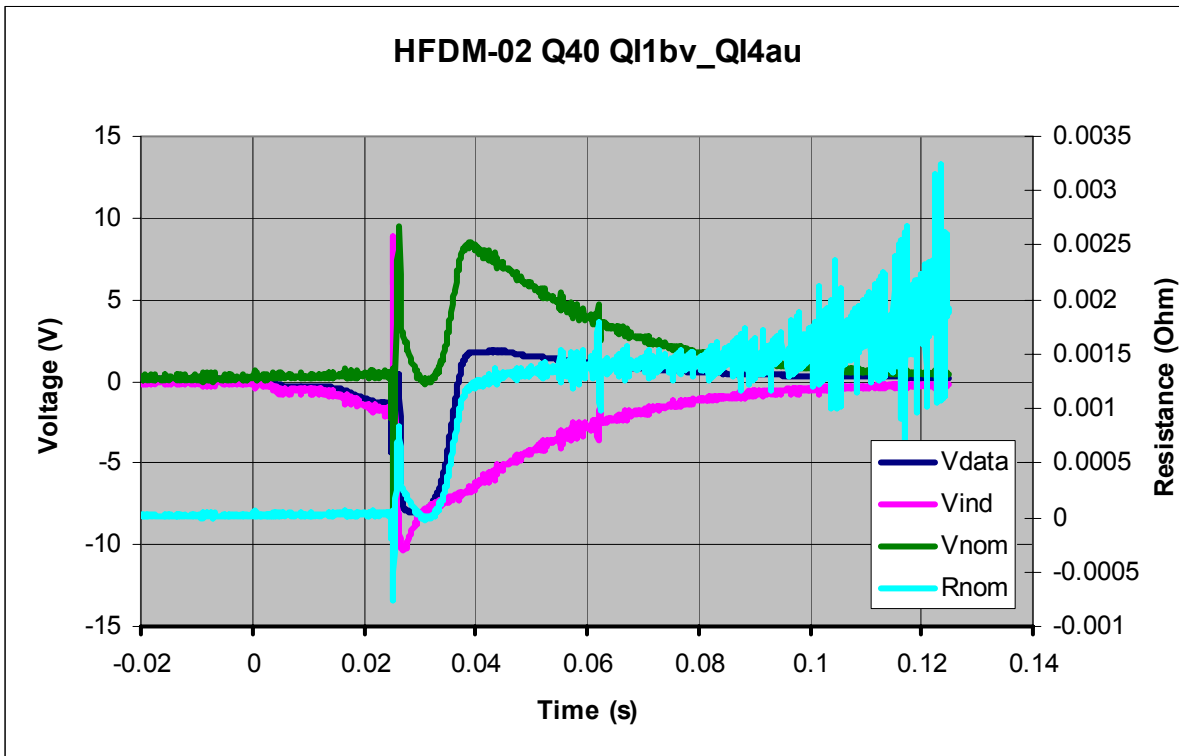


Fig. 59

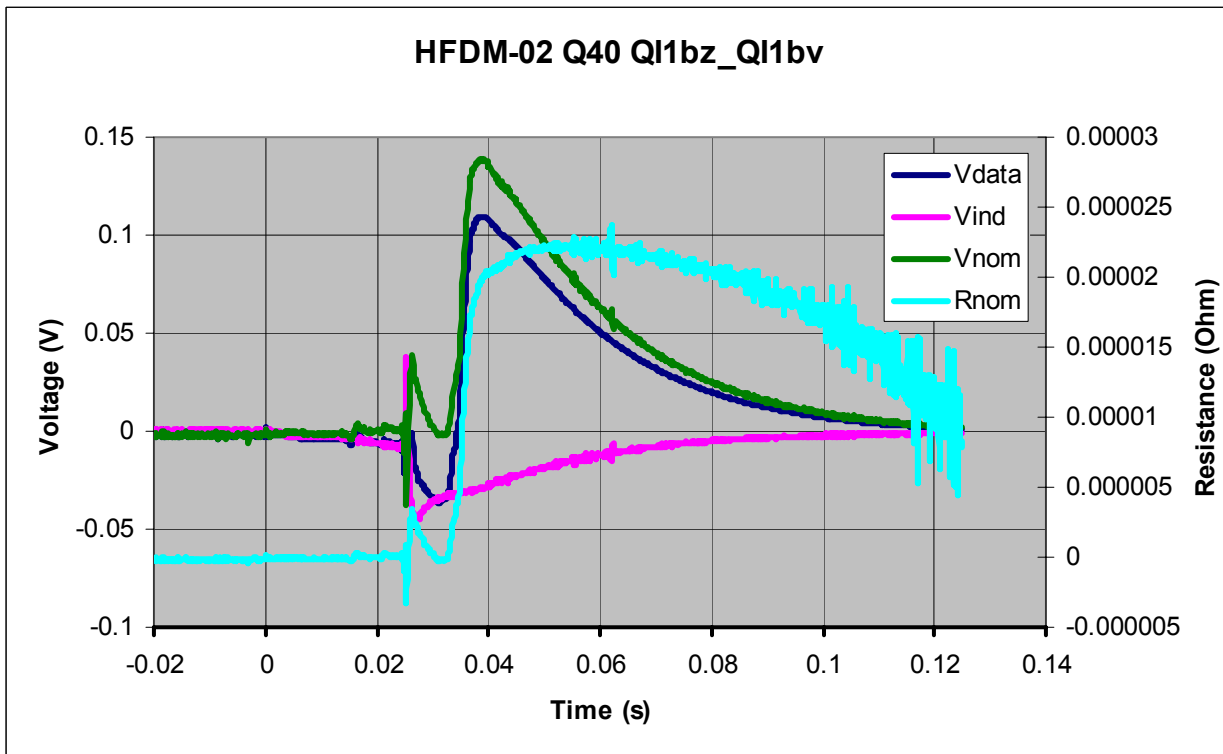


Fig. 60

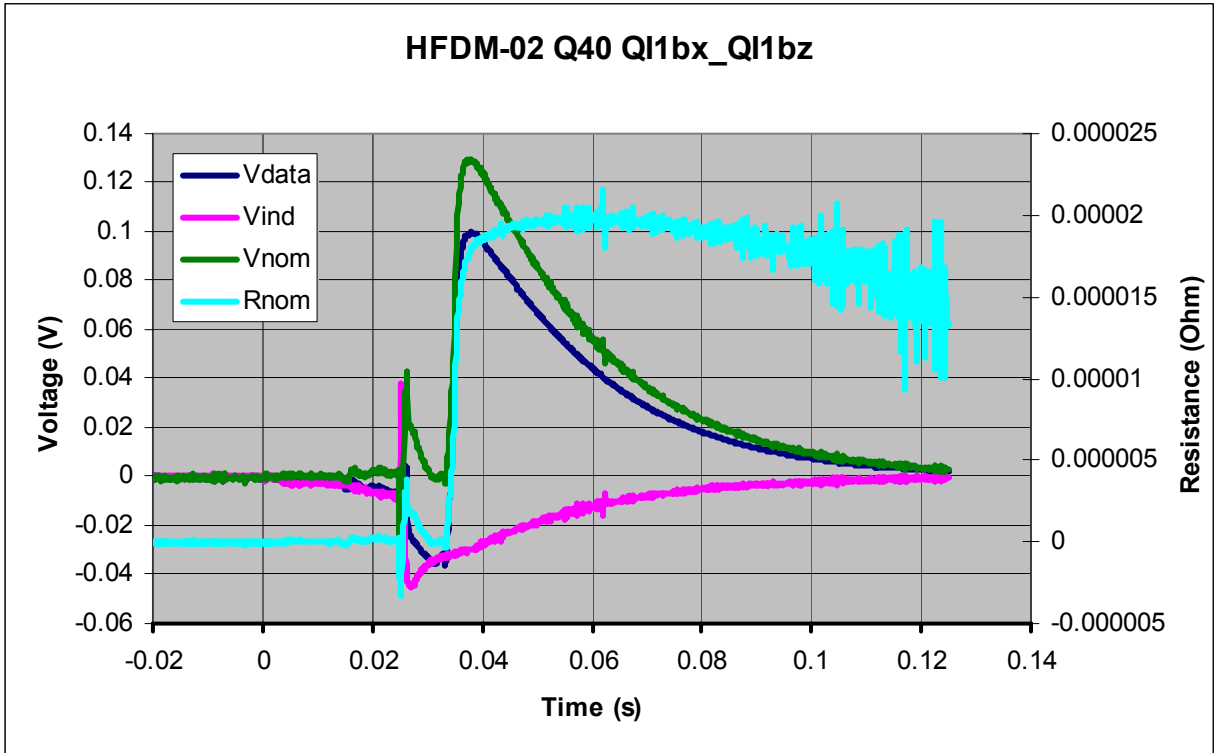


Fig. 61

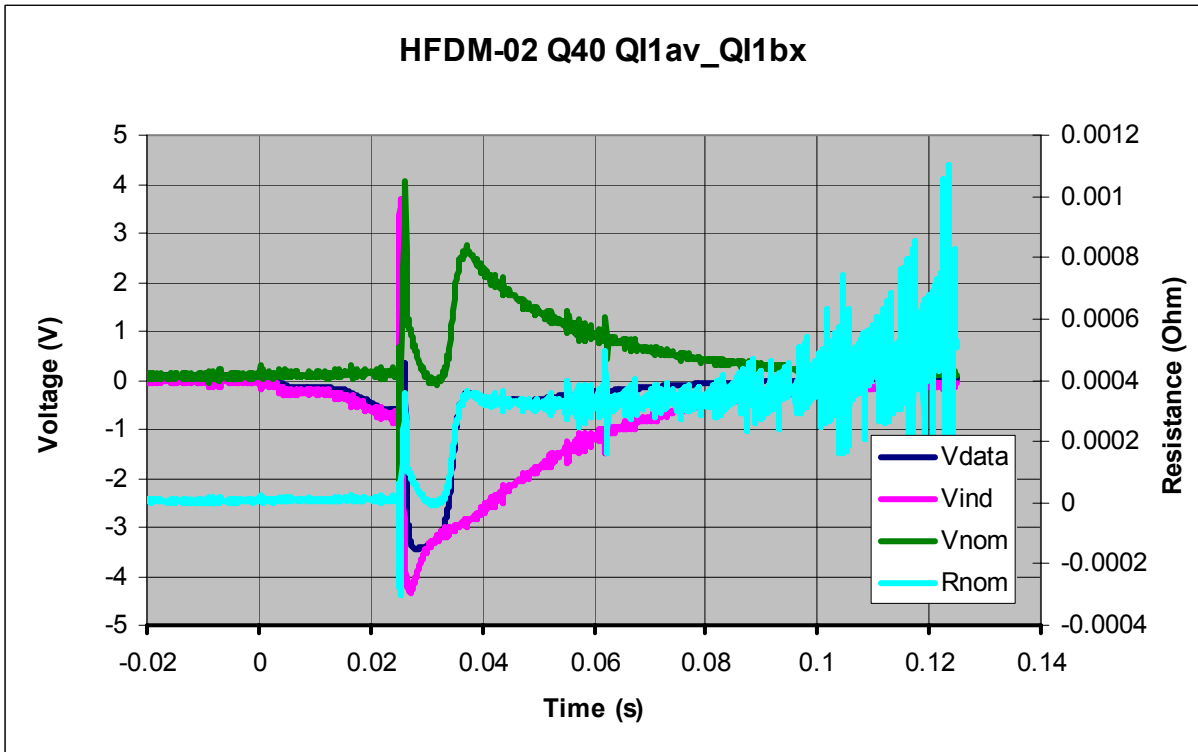


Fig. 62

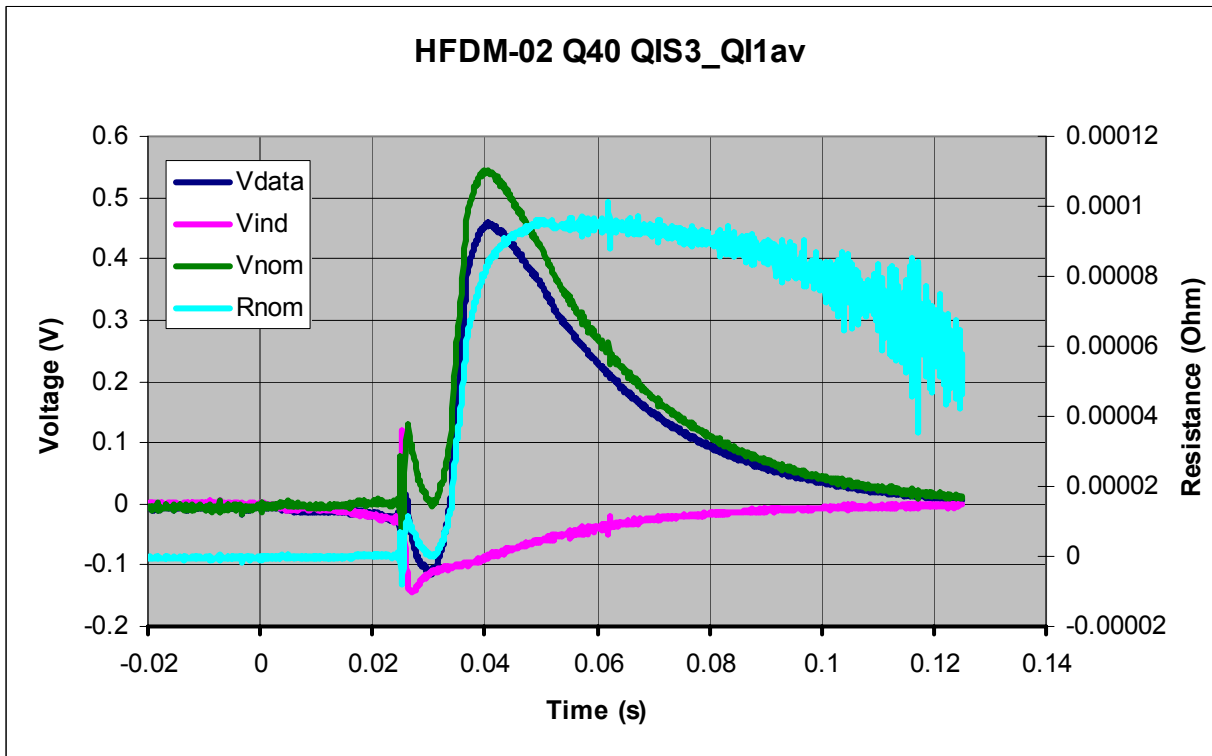


Fig. 63

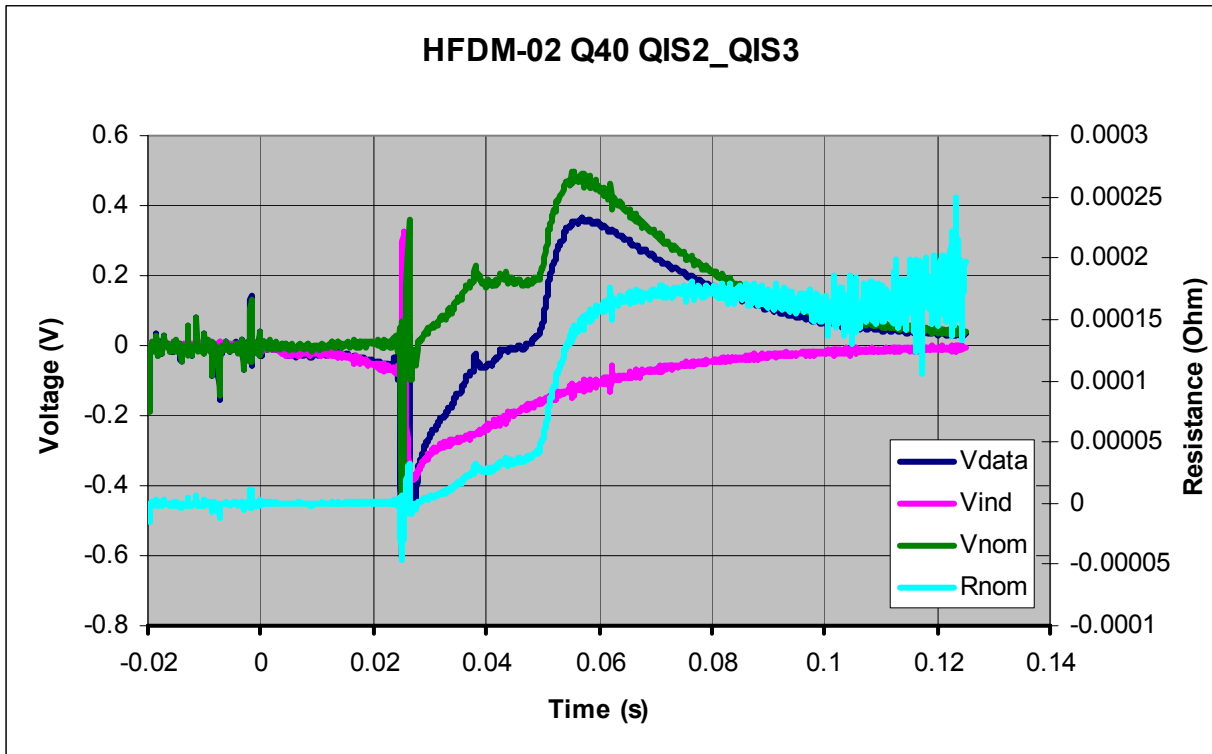


Fig. 64

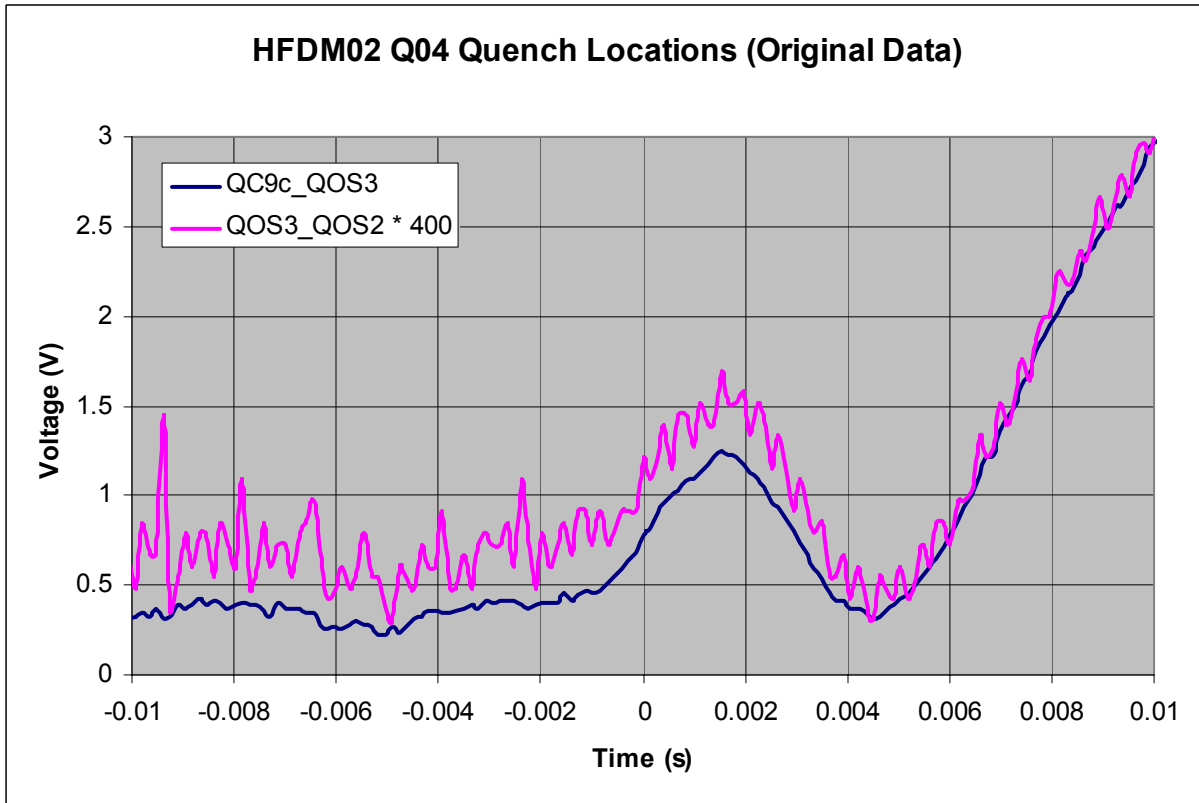


Fig. 65

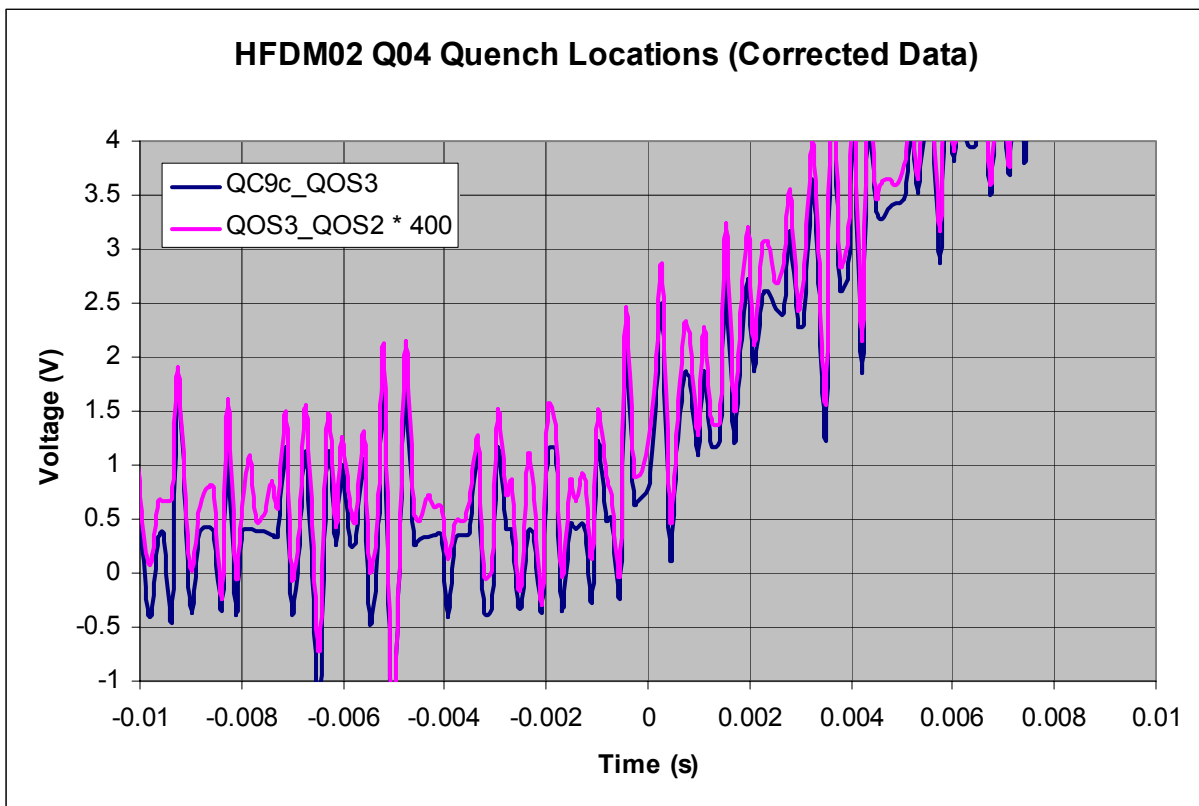


Fig. 66

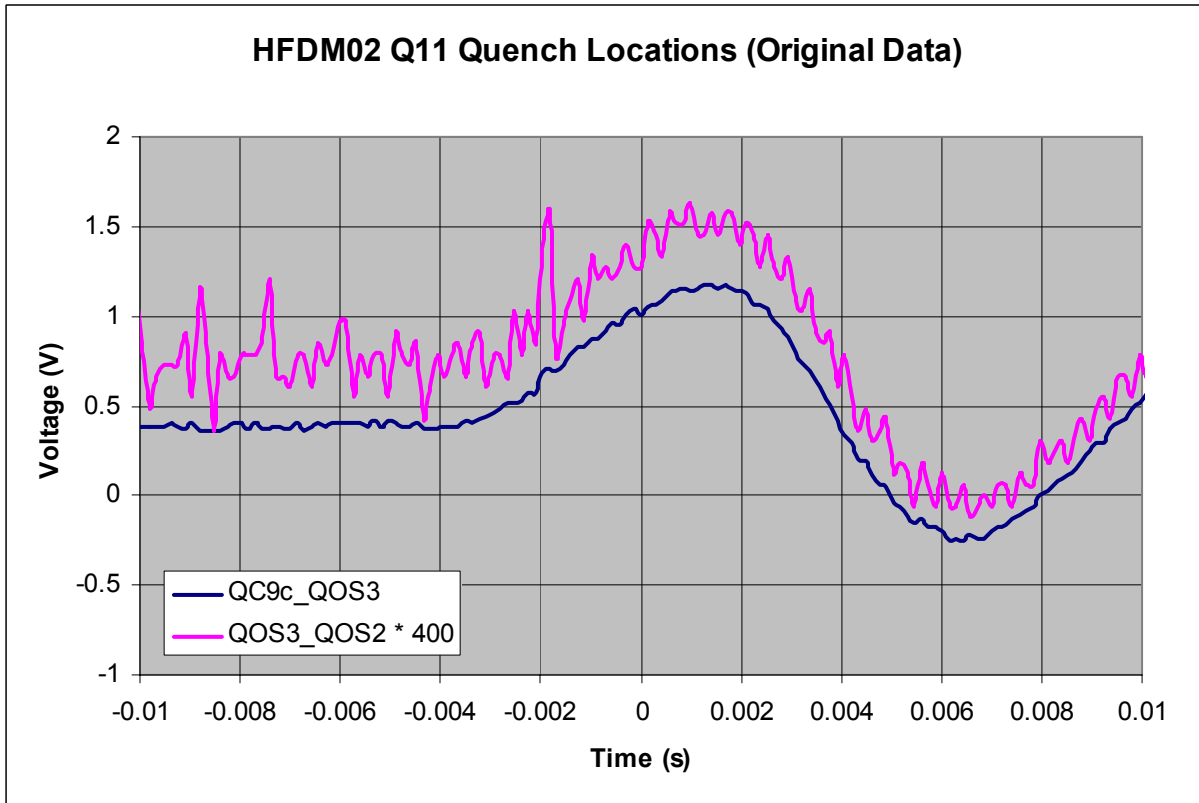


Fig. 67

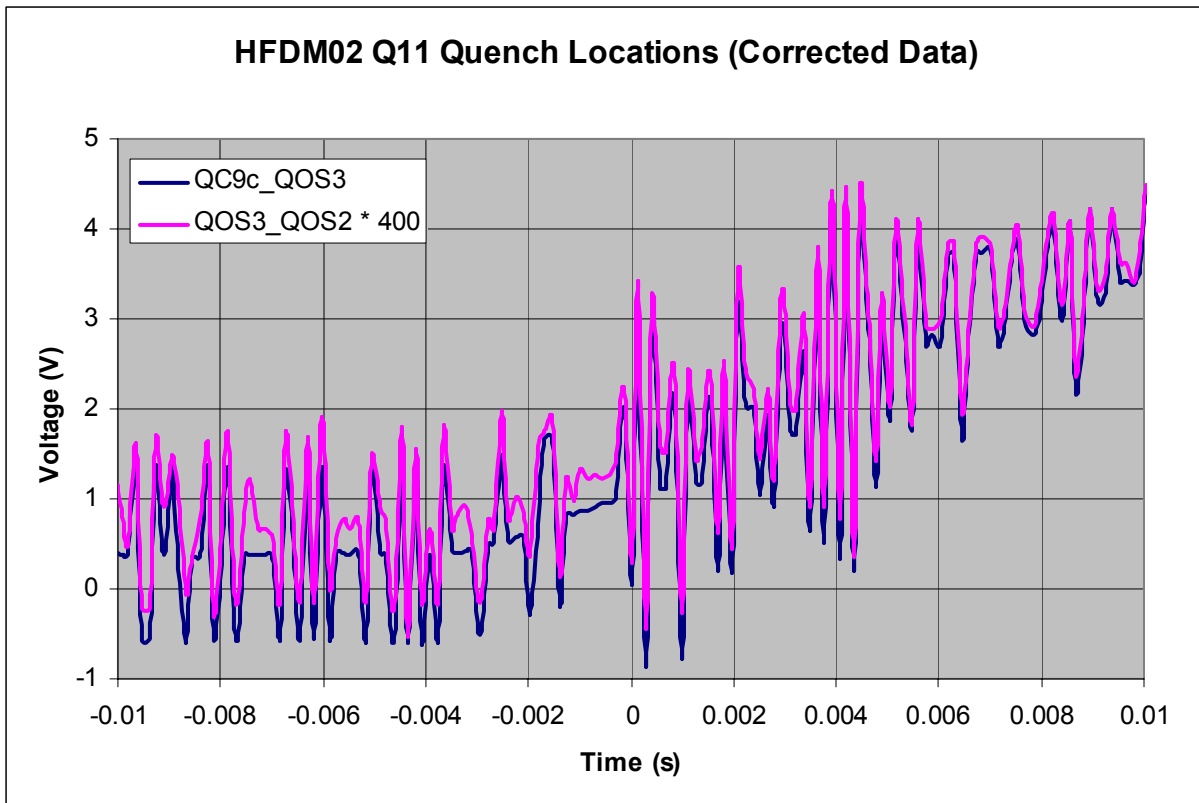


Fig. 68